AD-A086 795 UNITED TECHNOLOGIES RESEARCH CENTER EAST HARTFORD CONN F/G 20/4
TWO-PHASE NOZZLE THEORY AND PARAMETRIC ANALYSIS.(U)
JUN 80 S C KUO, C W DEANE N00014-79-C-0344
UNCLASSIFIED UTRC/R80-954624-2 NL

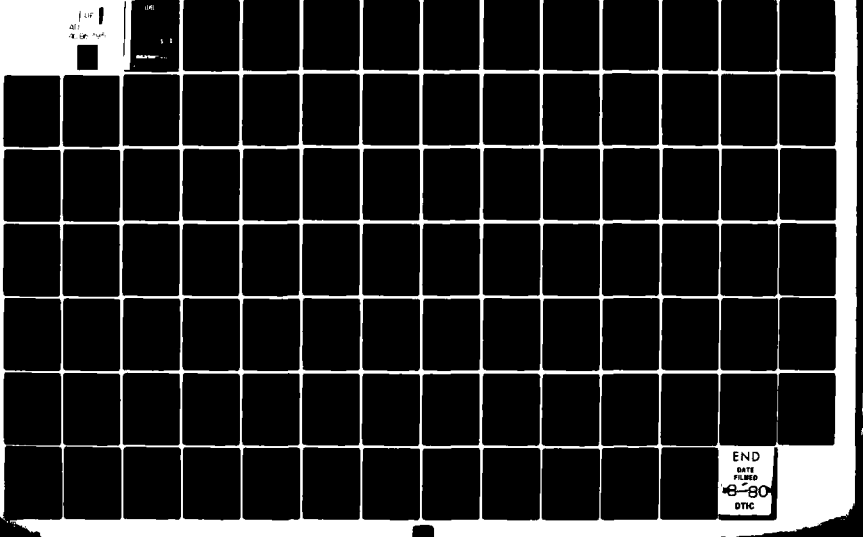

END
DATE FILED
8-80
DTIC

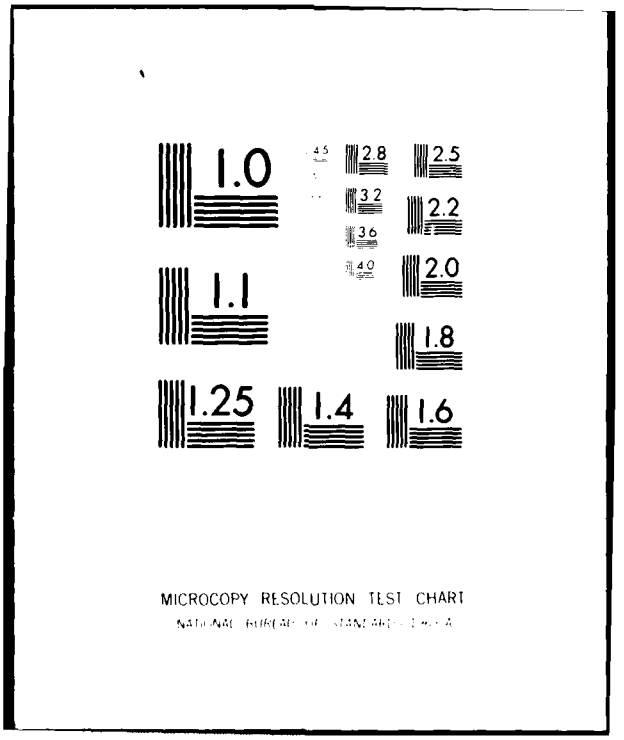
1.0
2.8
2.5
3.2
2.2
3.6
4.0
2.0
1.1
1.8
1.25
1.4
1.6
MICROCOPY RESOLUTION TEST CHART

UTRC Report R80-

Two-Phase Nozzle Theory and Parametric Analysis

Annual Technical Report
June 1980

C.W. Deane
S.C. Kuo, Principal Investigator

Prepared for
The Office of Naval Research, Arlington, Virginia
Under Contract No. N00014-79-C-0344

UNITED TECHNOLOGIES
RESEARCH CENTER
EAST HARTFORD, CONNECTICUT 06108

UNCLASSIFIED

SECURITY CLASSIFICATION OF THIS PAGE (When Data Entered)

REPORT DOCUMENTATION PAGE

READ INSTRUCTIONS BEFORE COMPLETING FORM

(14) 1. REPORT NUMBER: UTRC R80-954624-2 | 2. GOVT ACCESSION NO.: AD-A086 795 | 3. RECIPIENT'S CATALOG NUMBER:

(6) 4. TITLE (and Subtitle): Two-Phase Nozzle Theory and Parametric Analysis.

5. TYPE OF REPORT & PERIOD COVERED: Annual Technical Report. May 15, 1979 to May 14, 1980

6. PERFORMING ORG. REPORT NUMBER: UTRC R80-954624-2

(10) 7. AUTHOR(s): Simion C. Kuo, Charles W. Deane

(15) 8. CONTRACT OR GRANT NUMBER(s): N00014-79-C-0344

9. PERFORMING ORGANIZATION NAME AND ADDRESS: United Technologies Research Center, Silver Lane, East Hartford, CT 06108

10. PROGRAM ELEMENT, PROJECT, TASK AREA & WORK UNIT NUMBERS: Program Element: 61153N; Project: RRO 24-03; Task Area: RRO 24-03-02; Work Unit: NR 097-411

11. CONTROLLING OFFICE NAME AND ADDRESS: Office of Naval Research, 800 North Quincy Street, Arlington, VA 22217

(12) 94

(11) 12. REPORT DATE: June 1980

13. NUMBER OF PAGES:

14. MONITORING AGENCY NAME & ADDRESS (if different from Controlling Office)

15. SECURITY CLASS. (of this report): Unclassified

15a. DECLASSIFICATION/DOWNGRADING SCHEDULE

(9) Annual technical rept. 15 May 79 - 14 May 80

16. DISTRIBUTION STATEMENT (of this Report): Approved for public release; Distribution unlimited

17. DISTRIBUTION STATEMENT (of the abstract entered in Block 20, if different from Report): Same as block 16

(16) RR024Ø3

18. SUPPLEMENTARY NOTES

(17) RR024Ø3Ø2

19. KEY WORDS (Continue on reverse side if necessary and identify by block number)

Two-Phase Gas-Liquid Flow
Two-Phase Nozzle
Two-Phase Turbine
Droplet Heat Transfer

this study sought

20. ABSTRACT (Continue on reverse side if necessary and identify by block number)

The object of the work presented in this report was to formulate a working theory with which the performance of two-phase nozzles can be analyzed parametrically over a wide range of flow conditions and fluid properties. As a basis for formulating the theory, the technical status of two-phase nozzles was assessed, the governing flow parameters were identified, and the flow domains were classified with the previously available theory. A working theory of two-phase nozzles suitable for parametric analyses and optimization was then

DD FORM 1 JAN 73 1473 EDITION OF 1 NOV 65 IS OBSOLETE S/N 0102-014-6601

UNCLASSIFIED

SECURITY CLASSIFICATION OF THIS PAGE (When Data Entered)

409252

formulated, incorporating the significant interphase effects of velocity slip, droplet breakup, and droplet heat transfer.

The technical status of two-phase nozzles was assessed by reviewing previous investigations, both analytical and experimental, and the ranges of parameters considered in previous investigations were summarized. The limitations of the previous models were documented, and areas where the theory could be improved or simplified for greater physical understanding of two-phase flow were reviewed. Liquid/gas combinations for two-phase nozzles, and suitable combinations for marine propulsion and other selected applications were discussed. Single-phase (or homogeneous) theory was also reviewed from the viewpoint of energy conversion in a nozzle and was compared with models applicable to separate phases in terms of their flow domains.

Finally, a working theory of two-phase nozzles was formulated based on the governing flow parameters and on the six basic equations that describe the two-phase flow. From this theory, a computer model was developed which includes the significant interphase effects of velocity slip, droplet breakup, and heat transfer and which is suitable for parametric analysis and optimization. Preliminary parametric calculations based on use of this model were compared with results from previous two-phase nozzle models and with available experimental data.

This study program was conducted by the Energy Conversion Systems Analysis Group at UTRC under Contract N00014-79-C-0344 from the Office of Naval Research, Power Program, Arlington, Virginia.

R80-954624-2

Two-Phase Nozzle Theory and Parametric Analysis

Annual Technical Report

Dr. Simion C. Kuo
Principal Investigator
(203) 727-7258

Prepared for:
The Office of Naval Research, Arlington, Virginia
Under Contract No. N00014-79-C-0344
Mr. M. Keith Ellingsworth, Program Monitor

June 1980

FOREWORD

The work described in this Annual Technical Report was performed at the United Technologies Research Center (UTRC) under Contract N00014-79-C-0344 entitled "Study of Two-Phase Nozzle Theory and Parametric Analysis", for the Office of Naval Research (ONR). This report summarizes results obtained for the Phase I - Two-Phase Nozzle Theory study program. Dr. Simion C. Kuo is the Principal Investigator for this contract, and Dr. C. W. Deane is the major contributor for this phase of the study.

The contract program was initiated with ONR on May 15, 1979, and the ONR Program Manager is Mr. M. Keith Ellingsworth, Power Program, ONR, Arlington, Virginia. Valuable guidance and comments received from Mr. Ellingsworth and Mr. John R. Satkowski, Director of Power Program at ONR are gratefully acknowledged.

TABLE OF CONTENTS

R80-954624-2

Two-Phase Theory and Parametric Analysis
Phase I - Two-Phase Nozzle Theory

SUMMARY

The object of the work presented in this report was to formulate a working theory with which the performance of two-phase nozzles can be analyzed parametrically over a wide range of flow conditions and fluid properties. As a basis for formulating the theory, the technical status of two-phase nozzles was assessed, the governing flow parameters were identified, and the flow domains were classified with the previously available theory. A working theory of two-phase nozzles suitable for parametric analyses and optimization was then formulated, incorporating the significant interphase effects of velocity slip, droplet breakup, and droplet heat transfer.

The technical status of two-phase nozzles was assessed by reviewing previous investigations, both analytical and experimental, and the ranges of parameters considered in previous investigations were summarized. The limitations of the previous models were documented, and areas where the theory could be improved or simplified for greater physical understanding of two-phase flow were reviewed. Liquid/gas combinations for two-phase nozzles, and suitable combinations for marine propulsion and other selected applications were discussed. Single-phase (or homogeneous) theory was also reviewed from the viewpoint of energy conversion in a nozzle and was compared with models applicable to separate phases in terms of their flow domains.

Finally, a working theory of two-phase nozzles was formulated based on the governing flow parameters and on the six basic equations that describe the two-phase flow. From this theory, a computer model was developed which includes the significant interphase effects of velocity slip, droplet breakup, and heat transfer and which is suitable for parametric analyses and optimization. Preliminary parametric calculations based on use of this model were compared with results from previous two-phase nozzle models and with available experimental data.

This study program was conducted by the Energy Conversion Systems Analysis Group at UTRC under Contract N00014-79-C-0344 from the Office of Naval Research, Power Program, Arlington, Virginia.

INTRODUCTION

The flow of two-phase mixtures through a nozzle is a complicated process which is receiving increasing attention since many engineering applications involve flows of a substance that is a suspension of liquid droplets or solid particles in a gas. A typical example is a two-phase nozzle where a gas and a liquid at a condition of high pressure and low velocity are mixed at a nozzle inlet and then expanded through the nozzle to a condition of low pressure and high velocity. Two types of two-phase flow are of interest here. "One-component" flow is the case where the gas phase is the vapor of the liquid being accelerated, and "two-component" flow is the case where the gas phase is of a different chemical species from that of the liquid. Among other applications, two-phase nozzles can be integrated with two-phase turbines for prime-mover applications and for geothermal power generation.

The major difference between single-phase (gas) nozzle flow and two-phase nozzle flow is the interaction between the phases: the transfer of momentum and heat between the two phases. In two-phase nozzle flow, as the gas expands, drag forces transfer momentum from the gas phase to accelerate the liquid droplets, while heat is being transferred between the liquid and the gas. However, the temperature of the gas phase decreases as the gas expands, therefore heat transfer from the liquid phase will partly offset this decrease, so the temperature decrease of the gas in a two-phase flow is less than that for the pure gas expanded through the same pressure. Hence, interphase effects must be considered in analyzing two-phase nozzle flows.

Previous analytical models of two-phase nozzle flow generally display one of two drawbacks. Either: only some of the significant interphase effects of velocity slip, droplet breakup, and droplet heat transfer were considered (e.g., Refs. 1 to 5); or these three effects were considered, but the model (e.g., Ref. 6) was generally formulated with a view towards detailed design and not with the intention of conducting parametric analyses and optimization where many cases must be quickly examined yet with reasonable accuracy. Therefore, to avoid these drawbacks, a working theory should be formulated which is suitable for parametric analyses and optimization yet includes the significant interphase effects of velocity slip, droplet breakup, and droplet heat transfer as well as provides details of the local flow conditions throughout the nozzle.

The object of the Phase I - Two-Phase nozzle theory study program was to formulate a working theory of two-phase nozzle flows for use in analyzing nozzle performance as a function of the governing flow parameters; the results

of this study program are presented in this report. The technical status of two-phase nozzles was assessed and summarized in Task I.1, and the governing flow parameters and their ranges of interest were identified in Task I.2. The flow domains of two-phase nozzles were classified and correlated in Task I.3 to identify the physical characteristics of these domains. Based on this work, a working theory of two-phase nozzle flow then was formulated that includes the significant interphase effects and that is suitable for parametric analyses and optimization while still providing detailed local flow conditions in the nozzle.

INTRODUCTION REFERENCES

1. Kliegel, J.R.: One Dimensional Flow of a Gas-particle System. Report No. TR-59-0000-00746, Space Technology Laboratories, Los Angeles, 1959.

2. Rudinger, G.: "Relaxation in Gas-particle Flow", Chapter in Non-equilibrium Flows - Part I, P. P. Wegener, ed., pp. 119-161. Marcel Dekker, Inc., 1969.

3. Hultberg, J. A. and S. L. Soo: Two-Phase Flow Through a Nozzle. Astronautica Acta, Vol. 11, No. 3, pp. 207-216, 1965.

4. Crowe, C. T., M. P. Sharma and D. E. Stock: The Particle-Source-In-Cell (PSI-Cell) Model for Gas Droplet Flows. ASME J. of Fluids Eng'g., pp. 325-332, 1977.

5. Comfort, W. J., T. W. Alger, W. H. Giedt and C. T. Crowe: Calculation of Two-Phase Dispersed Droplet-In-Vapor Flows Including Normal Shock Waves. ASME J. of Fluids Eng'g., pp. 355-362, 1978.

6. Elliott, D. G. and E. Weinberg: Acceleration of Liquids in Two-Phase Nozzles. JPL Report 32-987, 1968.

RESULTS AND CONCLUSIONS

1. A working theory of two-component two-phase (gas-liquid) nozzles was developed which includes the interphase transport of momentum and thermal energy but without mass transfer and frictional losses. This working theory provides reasonably rapid yet accurate computerized numerical solutions suitable for parametric and optimization analyses of these nozzles with gas-liquid flows.

2. Previous two-phase nozzle theories generally display one of two drawbacks: either they considered only some of the interphase transport effects for simplicity of solution, or they used excessively tedious computational procedures to calculate design details of individual two-phase nozzles.

3. The departure of two-phase nozzle behavior from that of a single-phase (gas) nozzle can be attributed to the interphase coupling of momentum and thermal energy transport. As a result, liquid droplets are accelerated by the expanding gas while heat transfer from the droplets retards expansion cooling of the gas which could expand nearly isothermally at a high liquid-to-gas loading ratio and with small droplets.

4. The principal interphase coupling effects which must be considered in formulating the two-phase nozzle theory are: 1) droplet drag due to velocity slip; 2) droplet breakup as dictated by the aerodynamic and surface tension forces; 3) heat transfer between droplets and the surrounding gas; and 4) mass transfer. The flow parameters which were identified as being significant are: velocity and temperature of the liquid and gas; pressure of the gas; the liquid-to-gas loading ratio; the droplet diameter; and the thermophysical properties of the two phases.

5. Use of a hot liquid at a temperature substantially higher than that of the gas will increase the enthalpy of the two-phase mixture as well as heat transfer from the droplets to the surrounding gas. Additionally, an external heater required to heat the liquid would be relatively small. Therefore, the potential application of such a nozzle as an integral component of a two-phase turbine would be enhanced.

6. Among the various liquid-gas combinations reviewed, a high-temperature synthetic heat transfer oil (such as one of those in the Dowtherm family) suspended in steam is an attractive potential combination for two-phase turbine applications.

Two-Phase Nozzle Theory and Parametric Analysis
Phase I - Two-Phase Nozzle Theory

The overall objective of this study program is to advance the basic understanding of two-phase nozzles. To meet this overall objective, the specific objective of Phase I is to develop a working theory of two-phase nozzles, based on the principal governing flow parameters and on previous work on two-phase nozzles in the literature. Phase I consists of four tasks: I.1) Technical Status of Two-Phase Nozzles; I.2) Identification of Governing Flow Parameters; I.3) Classification of Flow Domains with Available Theory; and I.4) Formulation of Working Theory for Two-Phase Nozzles. The results obtained in each of these four tasks are presented in this report.

I.1 Technical Status of Two-Phase Nozzles

A nozzle is a flow channel in which the velocity of the fluid is increased and the pressure is reduced, thereby converting pressure energy into kinetic energy. For the two-phase nozzles being investigated in this program, the fluid is a two-phase mixture consisting of hot liquid droplets suspended in a gas. Because the hot liquid acts as a heat source in a two-phase nozzle, part of the thermal energy of the liquid is transferred efficiently to the gas phase, and the resulting two-phase enthalpy is then converted into kinetic energy.

As an example of flow in a two-phase nozzle, small droplets of a hot liquid which has a low vapor pressure (such as mineral-oil hydraulic fluids) can be mixed at the nozzle inlet with a liquid that has a higher vapor pressure (such as water). If the hot liquid is at a sufficiently high temperature, the cold liquid with its high vapor pressure can be vaporized by the heat from the hot liquid, and the resulting two-phase mixture is then expanded through a nozzle to low pressure and high velocity. The high-velocity vapor drags the oil droplets along to a high velocity, and the presence of the finely dispersed liquid droplets means that the same level of momentum flux is obtained but with a much lower gas velocity (or spouting velocity) when compared to a single-phase gas nozzle, because the average molecular weight of the two-phase mixture is higher than that of the gas. For the prime mover application, for example, two-phase nozzles can be integrated with a two-phase turbine for efficient operation at much lower rotor speeds than a turbine with a single-phase gas as the working fluid. Hence, the two-phase turbine can offer high torque at low rotor speed.

Flow in two-phase nozzles involves changes in the gas velocity and temperature that are brought about by the gas-droplet interactions of viscous drag and heat transfer. Because of the short residence time of the two-phase mixture in the nozzle, considerable departures from velocity and temperature equilibrium between the two phases can occur in the nozzle. Hence, nonequilibrium effects should be included in analytical models of two-phase nozzle flows.

Previous work on two-phase nozzles can be divided into three general areas: 1) gas-particle, 2) gas-liquid, and 3) vapor-liquid flows. Gas-particle nozzles are applied mainly to metallized solid propellant flows in rocket motors and are the simplest to analyze. Gas-liquid nozzles are more complex, primarily because of droplet effects, but are of interest in a wide variety of applications, including low-speed power turbines, gas-driven jet pumps, MHD power generators, and atomization and spraying equipment. Vapor-liquid nozzle flows are the most complex because of the interphase transfer mechanisms and find application in such areas as geothermal power turbines and high-quality steam-water flows in steam turbines.

I.1.1 Physical Models and Solutions

A number of previous investigators have proposed physical models for two-phase flows in nozzles, and several of these models are discussed in the following section. Table I.1 summarizes the important aspects of these models, all of which are one-dimensional (except for Crowe's model). Generally, the early models neglected droplet breakup for one of two reasons: either to simplify the analysis, or to reflect the fact that the analysis was applicable to constant-diameter solid spheres in rocket exhaust nozzles. Most of the models listed also neglect shock effects, in part either to simplify the analysis or to reflect the fact that shock effects are important only at drop sizes significantly smaller than those anticipated for their application.

As seen in Table I.1, Tangren et al. (Ref. 1) conducted one of the early investigations of two-phase flows in two-phase nozzles, and nozzle characteristics for isothermal frictionless flow were calculated. The isentropic flow was also assumed to be homogeneous, which assumption means that differences in velocity and temperature were neglected. The qualitative behavior of the homogeneous nozzle flow and the methods of solution for the homogeneous model are very similar to the classic closed-form analytical solution for the single-phase nozzle discussed by Shapiro (Ref. 2). The Tangren analysis applies to bubbly flow, but should also be valid for dispersed (or spray) flow because almost all of the mass flux is also due to the liquid. Further, when the liquid comprises most of the mass in the flow, the liquid will act as a heat source for the expanding gas, and the expanding two-phase flow may be nearly isothermal. This depends on the droplet size which affects the

heat transfer rate in terms of both the heat transfer area and the heat transfer coefficient between the gas and the droplets. The Tangren analysis produces a local Mach number which is a function of the ratio of the local pressure to the reservoir (or inlet) pressure, and the throat area which will pass a given amount of the two-phase mixture. However, the homogenous theory does not account for differences in velocity and temperature between the two phases, and because differences which occur in the real nozzle flow lead to nozzle inefficiencies, a prediction based on the homogeneous model would be optimistic.

As indicated in Table I.1, work by Kliegel (Ref. 3) took into consideration differences in velocity and temperature between the two phases. The analysis was applied to gas-solid flows in rocket exhaust nozzles, where the size of the solid particle is both constant and known. In this case, too, a closed-form analytical solution was obtained. Kliegel assumed that the nozzle shape was such that the ratio of particle (or droplet) velocity to the local gas velocity was constant and that the lag of the particle temperature is directly proportional to the lag of the gas temperature. (The lag of the temperature is simply the temperature relative to the reservoir conditions of the flow.) These nozzles are known as "constant-fractional-lag nozzles". If the volume fraction of the particles is neglected, then the flow equations for these nozzles reduce to the form that applies to the flow of a perfect gas which has an apparent specific heat and a modified Mach number. The shape of the nozzle which results for the assumption of constant fractional lag is arbitrary, but no more arbitrary than other shapes. And the simplifications thereby possible in the analysis allow insight into the behavior of the two-phase flow.

Rudinger (Ref. 4) extended Kliegel's concept of the constant-fractional-lag nozzle to high particle loadings where the particle volume must be considered. For this situation, computerized solutions are necessary because of the complicated analysis. Under certain flow conditions, the computerized solutions indicate, however, that the gas and particle (or droplet) temperatures remain essentially constant throughout the length of the nozzle during certain operating conditions, namely those with high loading ratios (which is the ratio of the liquid droplet/particle mass flow rate to the gas flow rate). These results are plausible because isothermal flow implies an isentropic expansion exponent of unity, a value which is rapidly approached as the loading ratio increases. For those cases where the flow can be assumed to be isothermal, then the equations result in a closed-form analytical solution convenient for hand calculation of velocity and flow area as a function of pressure along the nozzle.

Netzer (Ref. 5) included the effects of droplet breakup by using the Weber number breakup criterion, although in his analysis, friction was neglected. For short nozzles, friction effects are negligible; however, in long nozzles,

friction effects are significant, and velocities were measured that were as much as 25 percent below those predicted by this frictionless model. Netzer's work is further limited by the fact that it allows for no temperature difference between the two phases.

Hultberg and Soo (Ref. 6) investigated two-phase mixtures of gas and solid particles (of constant diameter). Their model included velocity slip and heat transfer between the particles and the gas phase. Iterative numerical methods were used to solve the governing equations using a prescribed nozzle profile, and the convergence of the solution was checked. Because the model was formulated for the flow of a metallized propellant containing alumina or magnesia (solid) particles in a rocket nozzle, the effects of droplet breakup were not considered.

Elliott and Weinberg (Refs. 7 and 8) synthesized a complex computerized model for two-phase nozzles which allowed for temperature, as well as velocity, differences between the two phases and included droplet breakup and friction effects for long nozzles. The only major effect not considered in their analysis was that of shock. This model was used (in Ref. 8) to study nozzle designs for an MHD application in which predictions were compared with experimental nitrogen-water results. For this application, the measured bulk velocities and flow rates agreed with those predicted by the analysis within 5 percent.

Recent work by Crowe et al. (Ref. 9) for spray cooling resulted in a two-dimensional model which includes coupling of mass, momentum, and energy between the two phases, although droplet breakup was not included. The flow field is divided into a series of cells, and finite-difference equations for mass, momentum, and energy conservation are written for the gas phase, while the droplet effects are treated as source terms in the gas flow equations. As a numerical example, Crowe analyzed the case of a spray issuing into a moving gas stream, and obtained predictions for the temperature and velocity flow fields of the gas and droplet phases.

Comfort et al. (Ref. 10) developed a one-dimensional analytical model of two-phase nozzle flows which can be applied to steam-water (one-component) mixtures from geothermal heat sources. With drop diameters of less than 10 microns (0.0004 in), shock effects in the flow can be important, and accordingly, those were included in the analysis. The importance of accounting for two-phase shock phenomena increases as the droplet size becomes smaller, because the mixture begins to behave as a homogeneous dense gas. Design considerations for the geothermal application generally require that the velocities in such devices as two-phase turbines be supersonic relative to both the two-phase choking velocity and the vapor choking velocity. In the Comfort analysis, thermal equilibrium between the two phases was assumed, because the heat transfer rate is very high when the drops are very small. For drop sizes which

may be encountered in a two-phase nozzle for the marine propulsion applications, however, thermal equilibrium may not exist, and shock effects will be less significant. Numerical analysis is required to solve Comfort's model which is capable of predicting pressure, velocity, droplet diameter, loading ratio, and normal shock waves as a function of axial distance through the nozzle.

I.1.2 Experimental Data

A number of investigators have conducted experiments with two-phase nozzles, and selected parts of these efforts are summarized in this section. Elliott and Weinberg (Ref. 8) summarized previous work as of 1968 and also conducted experiments with room-temperature nitrogen and water mixtures in a large-scale 1.32 m (52 inch) long nozzle for an MHD application. Their inlet pressures ranged from 10.3 to 15.9 bar (150 to 230 psi), and their expansion pressure ratio ranged from 10:1 to 16:1. With a loading ratio (liquid/gas) of 40, the predicted temperature drop of the liquid was approximately 0.8 C (1.5 F) while that of the gas was 6 C (11 F). Without the water, the isentropic expansion of the nitrogen would have resulted in a temperature drop of 139 C (250 F). Hence, in the two-phase expansion, the liquid acted as a heat source for the gas, with liquid enthalpy being converted into gas enthalpy. Experimentally, axial pressure profiles and bulk exit velocities were measured and compared with the analytical predictions. The flow rate data generally were in the range between that predicted for flow with friction and that for isentropic flow (which was 8 percent lower). The isentropic prediction is lower because the gas velocity is the lowest in the absence of slip, and hence the gas flow rate is lower. And with the loading ratio fixed, then the total flow rate is lower. Elliott and Weinberg attributed the slightly higher predictions of flow rate to the underestimation of the droplet drag. Solid sphere drag data was used, whereas the actual liquid droplets become flatter and offer more aerodynamic resistance than do spherical droplets. Exit velocities were also measured and are about 3 to 5 percent higher than those predicted for flow with friction - the difference is again attributed to underestimation of droplet drag. The isentropic velocity is 13 to 18 percent higher than that for the prediction of flow with friction. Tests were also run in the same nozzle using Freon 1301 ($CBrF_3$) as a liquid at the nozzle inlet in place of the nitrogen to verify that the gas phase could be produced by contact vaporization at the inlet of a two-phase nozzle. Because the data agreed as well with the theory as in the nitrogen-water tests (where the nitrogen was already a gas at the nozzle inlet), Elliott and Weinberg concluded that complete vaporization of the Freon 1301 did occur.

Elliott also reported (Ref. 7) the results of earlier water-air experiments using a 0.15-m (6-in.) long converging-diverging nozzle at inlet conditions of 12 C (54 F) and 35.4 bar (514 psia). These results were compared with those of their later analytical model (Ref. 8). The measured flow rates were only 1 to 2 percent lower than those predicted for flow with friction and the measured

bulk exit velocities straddled by ± 3 percent the prediction for flow with friction. For this short nozzle, the effect of friction was to decrease the flow rate prediction based on the frictionless prediction criterion by 3 percent, and the bulk exit velocity prediction by 6 percent.

Starkman et al. (Ref. 11) measured flow rates of one-component, two-phase (water-steam) mixtures expanding through a converging-diverging deLaval nozzle, with the inlet quality ranging from zero to 20 percent and inlet pressures up to 69 bar (1000 psia). The data were compared with the results of three simple models: isentropic expansion with thermal equilibrium but no slip; frozen composition with no slip or heat transfer; and slip flow with limited momentum exchange between the phases. The measured flow rates agreed satisfactorily with the results from all three models, except at low inlet qualities (where the mixture is mostly saturated liquid). When the nozzles were run at overexpanded conditions, it was observed that there was a two-phase "shock" which was much weaker and less distinct than that found in single-phase gas flows. Schrock et al. (Ref. 12) extended the work of Starkman et al. and examined the effect of inlet subcooling on the flashing flow of water in converging-diverging nozzles. A two-step model based on a nucleating delay with a discontinuous transition to a frozen composition gave reasonable predictions of flow rates and pressure profiles in the convergent section.

For the geothermal application of hot water deposits, Alger (Ref. 13) tested a small nozzle (0.1-m(4-inches)long) with mixtures of steam-water of 19 percent inlet quality at 24.8 bar (360 psia) and 224 C (435 F). This nozzle could be incorporated into a two-phase impulse turbine, although, to achieve a maximum efficiency turbine, droplet sizes of less than 4 microns (0.00016 in) would be required so that the droplets will follow the vapor streamlines and not collide with the blade walls. The thrust of Alger's work was to measure droplet phase characteristics (primarily drop sizes), and the results suggest that the droplets break up at diameters which are less than about one third of the diameter predicted by a critical Weber number of 6. (The Weber number is defined as the dimensionless ratio of the aerodynamic force to the surface tension force on the droplets, and the critical Weber number is the value at which droplet breakup occurs.)

Cerini (Ref. 14) tested a 0.63-m (25-inch) long steam-water nozzle for a geothermal application where inlet conditions were 5.5 bar (80 psia) and 5 percent quality. The measured flow rates agreed to ±3 percent with the predictions from the computerized model with friction developed by Elliot and Weinberg (Ref. 8).

Most of the recent experimental work on two-phase nozzles has concentrated on geothermal applications, where the steam-water mixtures are one-component and mass-transfer effects are very important. However, two-phase nozzles with two-component flows are of interest for applications in marine power and thrust augmentation in turbofan engines.

I.1.3 Two-Phase Nozzle Applications

Two-phase nozzles are of interest in a number of fields, and Table I.2 lists several of these applications. As can be seen, two-phase nozzles are being used in such areas as propulsion, energy conversion, and transportation. Two-phase nozzles are used in two-phase turbines which, because of the higher density of the two-phase working fluid, have lower rotor speeds than do turbines using gas as the working fluid. With the lower rotor speeds, two-phase turbines (Ref. 15) offer the possibility of either a smaller gearbox or no gearbox in the marine and automotive propulsion applications. With a two-phase nozzle, the liquid/gas ratio can be varied to control the nozzle exit velocity, a feature which is unique to two-phase nozzles. As a result, the turbine speed can be varied at nearly constant efficiency. At part-load conditions, the efficiency of a two-phase turbine cycle can be higher than that of a single-phase steam turbine, because the efficiency of a two-phase turbine cycle is nearly flat over a large portion of its turbine speed range. Further, the usual boiler could be eliminated because a single-phase liquid heat exchanger could be used to heat the liquid which, in turn, would be mixed with a high-vapor-pressure liquid. The resulting vapor would be expanded through the the nozzle carrying with it the hot liquid drops (of the low-vapor-pressure fluid).

Another application of great current interest is geothermal power, where the steam is frequently unsaturated, and where potential erosion problems play a decisive role in the design of the turbine. With the higher density of the two-phase mixture, the turbine rotor speed is lower than in a gas turbine, and erosion problems would be less severe.

Water injection in the fan exhaust nozzle of a turbofan engine can be used to augment the thrust. Work on this two-phase nozzle (Ref. 16) using a water-augmented turbofan engine for high-speed ships showed a theoretical augmentation in thrust of 380 percent at 12.9 m/sec (25 knots) and of 90 percent at 51.4 m/sec (100 knots).

Work by Elliot and Weinberg (Ref. 8) was directed toward MHD power generation, where liquid lithium and cesium vapor are the two components. Ahmad and Hays (Ref. 18) have investigated the use of a two-phase turbine system to recover waste heat in a bottoming cycle of a stationary diesel engine, and a fuel saving of as much as 30 percent is calculated.

I.2 Identification of Governing Flow Parameters

Preparatory to formulating a working theory of two-phase nozzle flows, the governing flow parameters and their ranges of values were identified. Liquid/gas combinations for the various two-phase nozzle applications were examined, and suitable combinations are discussed for selected applications.

I.2.1 Governing Flow Parameters

The principal governing flow parameters were identified on the basis of the previous investigations that were described in Section I.1. Fig. I.1 is a schematic of a converging-diverging nozzle with the governing flow parameters: the velocity(v), mass flow rate($\dot{m}$), and temperature(T) of both the gas-phase (subscript g) and liquid-phase (subscript ℓ) streams, and the droplet diameter(D). The thermophysical properties of each stream must also be known. For the gas phase, these properties include the density (ρ_g), specific heat (C_{pg}), thermal conductivity (k_g), and viscosity (μ_g). For the liquid phase, these properties include the density (ρ_ℓ), specific heat (C), and the surface tension (σ) for use in estimating droplet sizes. The local differences in velocity and temperature between the two phases affect the interphase transfer mechanisms of momentum and energy. The velocity difference affects the droplet drag, the heat transfer coefficient between the liquid droplet and the gas, and the droplet breakup. The temperature difference is the driving force for heat transfer between the liquid and the gas. The flow rates of each phase determine the loading ratio ($\dot{m}_\ell/\dot{m}_g$) of the nozzle and the mass flux of each phase in the nozzle. The droplet diameter affects the coefficients of drag and heat transfer and is obtained from the Weber droplet breakup criterion which in turn depends on the velocity difference between the two phases.

The range of parameters considered in previous investigations of two-phase nozzles is shown in Table I.3 in terms of the gas/liquid combination, the design-point temperature and pressure, the liquid mass and volume fractions, and the droplet diameter (when indicated by the investigator). In a given investigation, the analytical and experimental aspects generally covered the same range of conditions, except when testing was done with fluids that are easier to handle. For example, Elliot and Weinberg (Ref. 8) examined the application of MHD power generation with liquid metals (lithium as the liquid and cesium as the gas phase) at inlet conditions of 982 C (1800 F) and 9.44 bar (137 psia), but their testing was done with mixtures of nitrogen and water at inlet conditions of 16 C (60 F) and 10.3 bar (150 psia).

In related investigations at the Lawrence Livermore Laboratory, Alger (Ref. 13) and Comfort and Beadle (Ref. 17) examined the geothermal application, and both testing and analysis were performed with steam/water mixtures at the actual operating conditions [224 C (435 F) and 24.8 bar (360 psia)] of a geothermal heat source. The liquid mass fraction of these investigations ranged from approximately 0.6 to 1.0 (which is all water).

The expected droplet diameter also covered a wide range, from 1 to 10 microns (3.9×10^{-5} to 3.9×10^{-4} in.) in Alger's investigation to large droplets of 1270 microns (0.050 in.) in Elliot and Weinberg's MHD investigation. Analytically, Alger showed that a large increase in the efficiency of a total-flow impulse turbine occurs when the droplet size is decreased because if the droplets are too large, they do not follow the vapor streamlines within the turbine blade passages and collide with the turbine walls, thereby resulting in reduced momentum exchange and liquid film pumping losses. However, in the separating type of two-phase turbine, smaller droplets can adversely affect the separation efficiency, because these smaller droplets are more difficult to separate from the gas in a centrifugal field.

Analytically, Elliot and Hays (Ref. 15) reviewed two-phase nozzles and turbines for the power turbine application, such as marine propulsion. Here, the nozzle inlet conditions for the mixture of steam and polyphenyl ether (which is a vacuum pump oil) were 327 C (620 F) and 100 bar (1450 psia), and the expected drop size approximately 25 microns (9.8×10^{-4} in.). In a related investigation (Ref. 18) for a bottoming cycle, the design conditions at the nozzle inlet were 349C (660 F) and 163 bar (2365 psia) for mixture of steam and Dowtherm A. As a point of reference, the critical point of steam is 392 C (705 F), above which point there is no phase change from a liquid to a vapor and the steam would act increasingly as a heavy liquid, thereby losing the acceleration effects of the compressible gas.

The ranges of the governing flow parameters for a two-phase nozzle to be used in a two-phase turbine can be estimated as follows. If a mixture of steam and heat transfer oil is selected as the working fluid, then the maximum working temperature will be about 370 C (700 F), because the heat transfer oil will begin to decompose at higher temperatures according to the manufacturer's data, and because the critical temperature of steam is 392 C (705 F). Hence, the inlet temperature will be in the vicinity of 316 C (600 F). As to the exit temperature, because of the anticipated high loading ratios, the equilibrium exit temperature of the mixture will be only slightly lower than the inlet temperature. The homogeneous flow model can be used to show this, as indicated by the results in Fig. I.2 for typical mixtures of steam and Dowtherm A at 316 C (600 F) and two pressure levels, 96.6 and 69 bars (1400 and 1000 psia). Here, the effect of loading ratio on the temperature drop of a homogeneous two-phase mixture expanding through a converging-diverging nozzle is shown, at two typical values of pressure ratio. For loading ratios larger than 10, the temperature drop of the homogeneous mixture is less than 3 percent at an expansion ratio of 2, and less than 9 percent at a ratio of 10. Hence, the homogeneous temperature will be nearly isothermal at some of the conditions of interest.

In actuality, however, heat transfer is a rate process, and the droplet size will also have a large effect on whether the expansion is nearly isothermal because the droplet size will affect both the value of the heat transfer coefficient between the gas and the droplet and the amount of heat transfer area of the droplet, as will be seen later. Fig. I.3 is a Temperature-Entropy diagram of the cycle paths for one-phase and two-phase turbines. As indicated by the cycle path above the cross-hatched area, the use of a two-phase nozzle can result in an expansion that is nearly isothermal, because the liquid acts as a heat source for the expanding gas (which otherwise would be cooled in a single-phase expansion). This heat transfer produces additional work which can be extracted by the two-phase turbine as represented by the heat in the integral of TdS shown as the cross-hatched area in Fig. I.3. The saturation pressure of steam at 316 C (600 F) is 107 bar (1550 psi), and hence, the nozzle inlet pressure should be established at this level so the area enclosed by the Temperature-Entropy diagram (as shown schematically in Fig. I.3 for the entire cycle) will be large. The exit pressure should be as low as possible so that the conversion of enthalpy to kinetic energy will be as large as possible. The condensing temperature will be typically 43 C (100 F), where the saturation pressure for steam is 0.088 bar (1.27 psia). Hence the nozzle exit pressure must be higher than that to allow for pressure drops through the system, and will be in the area of 1 bar (14.5 psia), which is low enough for nozzle expansion and yet high enough to allow for pressure in the flow path to the condenser.

Based on work by Elliot and Hays (Ref. 15), the loading ratio ($\dot{m}_\ell/\dot{m}_g$) of the nozzle will range from about 10 to 50. At a loading ratio of 50, the speed of the two-phase turbine will be about one-third that of the all-gas turbine, with only a slight drop in cycle efficiency. Larger values of the loading ratio result in a significant drop in cycle efficiency. At the other end, a loading ratio of 10 is near the lower limit, because ratios lower than that result in turbine speeds that approach the all-gas turbine speed, and the low-speed advantage of a two-phase turbine would then be lost.

The expected droplet size can be deduced from the Weber number droplet breakup criterion. Fig. I.4 shows calculated results for the diameter of droplets of Dowtherm A in steam as a function of steam velocity, when the maximum Weber number is equal to 6. (The Weber number is a dimensionless criterion which is the ratio of the aerodynamic pressure forces which are trying to deform and fragment the droplet and the surface tension forces which are trying to maintain the droplet in spherical form. The critical value of the Weber number is experimentally determined.) At the nozzle inlet where the gas (steam) velocity will be approximately 30.5 m/sec (100 ft/sec) and droplet velocities will be in the range of 18.3 to 24.4 m/sec (60 to 80 ft/sec), the expected drop size will be in the range of 50 to 180 microns (0.002 to 0.007 in.).

I.2.2 Liquid/Gas Combinations

A liquid/gas combination suitable for each two-phase nozzle application must be selected. In general, there are two types of two-phase liquid/gas flows. If the gas phase is the vapor of the liquid phase, then the flow is "one-component" flow, and an example of this type is steam and water flow. If the gas phase is of a different chemical species than that of the liquid, then the flow is "two-component" flow, and an example of this would be a mixture of steam and an organic liquid with a low vapor pressure. The expansion of a one-component system occurs along the saturation line, while the expansion of a two-component, system can be nearly isothermal if the loading ratio is high enough. A nearly isothermal expansion is advantageous for a two-phase nozzle in a two-phase turbine. For a two-component system, the main factors in the selection of the liquid are sufficiently high density, low vapor pressure, and inertness, while the main requirements for the gas are immiscibility with the liquid and a reasonable condensing pressure. This pressure must not be so low as to require a huge nozzle exit area, and not be so high as to require high nozzle exit area.

For many applications, the liquid/gas combination is an inherent characteristic of that application: the steam/brine mixture for the geothermal application because the thermal energy is already contained in that mixture, or the air/water mixture for thrust augmentation in marine propulsion because air is the working fluid of the gas turbine and water is both suitable and inexpensive for this open-cycle process. The MHD power generation application requires high working temperatures in the vicinity of 982 C (1800 F), which means that all working fluids except for the liquid metals are ruled out. Here, the liquid/gas combination of greatest interest (Ref. 8) is the two-component system of liquid lithium and cesium vapor, but a one-component system of potassium and potassium vapor is also of interest for MHD. Another application of two-phase nozzles (Ref. 7) is that of jet pumps (with no moving parts) for rocket engines. Here, a non-condensible gas (such as hydrazine decomposition products) is used to pump a liquid propellant (such as nitric acid, hydrogen peroxide, JP-5 jet fuel, or hydrazine, etc).

Recently, Ahmad and Hays (Ref. 18) have studied the use of a two-phase turbine for a diesel bottoming cycle. The nozzle inlet temperature is 349 C (660 F), and after an extensive cycle study, a mixture of Dowtherm A and steam was chosen as the liquid/gas combination. The use of a liquid with a lower specific heat than Dowtherm A would mean a higher loading ratio and hence a lower nozzle exit velocity, but the fluid with the lowest specific heat that they found was a "Therminol" fluid, which may have toxicity problems. The thermophysical properties (vapor pressure, specific heat, density, viscosity, and thermal conductivity) are tabulated as a function of temperature in Ref. 16 for 11 fluids of potential interest for an application at the 316 C (600 F) level. Included among these fluids are 3 kinds of Therminol, 2 kinds of Dowtherm, and

2 kinds of DowCorning fluids. (Another fluid of possible interest is polyphenyl ether, and three chemical firms were contacted: Union Carbide does not make it, Dow Chemical stopped making it 20 years ago, but Monsanto does make it for use in vacuum diffusion pumps and sells it for approximately $1000/gal.) These same eleven fluids are also of interest in the marine propulsion application because the range of operating temperatures is similar.

Two-phase turbines are being considered (Ref. 15) for marine and automotive propulsion applications because of their low-speed characteristics which result in reduced gearbox requirements. High-temperature synthetic, organic heat-transfer oils (such as the Dowtherm family) seem to offer the most advantages as the liquid for this application where steam would be the gas phase. These oils have a density only about 15 percent less than that of water and a very low vapor pressure. Their specific heat is in the range of 0.5 cal/gm-C (0.5 BTU/lbm-F) which means that the liquid flow rate (and hence the loading ratio) will be high enough to result in a reasonably low nozzle exit (or spouting) velocity. Further, most of these oils are inert and have a low level of toxicity. For the gas phase, water is a well-known working fluid which has a reasonable vapor pressure characteristic, and is immiscible with the heat transfer oils under consideration for the liquid phase. In general, fluorocarbons are not suitable for use as the gas phase for three reasons. First, as seen in Fig. I-5, their vapor pressures are significantly higher than that of water at the same pressure. Second, as also seen in Fig. I.5, their critical temperatures are significantly lower than that of water, which means that if operating above the critical temperature, compressibility effects in accelerating the mixture would be lost because the fluorocarbon would behave essentially as a heavy liquid. Third, these fluorocarbons decompose (into toxic substances) at temperatures above 177 C (350 F), and this decomposition is only aggravated by the presence of foreign substances such as water or oils.

I.3 Classification of Flow Domains With Available Theory

The flow domains considered and the theories used in previous investigations of two-phase nozzles were examined for their usefulness in classifying and correlating flow domains. Single-phase (or homogeneous) theory was reviewed from the viewpoint of energy conversion in a nozzle and was compared to models with separate phases in terms of their applicability to these flow domains. Gas dynamic aspects of two-phase nozzle flows were examined in terms of the speed of sound in a two-phase mixture and of choked flow at the nozzle throat.

I.3.1 Single-Phase Nozzle Theory

For some operating conditions of two-phase nozzles, the flow regime will be dispersed flow, where the liquid phase is in the form of uniformly dispersed,

small-diameter droplets suspended in the gas. In many ways, the behavior of droplets suspended in a gas is similar to the behavior of bubbly flow where the small bubbles are suspended in the liquid. In bubbly flow, most of the inertia is in the liquid phase, and the drag forces on the gas bubbles are large relative to the momentum forces. As a result, the bubbles follow the forced convection motion of the surrounding liquid very closely. For dispersed flow where the situation is reversed with the liquid droplets suspended in the gas, the momentum forces are much larger than the drag forces, and the droplets do not adjust to the flow of the surrounding gas as fast. For this reason, homogeneous flow models are not expected to describe the situation that obtains in dispersed flow as well as in bubbly flow, but useful understanding of the basic flow processes can still be obtained from a homogeneous model.

The theory for single-phase incompressible flow is valid for two cases. The first case is when the nozzle exit pressure is only slightly less than the inlet pressure and the flow (either gas or liquid) can then be treated as incompressible because density effects are negligible. The second case is when the flow is all liquid (which corresponds to a loading ratio of infinity), and there are no compressibility effects. Essentially, the continuity equation is then used to calculate nozzle performance, as there is no pressure effect and only a small temperature effect on liquid density. If the flow were mostly liquid with only a few small bubbles, then the flow would be expected to behave as a liquid with only small compressibility effects.

At the other extreme where the single-plase flow is all gas (and the loading ratio is zero), the classical isentropic compressible gas theory (Ref. 2), describes the flow situation. For the flow situations between the all-liquid and the all-gas flows, single-phase isentropic theory has been developed to describe the liquid/gas mixture in terms of average properties, assuming thermal equilibrium ($T_\ell = T_g$) and no velocity slip ($V_\ell = V_g$). The main influences on the behavior of such a mixture are the compressibility of the gas phase and the inertia of the liquid. This theory (called the homogeneous flow theory and given in Ref. 23, for example) treats the liquid/gas mixture as a pseudo gas which is then shown to obey the well-known one-dimensional flow relationships of classical gas dynamics. The isentropic expansion exponent of the mixture, Γ, is:

$$\Gamma = \gamma_g \left[\frac{1 + r\delta}{1 + \gamma_g r\delta} \right] \qquad (I.1)$$

where γ_g is the isentropic expansion exponent of the pure gas, r is the loading ratio ($\dot{m}_\ell/\dot{m}_g$), and δ is the ratio of the specific heat of the

liquid to the specific heat of the gas at constant pressure (C/C_{pg}). For the all-liquid extreme, the loading ratio (η) is infinite and $\Gamma = 1$. At the all-gas extreme, the loading ratio is zero and $\Gamma = \gamma_g$. Then the temperature and density after an isentropic expansion are given by the expressions:

$$\frac{T}{T_o} = \left(\frac{P}{P_o}\right)^{\frac{\Gamma-1}{\Gamma}} \quad ; \quad \frac{\rho}{\rho_o} = \left(\frac{P}{P_o}\right)^{1/\Gamma} \tag{I.2}$$

where the subscript zero refers to nozzle reservoir (or inlet) conditions. This expression for temperature in an isentropic expansion was used to obtain the results shown earlier in Fig. I-2. The nozzle exit velocity, V_2, is given by the expression:

$$V_2 = \sqrt{\left(\frac{2\Gamma}{\Gamma-1}\right)\left(\frac{R_g T_o}{1+r}\right)\left[1 - \left(\frac{P}{P_o}\right)^{\frac{\Gamma-1}{\Gamma}}\right]} \tag{I.3}$$

where R_g is the gas constant of the pure gas. An expression for the momentum flux at the nozzle exit can be obtained using continuity and the above expressions for the nozzle exit velocity and density:

$$\frac{\dot{m}V_2}{A} = \rho_g\Big)_o \; 2RT_o \left(\frac{\Gamma}{\Gamma-1}\right)\left[1 - \left(\frac{P}{P_o}\right)^{\frac{\Gamma-1}{\Gamma}}\right]\left(\frac{P}{P_o}\right)^{1/\Gamma} \tag{I.4}$$

Results calculated from these expressions for exit velocity and momentum flux for mixtures of steam and Dowtherm A are shown in Fig. I.6 as a function of the loading ratio. Several observations can be made from these results. First, the all-gas flow corresponds to a loading ratio of zero, while the all-liquid extreme is approached as $r \to \infty$. Second, the momentum flux is nearly independent of loading ratio, because the amount of enthalpy converted into kinetic energy (in the form of momentum) is essentially fixed by the expansion ratio. Third, as the loading ratio increases, the nozzle exit velocity decreases. Again, this is expected because the momentum flux is nearly constant, and the density of the homogeneous two-phase mixture is increasing as the loading ratio is increased.

I.3.2 Comparison of Homogeneous Model With Separate-Phase Models

A flow model with partially separate phases was developed by Rudinger (Ref. 4) when he extended Kliegel's constant-fractional-lag model (Ref. 3) to include the effect of the particle volume fraction. Using the equations of continuity, momentum, energy, and the heat balance on a particle (or droplet),

a model was developed and computerized numerical solutions were obtained. But these solutions indicated that the gas and particle temperatures remained substantially constant throughout the nozzle over a wide range of operating conditions of interest. With the assumption of isothermal flow ($T_\ell = T_g = T_o$), then the energy and the heat balance equations are eliminated, and a particularly simple result is obtained for the gas velocity in the nozzle as a function of pressure:

$$V_{g2}^2 = V_g)_o^2 + \frac{2R_g T_o}{1+rK}\left[\ln\left(\frac{P_o}{P}\right) + \frac{\epsilon_o}{1-\epsilon_o}\left(1-\frac{P}{P_o}\right)\right] \qquad (I.5)$$

where K is the velocity lag ($K \equiv V_\ell/V_g$), and ϵ is the particle volume fraction. The subscript zero refers to inlet or reservoir conditions. For the special case when no particles (or droplets) are present in the flow, both the loading ratio (r) and the inlet particle volume fraction (e_o) are zero, and the isothermal solution of Eq. I.5 reduces to:

$$V_{g2}^2 = 2R_g T_o \ln\frac{P_o}{P} \qquad (I.5a)$$

if the inlet velocity is zero. For steam at 260 C (500 F), the calculated exit velocity from Eq. I.5a for an isothermal expansion is 502 m/sec (1646 ft/sec) at an expansion ratio (P_o/P) of 1.66, and 1066 m/sec (3496 ft/sec) when P_o/P is 10. In contrast, for the isentropic expansion of pure steam (in the absence of liquid oil droplets), the homogeneous model of Eq. I.3 yields an exit velocity of 488 m/sec (1599 ft/sec) at an expansion ratio of 1.66, and 939 m/sec (3079 ft/sec) when P_o/P is 10. Hence, the isothermal model for pure steam predicts nozzle exit velocities that are 5 to 10 percent higher than the homogeneous model. Continuity considerations would lead one to expect a higher velocity for the isothermal case where the temperature is higher (and hence the gas density is lower at the same pressure). For the isothermal model, expressions for the other variables are:

$$\frac{\epsilon}{1-\epsilon} = \frac{\epsilon_o}{1-\epsilon_o}\frac{P}{P_o} \qquad (I.6)$$

and

$$\frac{A}{A_o} = \frac{V_g)_o P_o}{V_g P}\left(\frac{1-\epsilon_o}{1-\epsilon}\right) \qquad (I.7)$$

By using the continuity equations of the gas and of the liquid, the following relationship between the local values of the flow variables can be obtained:

$$r = \frac{\varepsilon}{1-\varepsilon} \frac{\rho_\ell}{\rho_g} \frac{V_\ell}{V_g} \qquad (I.8)$$

The numerical relationship between the variables of Eq. I.8 is shown in Fig. I.7. For example, mixtures of saturated steam and Dowtherm A at 260 C (500 F) and 46.9 bar (680 psia) have a density ratio (ρ_ℓ/ρ_g) of approximately 36. Thus, for a loading ratio of 20 (that could be typical for a marine propulsion application), the particle volume fraction is over 0.40 for the slip ratio in a typical range of 0.6 to 0.8. In other words, the gas volume accounts for under 40 percent of the total volume at these operating conditions.

Rudinger's analytical results (Eqns. I.5, I.6, and I.7) for the isothermal case can be used to calculate nozzle parameters. Fig. I.8 shows typical results for gas velocity, dimensionless nozzle area, and the particle volume fraction as a function of pressure (and hence axial distance) through the nozzle, for the expansion of a two-phase mixture of air (with a molecular weight (MW) of 28) and a liquid with an inlet particle volume fraction of 0.2 and an inlet temperature of 260 C (500 F). As seen by inspecting Eq. I.5, the only quantity which is a function of the specific liquid/gas combination is the gas constant. Hence, only the molecular weight of the gas need be specified to use Eq. I.5, and the results are independent of the liquid phase. If steam were the gas (MW = 18) at the same pressure level, then the velocities would be higher, and the required flow areas through the nozzle would be smaller fractions of the inlet area to pass the same flow rate, as deduced from Eq. I.7. In other words, a nozzle for a steam/liquid flow would be relatively more constricted at the throat than that for an air/liquid nozzle. For these constant-fractional-lag nozzles, the droplet velocities in this example are 60 percent of the local gas velocities in the nozzle.

Equation I.5 can be used to determine the effect of particle volume fraction on the gas exit velocity, as compared to the case when $\varepsilon_o = 0$ (the all-gas case), and Fig. I.9 shows the results. For values of ε_o less than 10 percent, the increase in calculated gas velocity is less than 4 percent when the effect of ε_o is included. At larger values of ε_o, however, the effect is not negligible. For example, at $\varepsilon_o = 0.4$, the increase in gas velocity is 12 percent when the pressure ratio (P_o/P) is 10.

The pressure ratio at the nozzle throat can be obtained analytically by determining the point at which the derivative of throat area with respect to pressure ratio goes to zero. When this is done, the effect of inlet particle volume fraction (ε_o) on the throat pressure ratio (P_t/P_o) can be estimated with the isothermal model, and Fig. I.10 shows calculated results of this effect. For the all-gas case ($\varepsilon_o = 0$), the throat pressure ratio is 0.607,

and as the inlet particle volume fraction is increased, the throat pressure ratio decreases from the all-gas value. For models which neglect the particle volume fraction, the predicted throat pressure ratio is simply 0.607. For example, at $\epsilon_o = 0.4$, the throat pressure ratio from this isothermal model is approximately 0.54.

Calculated results from the homogeneous and the separate-phase models can be compared with each other, and Fig. I.11 shows calculated results for gas and liquid velocities as a function of exit pressure from three different models for a two-phase mixture of nitrogen and water with inlet conditions of 10.3 bar (150 psia) and 10 C (60 F) expanding through a converging-diverging nozzle at a loading ratio of 40. These conditions were selected because Elliot and Weinberg (Ref. 8) present results for these conditions from their computerized comprehensive model which includes the effects of velocity slip, temperature difference between the phases, and droplet breakup. Results for the mixture velocity from the homogeneous model are shown. Because the value of the loading ratio is 40, the velocity of the mixture is essentially that of the liquid. Also shown are calculated results from Rudinger's isothermal model, at two values of the velocity ratio (V_ℓ/V_g): 0.71 and 1.0. Rudinger's model can be considered as partially separated, because slip is included. The value of 0.71 was selected because it is characteristic of the velocity ratio over most of the length of the nozzle of Elliott and Weinberg. The calculated gas and liquid velocities from Elliott and Weinberg's model are shown as triangles. The estimates for the gas and liquid velocities from Rudinger's isothermal model at $V_\ell/V_g = 0.71$ coincide closely with the corresponding results from Elliott and Weinberg's comprehensive model, and the prediction from the homogeneous model agrees well with the liquid predictions of the other two models.

Results calculated from the homogeneous model and Rudinger's model are shown in Fig. I.12 for expansion of a steam/Dowtherm A mixture with typical inlet conditions and a loading ratio of 40. (Predictions from Elliott and Weinberg's model are not shown because a listing of their comprehensive computerized code is not available in the open literature.) For these conditions at an exit pressure of $P/P_o = 0.2$, the homogeneous model predicts velocities about 16 percent lower than the liquid velocity from the isothermal model at a slip ratio of 0.8.

Figure I.13 is a comparison of the momentum flux at the nozzle exit as calculated with the homogeneous theory (Eq. I.4) and with Rudinger's isothermal theory. The total momentum of the two-phase mixture is the sum of the momentums of the gas and liquid streams, and the momentum flux is the total momentum divided by the flow area. With this definition and the equation of continuity, the momentum flux can be shown to be:

$$\left.\frac{\Sigma \text{ Mom}}{A}\right]_{\text{exit}} = \left[\rho_\ell V_\ell^2 \left(\frac{1 + \frac{1}{rK}}{1 + \frac{K\rho_\ell}{r\rho_g}}\right)\right]_{\text{exit}} \qquad \text{(I.9)}$$

Now, $V_\ell = KV_g$, and the gas exit velocity for the isothermal model can be calculated with Eq. I.5 as a function of the selected operating conditions. As seen in Fig. I.13, the iosthermal model predicts higher momentum fluxes at loading ratios larger than approximately 5 at the operating conditions typical for the marine propulsion application.

An estimate of the effects of the heat transfer rate process on the temperature difference between the liquid and the gas as the gas expands through the nozzle can be made using a simple model. Heat transfer is a rate process, and the residence time determines the quantity of heat transferred. For heat transfer to occur between the liquid and the gas, there must be a temperature difference. Even if the liquid and the gas enter the nozzle at the same temperature, the temperature of the gas will drop relative to the liquid as the gas expands, thereby creating the temperature differential which is the driving force for heat transfer. To make numerical estimates, some approximations can be made: as the liquid and gas flow along an axial increment through the nozzle, assume that the liquid temperature is constant over this increment, and that the gas temperature drops according to an (adiabatic) isentropic expansion. Then, for this small axial increment, the amount of heat transfer from the gas to the liquid can be calculated, and the temperatures of the gas and the liquid can be adjusted at the end of this increment to account for this heat transfer. With these assumptions and for an assumed pressure drop over the axial increment, the gas temperature at the end of the increment can be calculated with the classical isentropic expression:

$$T_g)_{out} = T_g)_{in} \left(\frac{P}{P_{in}}\right)^{\frac{\Gamma-1}{\Gamma}} \qquad (I.10)$$

Figure I.14 depicts the model, where the star conditions reflect the temperatures as adjusted at the end of the increment for heat transfer. The heat balance on a liquid droplet is:

$$Q_{drop} = mC\left[T_\ell)_{in} - T_\ell)^*_{out}\right] = \left(hA_h\Delta T_{\ell-g}\right)\Delta t \qquad (I.11)$$

where m is the mass of the droplet, C is its specific heat, h is the heat transfer coefficient between the droplet and the gas, A_h is the heat transfer surface area of the droplet, $\Delta T_{\ell-g}$ is the average temperature differential between the liquid and the gas, and Δt is the residence time of the droplet in the axial increment ($\Delta t = \Delta X/V_\ell$). The value of $\Delta T_{\ell-g}$ can be estimated simply as:

$$\Delta T_{\ell-g} = T_\ell)_{in} - \frac{1}{2}\left[T_g)_{in} + T_g)_{out}\right] \qquad (I.12)$$

For relative droplet Reynolds numbers in the range of $25 < Re_{Rel} < 100{,}000$, the heat transfer coefficient can be estimated with the relation (as recommended in Ref. 19):

$$\frac{hD}{k_g} = 0.37\ Re_{Rel}^{0.6} \qquad (I.13)$$

The mass of the droplet is $\rho_\ell \cdot$ Vol, and for spherical droplets, $Vol/A_h = D$. Hence the value of $T_\ell)^*_{out}$ can be calculated from Eq. I.11. The value of the gas exit temperature $T_g)^*$, adjusted from the isentropic value to account for heat transfer, can be calculated from a heat balance on the liquid and the gas:

$$m_\ell C \left[T_\ell)_{in} - T_\ell)^*\right] = m_g C_{pg} \left[T_g)^*_{out} - T_g)_{out}\right] \qquad (I.14)$$

The ratio of the mass of liquid droplets (m_ℓ) to the mass of gas (m_g) in the axial increment is simply equal to the loading ratio, r. Hence, Eq. I.14 reduces to:

$$T_g)^*_{out} = T_g)_{out} + r\,\frac{C}{Cpg}\left[T_\ell)_{in} - T_\ell)_{out}\right] \qquad (I.15)$$

and the adjusted gas exit temperature can be calculated. This simplified model was used to estimate the effect of the heat transfer rate process on the temperature difference between the liquid and gas at typical operating conditions. Fig. I.15 shows such estimates for mixtures of steam and Dowtherm A at an inlet temperature of 260 C (500 F) as a function of loading ratio, droplet diameter, and velocity level at a slip ratio (V_ℓ/V_g) of 0.8. The temperature of 247.1 C (476.9 F) occurs when steam is expanded over a pressure of $P/P_o = 0.9$. Three factors can cause the gas temperature in the nozzle to approach that of the liquid: first, a decrease in drop diameter, because the heat transfer coefficient and the volumetric heat transfer area both increase; second, an increase in loading ratio, because the amount of gas relative to the amount of liquid is reduced; and third, a decrease in velocity, because the residence time increases faster than the heat transfer coefficient decreases. Actually, the model is over-simplified in that it does not predict the asymptote of 960 R as the loading ratio is increased and the asymptote must be faired in, but the model does indicate the conditions at which the heat transfer rate can have an effect on nozzle performance. Fig. I.16 shows calculations from the model when the inlet temperature of the Dowtherm A is 56 C (100 F) above the steam inlet temperature, and the same trends occur as in Fig. I.15. this simplified heat transfer model indicates the conditions under which the flow is likely to be isothermal and hence under which the isothermal theory is valid.

I.3.3 Gas Dynamics Aspects

Gas dynamics aspects of nozzle flow were examined in terms of the speed of sound in a two-phase mixture and choked flow at the nozzle throat. The change in operating conditions at one point in a flow system is telegraphed to other points by pressure waves which travel at the speed of sound and result in the necessary flow adjustments. If thermodynamic equilibrium (temperature, pressure, and kinetic equilibrium) between phases is assumed for a homogeneous two-phase mixture, then the sonic velocity can be defined as the square root of the isentropic gradient of the pressure with respect to density, as in the case of the classical gas dynamics theory. With this definition, the two-phase choking velocity is always lower than the choking velocity of the pure saturated vapor at the same temperature and pressure. Rudinger (Ref. 20) has shown that the equilibrium speed of sound a_e in the mixture relative to that of the pure vapor a_o is:

$$\frac{a_e}{a_o} = \left[\frac{1+r\delta}{(1+r)\ (1+\gamma r\delta)}\right]^{1/2} \left(1 + \frac{r\rho_g}{\rho_\ell}\right) \qquad \text{(I.16)}$$

where the last term accounts for the finite droplet volume fraction at high values of the loading ratio. Fig. I.17 shows typical results from Eq. I.16 for a mixture of saturated steam and Dowtherm A at 260 c (500 F). The two-phase-mixture speed of sound reaches a minimum of 0.29 a_o, at a loading ratio of approximately 20. The value of a_o at 260 C (500 F) is 566 m/sec (1857 ft/sec), so the choked velocity of a homogeneous mixture is 164 m/sec (539 ft/sec) in the nozzle throat. As seen earlier in Fig. 1.7, the inlet particle volume fraction for this mixture is expected to be between 0.4 and 0.48 at a loading ratio of 20. Hence, from Fig. 1.10, the throat pressure ratio (P_t/P_o) is between 0.52 and 0.54 for this range of inlet particle volume fractions. From Fig. I.17, for a pressure ratio in this range, the isothermal model predicts a gas velocity of between 137 and 140 m/sec (450 and 460 ft/sec), at a slip ratio (V_ℓ/V_g) of 0.8. At this same pressure ratio, the homogeneous model predicts a velocity of between 85 and 88 m/sec (280 and 290 ft/sec). These estimates suggest that the mixture velocity at the nozzle throat at these operating conditions is below the choked flow velocity.

Comfort and Crowe (Ref. 21) investigated the effect of droplet size on shock characteristics of a steam/water flow in a converging-diverging nozzle. As the droplet size is reduced, the mixture behaves as a continuum and sharp velocity discontinuities occur at velocities above the two-phase choking velocity but below the vapor sonic velocity. Analytically, for their conditions and droplet diameters below about 2 microns (7.8×10^{-5} in.), then the mixture

behaves as a continuum, and the shock conditions can be carried upstream because the sonic velocity is higher than the actual gas velocity. For larger droplet diameters, the change in velocity is very gradual, without discontinuity as the mixture no longer behaves as a continuum. Because the mass fraction of the dispersed liquid droplets strongly affects the choking velocity, relatively low-velocity flows can be supersonic with respect to the homogeneous two-phase choking velocity. At another operating condition, where the gas velocity is above the vapor sonic velocity, Comfort and Crowe calculated that the maximum isentropic velocity (of the vapor) in the diverging section of their nozzle with steam/water flow would be approximately Mach 1.2 relative to the vapor sonic velocity and Mach 3.3 relative to the two-phase choking velocity for a homogeneous-mixture model. Here the droplet size has little effect on the sharpness of the shock, because the shock is not felt upstream when the gas velocity is above the vapor sonic velocity. Hence, unless the droplets are very small or unless the gas velocity is above the vapor sonic velocity, the flow disturbance is very gradual and the sharp discontinuities of classical gas dynamics are not expected. Rudinger (Ref. 22) has shown that the distance that a droplet travels while achieving velocity and temperature equilibrium with the gas is orders of magnitude larger than the distance for shock transition in a pure gas, and this is the reason why flow disturbances attributable to shock conditions in a two-phase mixture can often be just gradual changes in flow conditions.

I.3.4 Correlation of Nozzle Flow Domains

The various nozzle flow domains were correlated and their physical characteristics were identified in terms of the governing flow parameters. For many of the two-phase-nozzle flow conditions, the flow regime will be that of dispersed flow, where the liquid phase is in the form of uniformly dispersed, small-diameter droplets. Dispersed flow through the nozzle is desirable, because uniformly dispersed small droplets result in enhanced heat transfer between the liquid and the gas phases as the droplet heat transfer coefficient and the volumetric heat transfer surface area both increase as the droplet diameter is reduced. The assumption of a homogeneous flow model implies small droplets uniformly dispersed over the cross-section of the flow area and in thermal equilibrium with the gas. In the limit, if the diameter of the droplets and their average spacing are both small as compared to the nozzle throat diameter, then the mixture begins to behave as a continuum. At a given loading, as the number of droplets is reduced, then the flow field becomes less uniform, and the limit is one droplet where it is apparent that the homogeneous theory no longer applies. The assumption of homogeneous flow conditions is sometimes made even though the flow is not homogeneous, because useful results can be obtained from the homogeneous flow model. The approximation of the homogeneous model can only be applied to flow situations where the two phases are well mixed, and this condition excludes such flow regimes

as slug, annular, or stratified flows. And the presence of any one of these flow regimes would suggest poor nozzle design in the first place, as their presence would negate the advantages of dispersed flow. Based on the work by Comfort and Crowe (Ref. 21) that was discussed above in Section I.3.3, however, the droplet size at which the mixture really behaves as a continuum in terms of shock characteristics is very small, on the order of less than 5 microns (2×10^{-4} in.) in diameter. With reference to the Weber number droplet breakup criterion shown in Fig. I.4, this size droplet would be expected at gas velocities higher than approximately 180 m/sec (600 ft/sec), and this velocity would probably exist near the exit of many two-phase nozzles. Even though truly homogeneous conditions may not obtain throughout the nozzle, the temperature and/or velocity of the two phases may be in sufficient equilibrium so that results from the homogeneous model could still be useful for examining many nozzle applications.

As indicated by the results obtained from the simplified heat transfer model of Fig. I.14, the two-phase flow becomes increasingly isothermal as the droplet size is reduced (because the heat transfer rate is increased) and as the loading ratio is increased (because the increased amount of liquid relative to the gas is a source of heat). As typified by the results in Fig. I.2, the homogeneous theory, with infinite heat transfer, indicates the values of the loading ratio at which isothermal conditions can be approached (depending on the droplet diameter), but the homogeneous model does not account for the fact that heat transfer is a rate process which requires residence time. For flow conditions which do lead to isothermal flow, however, Rudinger's isothermal model is applicable and still allows for slip between the liquid and the gas.

An indication of the degree of velocity slip can be obtained by looking at the relaxation time for the particle velocity, τ_v, which is a qualitative measure of the time to achieve velocity equilibrium between the gas and the droplet. Consider the motion of a single droplet in a gas flow, and assume that Stokes drag is valid. Equate the drag of the gas with constant velocity, V_g, to the droplet acceleration:

$$\frac{dV_\ell}{dt} = \frac{18\mu_g}{D^2\rho_\ell}\left(V_g - V_\ell\right) \qquad \text{(I.17)}$$

The solution to this simplified equation is:

$$\frac{V_g - V_\ell}{V_g - V_\ell)_o} = e^{-t/\tau_v} \qquad \text{(I.18)}$$

where $V_\ell)_o$ is the initial velocity at time zero, and τ_v is the relaxation time for the particle velocity:

$$\tau_v = \frac{D^2 \rho_\ell}{18\mu_g} \qquad (I.19)$$

Now, the residence time of the mixture with average gas velocity, $V_g)_{ave}$, in the nozzle of length L is: $t_{res} = L/V_g)_{ave}$

Hence a dimensionless residence time can be formed by the ratio:

$$\frac{t_{res}}{\tau_v} = \frac{L}{V_g)_{ave}} \frac{18\mu_g}{D^2 \rho_\ell} \qquad (I.20)$$

When the residence time is large compared to the velocity relaxation time, then velocity equilibrium between the gas the the liquid can be expected. Fig. I.18 shows Eq. I.20 plotted for typical conditions of a steam/Dowtherm A mixture. Several trends can be observed: the direction of increasing velocity equilibrium is smaller droplet diameter, lower gas velocities, and longer nozzles, with droplet diameter being the single most important factor. For example, with a 0.15-m (6-inch) long nozzle and an average gas velocity of 152 m/sec (500 ft/sec), the droplet diameter would have to be less than 12.5 microns (0.0005 inches) to approach conditions of velocity equilibrium between the gas and the droplet.

I.4 Formulation of Working Theory For Two-Phase Nozzles

The objective of this task was to formulate a working theory of two-phase nozzle flow based on considerations of the governing flow parameters and the flow domains. The theory had to be in a form suitable for parametric analyses and optimization of two-phase flow nozzles. Two simplified models have been developed and computerized: an Isothermal Model which is valid only for certain operating conditions; and a Model with Droplet Heat Transfer which is a more general model and is valid for a wide range of operating conditions since it includes the effects of heat transfer between the liquid droplets and the gas phase. Both models include the interphase effects of velocity slip and droplet breakup.

Both models assume a two-component, two-phase mixture, where the liquid phase is in the form of droplets. One-dimensional flow, with variables changing only in the axial flow direction of the nozzle, was selected so

both the model and the results will be tractable in terms of parametric analysis and optimization of nozzles. A two-component mixture was chosen for the marine propulsion application because the expansion of a two-component system can be nearly isothermal (depending on the loading ratio) when compared with a one-component system which expands along its saturation vapor line. As discussed in Section 1.2.1, more area is enclosed by the integral of TdS (Fig. I.3) when the expansion is nearly isothermal than when an adiabatic, one-component expansion is experienced.

Numerical marching-type solutions have been selected for both models because closed-form analytical solutions are possible only for certain simplified situations as discussed in Section I.3. In computing the solutions, the nozzle is divided into numerous small axial segments of equal length, and the flow conditions at the exit of each segment are calculated from the governing flow equations and the upstream flow conditions at the inlet of that axial segment. The exit flow conditions of a given segment then become the inlet flow conditions for the adjacent downstream segment, hence the description, "marching-type" solution, as the calculations proceed from one segment to the next downstream segment. A six-inch-long nozzle, for example, could be divided into 1000 segments, each 0.006 in. long (which could be larger than the droplet diameter for many flow conditions). Care must be shown to select enough segments so that the equations are numerically stable.

In the *Model with Droplet Heat Transfer*, the variations of the thermophysical properties of the gas and the liquid with temperature and/or pressure along the nozzle are included in the marching-type solution by recalculating the value of the property for the local temperature or pressure at each segment. In the Isothermal Model, the thermophysical properties are not temperature-dependent because the flow is assumed as isothermal.

I.4.1 Isothermal Model

In the Isothermal Model, the assumption is made that the liquid and gas temperatures are equal and constant throughout the nozzle ($T_\ell = T_g = T_{in}$). This assumption implies that the heat transfer rate between the liquid droplets and the gas phase is very high and that the liquid droplets act as a heat source so that the gas temperature does not decrease as the gas expands through the nozzle. This assumption means that the Isothermal Model is suitable only for certain operating conditions, such as very small droplet size and high values of the loading ratio ($\dot{m}_\ell/\dot{m}_g$). For the isothermal situation to occur even in theory, it would require either an internal heat source, or an external heat input, for the expansion of the two-phase mixture in the nozzle to be isothermal.

In addition to the Isothermal Model being valid for certain operating conditions, this model serves as a useful adjunct to a model that does account for finite droplet heat transfer, that is, it is useful because the calculated results from its momentum equations can be compared with the results from the analytical isothermal model of Rudinger (Ref. 4).

The following four basic equations describe the isothermal one-dimensional, two-phase nozzle flow:

Continuity
Momentum
Droplet Drag
Droplet Breakup

These equations describe the flow conditions in and across each segment of finite length, and each has been transformed into a form suitable for computerized numerical solutions.

The Isothermal Model makes allowance for velocity slip between the liquid droplets and the gas and also includes the effects of droplet drag and droplet breakup. The nozzle inlet conditions are specified as input to the model, and the pressure distribution along the axial length of the nozzle is also required.

1.4.1.1 Continuity Equation

At a given nozzle cross-section, the total flow area (A) can be considered as the sum of the liquid flow area (A_ℓ) and the gas flow area (A_g):

$$A = A_\ell + A_g \tag{I.21}$$

For one-dimensional flow through a cross-section, the continuity equations for each of the two components can be written as:

$$\dot{m}_g = \rho_g V_g A_g \quad ; \quad \dot{m}_\ell = \rho_\ell V_\ell A_\ell \tag{I.22}$$

These forms of the continuity equation imply the assumptions that the gas does not dissolve in the liquid and that the vapor pressure of the liquid is so low that the liquid does not vaporize.

Recalling the definition of the loading ratio ($r \equiv \dot{m}_\ell / \dot{m}_g$), then the expressions in Eq. I.22 can be substituted into Eq. I.21 to produce:

$$A = \dot{m}_g = \left(\frac{1}{\rho_g V_g} + \frac{r}{\rho_\ell V_\ell} \right) \tag{I.23}$$

This is the form of the continuity equation that is used with the momentum equation.

I.4.1.2 Momentum Equation

A differential force balance on a control volume with cross-section A and infinitesimal axial length dx describes the conversion of pressure drop (dP) into momentum:

$$d\dot{M} = -A\, dP \tag{I.24}$$

where the total momentum ($\dot{m}$) of the two-phase mixture is equal to the sum of the momentum of each of the two streams:

$$\dot{M} = \dot{m}_g V_g + \dot{m}_\ell V_\ell = \dot{m}_g \left(V_g + r V_\ell \right) \tag{I.25}$$

The mass-weighted mean velocity ($\bar{V}$) is defined as:

$$\bar{V} \equiv \frac{V_g + r V_\ell}{1 + r} \tag{I.26}$$

Hence, in terms of the weighted velocity, Eq. I.26 for the total momentum becomes:

$$\dot{M} = \left(\dot{m}_g + \dot{m}_\ell \right) \bar{V} \tag{I.27}$$

Taking the differential of Eq. I.27, and recalling that ($\dot{m}_g + \dot{m}_\ell$) is constant by conservation of mass, results in:

$$d\dot{M} = \left(\dot{m}_g + \dot{m}_\ell \right) d\bar{V} \tag{I.28}$$

Then, substituting Eqns. I.28 and I.23 into the basic force balance of Eq. I.24 yields a differential expression for the weighted velocity:

$$d\bar{V} = -\left(\frac{1}{1+r}\right)\left(\frac{1}{\rho_g V_g} + \frac{r}{\rho_\ell V_\ell}\right) dP \qquad (I.29)$$

Actually, $\bar{V}$ is a function of the phase velocities, V_g and V_ℓ, and expressions which relate these three velocities are developed below.

The local velocity ratio (K) is defined as: $K \equiv V_\ell/V_g$. Combining this definition with the mean-velocity definition (Eq. I.26) produces expressions for the local phase velocities, V_ℓ and V_g, in terms of the local velocity ratio and the local mean velocity:

$$V_\ell = \left(\frac{1+r}{1+rK}\right) K\bar{V} \equiv L\bar{V} \qquad (I.30)$$

$$V_g = \left(\frac{1+r}{1+rK}\right) \bar{V} \equiv G\bar{V} \qquad (I.31)$$

Using these two expressions, Eq. I.29 can be rewritten as:

$$\bar{V}\, d\bar{V} = -\left(\frac{1}{1+r}\right)\left(\frac{1}{\rho_g G} + \frac{r}{\rho_\ell L}\right) dP \qquad (I.32)$$

Equation I.32 can now be transformed into a form for numerical integration:

$$d(\bar{V}^2) = \Delta\, \bar{V}^2 = -\int_P^{P+\Delta P} \left(\frac{2}{1+r}\right)\left\{\frac{RT_g}{GPM_g} + \frac{r}{\rho_\ell L}\right\} dP \qquad (I.33)$$

where the perfect gas law is assumed for the density of the gas phase ($\rho_g = PM_g/RT_g$), and where ΔP is the pressure change over the length of the segment ΔX as the two-phase mixture flows from position X to downstream position, $X + \Delta X$. M_g is the molecular weight of the gas and R is the universal gas constant. If the assumption is made that the quantities T_g, G, L, and ρ_ℓ vary only slowly over the small pressure increment ΔP, then the values of these quantities can be assumed to be constant over the small segment and can be assigned the numerical value that exists at the inlet of each segment. The values

of these quantities are then recalculated for each segment. With this assumption, Eq. I.33 can be integrated to:

$$\Delta\bar{V}^2 = -\left(\frac{2}{1+r}\right)\left\{\frac{RT_g}{GM_g}\ \ell n\left(\frac{P+\Delta P}{P}\right) + \frac{r\,P}{\rho_\ell L}\right\} \qquad (I.34)$$

This is the form of the momentum equation that is used in the computerized numerical solution.

I.4.1.3 Droplet Drag Equation

Droplet drag provides the mechanism by which the gas-phase momentum, which increases during expansion, is transferred to the liquid droplets. Accordingly, this momentum transfer produces droplet acceleration. Using a force balance on the droplet, as shown schematically in Fig. I.19, the droplet acceleration force is equal to the drag force less the force caused by the pressure gradient of the gas phase:

$$F_{Drag} - F_{Press} = F_{Accel} \qquad (I.35)$$

Because the pressure gradient is negative, the pressure is lower on the downstream side of the droplet than on the upstream side, and the overall effect of the pressure-gradient force is, therefore, to accelerate the droplet.

The drag force on the droplet is represented by the expression:

$$F_{Drag} = \frac{1}{2}\rho_g V_{Slip}|V_{Slip}|C_D\frac{\pi D^2}{4} \qquad (I.36)$$

where V_{slip} is the velocity slip between the two phases ($V_{slip} = V_g - V_\ell$) and the absolute symbol around V_{slip} accounts for the direction of the drag force. If V_ℓ is larger than V_g, then the drag force on the droplet would be negative (and the direction of the force is properly predicted by Eq. I.36). A convenient definition (Ref. 8) is the velocity slip relative to the mass-weighted mean velocity:

$$S \equiv \frac{V_{Slip}}{\bar{V}} \qquad (I.37)$$

The pressure-gradient force on a small droplet in a pressure gradient is represented by the expression (Ref. 23):

$$F_{Press} = V_D \frac{dP}{dX} \tag{I.38}$$

where V_D is the volume of the droplet. For spherical droplets, $V_D = \pi D^3/6$, and Eq. I.37 becomes:

$$F_{Press} = \frac{\pi D^3}{6} \frac{dP}{dX} \tag{I.38a}$$

Even if the velocity slip (V_{slip}) is zero and the drag force is therefore zero, the pressure gradient caused by the gas phase still exists and exerts a force on the droplet.

The acceleration force on the droplet is:

$$F_{Accel} = ma = \left(\rho_\ell \frac{\pi D^3}{6}\right)\left(V_\ell \frac{dV_\ell}{dX}\right) \tag{I.39}$$

Combining the three force equations into the force balance of Eq. I.35 and using the convenient definition of Eq. I.37, the following equation results:

$$dV_\ell = \frac{3\rho_g |S| S \bar{V}^2 C_D \, dX}{4 \rho_\ell V_\ell D} - \frac{dP}{\rho_\ell V_\ell} \tag{I.40}$$

The definitions of the mean velocity (Eq. I.26) and the slip (Eq. I.37) can be combined to eliminate the explicit variable V_g, thereby obtaining an expression for V_ℓ in terms of $\bar{V}$ and s:

$$V_\ell = \left(1 - \frac{S}{1 + r}\right)\bar{V} \tag{I.41}$$

This expression is consistent with Eq. I.30 for V_ℓ in terms of $\bar{V}$ and K. For the cases considered here, the assumption is made that no mass transfer occurs between the phases. Hence the loading ratio (r) is constant throughout

the nozzle. Noting this and taking the first differential of Eq. I.41 results in:

$$dV_\ell = \left(1 - \frac{S}{1+r}\right) d\bar{V} - \frac{\bar{V}}{(1+r)} dS \qquad (I.42)$$

Then, Eqns. I.42 and I.40 can be combined to eliminate the term, dV_ℓ:

$$dS = \left(\frac{1+r}{\bar{V}}\right)\left[\left(1 - \frac{S}{1+r}\right) d\bar{V} - \left(\frac{3\rho_g |S| S \bar{V}^2 C_D dX}{4 \rho_\ell V_\ell D} - \frac{dP}{\rho_\ell V_\ell}\right)\right] \qquad (I.43)$$

Recalling that $V_\ell = L\bar{V}$ from Eq. I.30 and noting that $d\bar{V}^2 = 2\bar{V}d\bar{V}$ (as $\bar{V}^2$ is the way that $\bar{V}$ appears in Eq. I.34 for the momentum), then Eq. I.43 takes the following form for an axial segment of finite length ΔX:

$$\Delta S = \frac{1+r}{2\bar{V}^2}\left(1 - \frac{S}{1+r}\right) \Delta\bar{V}^2 - \frac{3\rho_g |S| S C_D (1+r) \Delta X}{4 \rho_\ell L D} + \frac{(1+r)\Delta P}{\rho_\ell L \bar{V}^2} \qquad (I.44)$$

This equation is valid for numerical analysis if the axial segments are short enough so that the equation can be linearized over the segment, and quantities can be evaluated at their inlet values (except for differential quantities). This equation represents the differential change of slip that occurs as momentum is transferred from the gas to the liquid by means of the interphase coupling from the drag force. The drag force and the buoyancy force caused by the pressure gradient across the droplet are balanced by the droplet acceleration force.

I.4.1.4 Droplet Breakup

The fourth relationship required to describe the two-phase flow in the Isothermal Model is the droplet breakup criterion. Droplet breakup in a two-phase mixture is governed primarily by the ratio of two forces: the aerodynamic pressure forces which are trying to deform the droplet, and the surface tension forces which are trying to maintain the droplet in spherical form. The ratio of these two forces is known as the Weber Number, We, defined as:

$$We \equiv \frac{\rho_g V_{slip}^2 D}{2\sigma} \qquad (I.45)$$

At high values of the Weber Number, the aerodynamic forces are large, and the droplets will deform and fragment into smaller droplets. At low values of the Weber Number, the surface tension forces dominate and the drops remain nearly spherical. The critical value of the Weber Number, $We)_{Crit}$, is experimentally determined and represents the maximum droplet size in terms of droplet diameter, D_{max}, that can exist at the local flow conditions in a two-phase flow:

$$D_{max} = \frac{2\ \sigma\ We)_{Crit}}{\rho_g\ V^2_{slip}} \qquad (I.46)$$

The generally accepted value of $We)_{Crit}$ is 6.0 (Ref. 23), within a factor of about 2 (for example, see Ref. 24). However, recent droplet size distribution measurements by Alger (Ref. 13) with steam-water nozzles suggest that the appropriate value of $We)_{Crit}$ should be approximately 1.0. Regions of high acceleration in the nozzle could produce greater droplet deformation and hence earlier breakup as compared to nearly spherical droplets in less accelerated regions. For the smaller droplets predicted which correspond to a smaller value of $We)_{Crit}$, the interphase coupling of momentum (and also heat transfer in the Model with Droplet Heat Transfer, to be discussed in Section I.42) will be enhanced.

I.4.1.5 Solution Technique

The four basic equations used in the Isothermal Model to solve the two-phase flow presented earlier include: continuity (Eq. I.23); momentum (Eq. I.34); droplet drag (Eq. I.44); and droplet breakup (Eq. I.46). The nozzle inlet flow conditions (gas and liquid velocities, loading ratio, temperature and pressure of the mixture and the pressure drop along the nozzle must be specified, as well as should the thermophysical properties of the gas (molecular weight and viscosity) and of the liquid (density and surface tension).

The solution technique is a marching-type solution, whereby the governing flow equations are solved for the first segment, and the calculated results from the first segment are then used as input for calculating the solution for the second segment, and so on through the nozzle. Basically, the quantity $\Delta\bar{V}^2$ is calculated for the segment using Eq. I.34 and the specified pressure distribution. Hence, the value of $\bar{V}$ at the exit of the segment can be calculated:

$$\bar{V})_{Exit} = \sqrt{\bar{V})^2_{Inlet} + \Delta\bar{V}^2} \qquad (I.47)$$

The change in the slip ratio, ΔS, over the segment can then be calculated using Eq. I.44, and the exit value of the slip ratio can be calculated from:

$$S)_{Exit} = S)_{Inlet} + \Delta S \qquad (I.48)$$

Using the exit values of the slip ratio and the weighted velocity, the value of the liquid velocity, V_ℓ, at the exit of the segment can be calculated using Eq. I.41. The exit value of the gas velocity can then be calculated from the definition of the slip ratio (Eq. I.37), and the nozzle area can be calculated as a function of axial distance using Eq. I.23 once V_g and V_ℓ are known.

Results which were calculated using the Isothermal Model for selected operating conditions are presented and discussed later in this section.

I.4.2 Model With Droplet Heat Transfer

The main difference between the Isothermal Model discussed above and the Model with Droplet Heat Transfer is that the latter includes the effect of heat transfer by allowing a varying temperature difference between the liquid droplets and the gas and an axial temperature decrease in the liquid and the gas. In addition to the four basic equations cited for the Isothermal Model, two additional governing equations, the energy equation and an equation for heat transfer from the liquid to the gas, are required so the liquid and gas temperatures of the two-phase flow can be calculated. The basic equations required are:

Continuity
Momentum
Droplet Drag
Droplet Breakup

Energy
Heat Transfer

The first four equations are used in the same form as are presented for the Isothermal Model. In the model with heat transfer, however, the thermophysical properties are temperature-dependent, including the temperature-dependence of the gas density based on the ideal gas equation that was used in the formulation of the momentum equation (Section I.4.1.2).

I.4.2.1 Energy Equation

The energy equation of the mixture states that the net energy flux into a volume element is zero, because the two-phase flow in the nozzle is steady state and assumed to be adiabatic. Hence, the total enthalpy of the mixture is constant:

$$V_g \frac{dV_g}{dX} + C_{pg} \frac{dT_g}{dX} + r \left[V_\ell \frac{dV_\ell}{dX} + C \frac{dT_\ell}{dX} + \frac{1}{\rho_\ell} \frac{dP}{dX} \right] = 0 \qquad (I.49)$$

The first two terms represent the gas enthalpy, and the other three terms represent the liquid enthalpy. Equation 1.49 applies throughout the nozzle, and the integrated form of the energy equation is:

$$\frac{V_g^2}{2} + C_{pg} T_g + r \left[\frac{V_\ell^2}{2} + C T_\ell + \frac{P}{\rho_\ell} \right] = \text{Constant} \qquad (I.50)$$

where the Constant term is determined from nozzle inlet conditions. The energy equation is an overall balance on the energy of the two-phase mixture. However, the temperatures of the gas and of the liquid can differ, yet satisfying the above energy equation.

I.4.2.2 Heat Transfer Equation

As the gas phase of the two-phase mixture expands through the nozzle, the temperature of the gas will decrease. It is assumed that the temperature of the liquid phase is always equal to or greater than that of the gas phase at the nozzle inlet. In this case, as the gas temperature drops, the temperature differential between the liquid and the gas will increase, and heat will be transferred from the liquid to the gas at an increased rate, other conditions being equal. A heat balance on the liquid droplet describes this phenomenon:

$$(\rho_\ell V_D) C \frac{\Delta T_\ell}{\Delta t} = h A_D (T_\ell - T_g) \qquad (I.51)$$

In this case, the rate of change of the enthalpy of the droplet is equal to the rate of heat transfer from the droplet to the surrounding gas. The heat transfer coefficient, h, is obtained from experimental data. For small segments, the time differential can be approximated as: $\Delta t = \Delta X / V_\ell$, and for spherical droplets, the volumetric density of heat transfer area is:

$$\left.\frac{A_D}{V_D}\right)_{Sphere} = \frac{6}{D} \qquad (I.52)$$

Hence, Eq. I.51 can be solved for the temperature change of a liquid droplet in the axial segment of length ΔX:

$$\Delta T_\ell = \frac{6h\ (T_\ell - T_g)}{\rho_\ell\ C V_\ell D}\ \Delta X \qquad (I.53)$$

Equation I.53 is then used to account for droplet heat transfer effects.

I.4.2.3 Solution Technique

The basic solution technique for the Model with Droplet Heat Transfer is very similar to that discussed in Section I.4.1.5 for the Isothermal Model, except that the energy equation (Eq. I.50) and the heat transfer equation (Eq. I.53) must now be included.

Again, a marching-type solution is used. Based on conditions at the inlet to the segment, the temperature change of the liquid droplets is calculated by using Eq. I.53. The heat transfer coefficient is calculated with correlations for droplet heat transfer based on the Reynold's Number. The liquid temperature at the exit of the segment is then known from the calculated change in temperature and the known inlet temperature. Next, the same procedure as in the Isothermal Model is used to calculate $\bar{V})_{Exit}$, $S)_{Exit}$, V_ℓ and V_g at the exit, and local nozzle area. Finally, the gas temperature at the segment exit is calculated with the heat balance of Eq. I.50.

The isentropic efficiency is a measure of nozzle performance and is defined as:

$$\eta \equiv \frac{\frac{1}{2}\dot{m}\ \bar{V}^2_{Exit}}{\dot{m}\ \Delta h)_{max}} = \frac{\bar{V}^2_{Exit}}{2\ \Delta h)_{max}} \qquad (I.54)$$

This efficiency is the ratio of the kinetic energy per unit mass of the exit mixture to the ideal change of enthalpy (into kinetic energy) for the isentropic expansion of a homogeneous two-phase mixture. The maximum enthalpy change through the nozzle, $\Delta h)_{max}$, is given by the expression:

$$\Delta h)_{max} = \left\{\left(\frac{1}{1+r}\right) C_{pg}\left[T_g)_{inlet} - T_{exit}\right]\right\} + \left\{\left(\frac{r}{1+r}\right)\left(C\left[T_\ell)_{inlet} - T_{exit}\right] + \frac{\Delta P}{\rho_\ell}\right)\right\} \qquad (I.55)$$

The $(\Delta P/\rho_\ell)$ term in the second brackets is included in the liquid enthalpy contribution because the process is not at constant (or even nearly constant) pressure. Although the temperatures of the gas and of the liquid could differ at the nozzle inlet, there is only one exit temperature for the homogeneous mixture, T_{exit}. This exit temperature is calculated by using the expression for an isentropic expansion:

$$\frac{T_{exit}}{T_{Mix)_{in}}} = \left(\frac{P}{P_o}\right)^{\frac{R}{r\bar{C}}} \tag{I.56}$$

where R is the gas constant and $\bar{C}$ is the mass-weighted specific heat:

$$\bar{C} \equiv \left(\frac{C_{pg}}{1 + r}\right) + \frac{rC}{1 + r} \tag{I.57}$$

and where $T_{Mix)_{in}}$ is the mass-weighted mixture temperature at the nozzle inlet:

$$T_{Mix)_{in}} = \frac{T_{g)_{inlet}}}{1 + r} + \frac{r\, T_{\ell)_{inlet}}}{1 + r}, \tag{I.58}$$

Equation I.56 is derived from the thermodynamic relations for an isentropic process (Ref. 25), where the integral form of the relationship for the entropy change of a perfect gas is:

$$\Delta S_g = C_p \ell n \frac{T_2}{T_1} - R \ell n \frac{P_2}{P_1} \tag{I.59}$$

The corresponding expression for the entropy change of a liquid (because there is no change in volume) is:

$$\Delta S_\ell = C \ell n \frac{T_2}{T_1} \tag{I.60}$$

Since the overall change in entropy for the process is zero:

$$r \Delta S_\ell + \Delta S_g = 0 \tag{I.61}$$

Therefore, Eqns. I.59, I.60, and I.61 can be combined, and the result is Eq. I.56, after the anti-logarithm is taken.

Calculated results using the Model with Droplet Heat Transfer for selected operating conditions are presented and discussed later in this section.

I.4.3 Comparisons Between Models and Test Data

To use the two models developed in Sections I.4.1 and I.4.2 for the calculation of nozzle designs, experimental data are required in three areas: droplet breakup (discussed in Section I.4.1.4 in terms of the Weber Number breakup criterion); the droplet drag coefficient; and the droplet heat transfer coefficient (required only for the Model with Droplet Heat Transfer). The empirical data base for the drag coefficient and the heat transfer coefficient have been developed from previous investigations published in the literature.

I.4.3.1 Drag and Heat Transfer Data

Experimental data are required to estimate the drag coefficient (C_D) of the droplets in the gas flow. The drag coefficient describes the viscous interaction between the gas and the droplets when the droplets are not in velocity equilibrium with the gas. For solid spheres, Stonecypher (as cited in Ref. 8) made the following least-squares fit of the drag data for spherical particles as tabulated by Perry et al., (Ref. 26):

$$\ell n\ C_D = 3.271 - 0.8893\ L_{Re} + 0.03417\ L_{Re}^2 + 0.001443\ L_{Re}^3 \qquad (I.62)$$

where $L_{Re} \equiv \ell n\ (Re_{Rel})$. This correlation is valid in the range of relative Reynolds Number, $0.1 < Re_{Rel} < 2 \times 10^4$ and is shown in Fig. I.20. Actually, this correlation applies to particles at low concentration in the gas so that no particle interactions occur and to flows with a large cross-section relative to the droplet diameter so that boundary effects are minimal. If the loading ratio is less than unity, then the average particle spacing is ten times or more the particle size, and the assumption of no particle interactions would seem reasonable for these conditions.

Ingebo (Ref. 27) measured drag coefficients of a particle cloud injected into a wind tunnel at particle mass fractions of about one percent, in the range of relative Reynolds Numbers of approximately 6 to 400. The data, which are correlated by the expression:

$$C_D = 27/Re_{Rel}^{0.84} , \qquad (I.63)$$

falls below those of Stonecypher's least-squares fit as seen in Fig. I.20. Ingebo attributed the lower drag coefficients to the fact that the particles were being accelerated, thereby implying non-steady-state flow.

In the flow behind weak shock waves, Rudinger (Ref. 28) measured drag coefficients for flows of suspensions of spherical glass particles in air. Mixtures of particles with average diameters of 29 microns (0.0011 in.) and of 62 microns (0.0024 in.) were tested, over a range of loading ratios from 0.05 to 0.36 and a range of relative Reynolds Numbers from 12 to 600. The data are higher than predicted by a correlation such as that of Eq. I.62 (which is based on single-sphere data), and the slope of the correlation (valid for $50 < Re_{Rel} < 300$) is much steeper:

$$C_D = 6000/Re_{Rel}^{1.7} \qquad (I.64)$$

Rudinger developed a model to account for these higher drag coefficients which were measured at loading ratios higher than those of Ingebo. This preliminary model allowed for both microscopic longitudinal and lateral perturbations of particle motion resulting from such effects as: particle interactions with the wakes of other particles; lateral effects caused by particle rotation; or electrostatic forces. The drag coefficient is evaluated for the local vectorial particle velocity relative to the gas by a correlation similar for that in Eq. I.62, and Rudinger attributed the higher effective drag coefficients to these perturbations in particle motion. In other words, the effective drag coefficient for the average motion differs from that applicable to the local microscopic motion.

A rigorous analytical study by Gluckman et al. (Ref. 29) examined the drag coefficient of spheres in an unconnected chain (with the flow direction being the same direction as the axis of the chain) in unbounded Stokes flow. Stokes flow generally exists at relative Reynolds Numbers below unity. Analytically, their work indicated a reduction in the drag coefficient on spheres in the middle of the chain. At a sphere spacing of four diameters, the drag is about 38 percent of the drag predicted by the classical Stokes drag ($C_D = 24/Re_{Rel}$); at a spacing of two diameters, the drag is about 24 percent; while at a spacing of one diameter (spheres touching), the drag is only about 14 percent. Hence, significant reductions in the drag are predicted, because the wake from one sphere influences the flow around the succeeding sphere.

Shown in Fig. I.20 are the data correlations and prediction for the drag coefficient that were just discussed. Based on these data, a wide range in the value of the drag coefficient would be expected. For the anticipated range of operating conditions ($100 < Re_{Rel} < 10{,}000$) of the two-phase nozzle, the data are in the vicinity of Stonecypher's curvefit, and accordingly, this is the comprehensive expression that is used in the computerized models to calculate the droplet drag coefficient. However, the sensitivity of the nozzle performance predictions to this assumption for the drag coefficient will be examined in Phase II of this study.

Similarly, experimental data are required to estimate the heat transfer coefficient (h) between the liquid droplets and the gas. McAdams (Ref. 19) presents data for heat transfer between spheres and a gas (air). In the range of relative Reynolds number ($Re_{Rel} \equiv \rho_g V_{slip} D/\mu_g$) of 25 to 10,000, the dimensionless correlation recommended by McAdams is:

$$\frac{hD}{k_g} = 0.37\ Re_{Rel}^{0.6} \qquad (I.65)$$

The relative Reynolds Number for some of the nozzle flow conditions of interest for marine propulsion will be in the range of 100 to 2000. For conditions where the Reynolds Number is much lower (e.g., in the range of 1.0 to 25.), Kreith (Ref. 30) recommends the following correlation:

$$\frac{hD}{k_g} = \frac{\mu_g C_{pg}}{k_g}\left[2.2 + 0.48\ Re_{Rel}^{0.5}\right] \qquad (I.66)$$

Equations I.65 and I.66 are the two correlations that are used to calculate the heat transfer coefficient in the Model with Droplet Heat Transfer.

I.4.3.2 Thermophysical Properties

Thermophysical properties of both the liquid and the gas are required to obtain numerical results from the models. Some testing (Ref. 8) has been done with mixtures of nitrogen and water at room temperature, and the thermophysical properties of these fluids at these conditions are known. As discussed in Section I.2.2, a liquid/gas combination of interest for the marine propulsion application is Dowtherm A/steam.

The thermophysical properties of steam (μ_g, k_g, ρ_g, C_{pg}) are known (for example, see Ref. 31) for the temperature and pressure range of interest for a marine propulsion application. Certain of the thermophysical properties

of Dowtherm A (DTA) that are required in the model (ρ_ℓ, C) are also known (Ref. 32) for the temperature range of interest, but the surface tension (σ) has apparently been measured only at relatively low temperatures, that is, in the range of 20 C (68 F) to 60 C (140 F). (The surface tension of the liquid is required to evaluate the Weber Number droplet breakup criterion.) The operating temperatures for the nozzle design, however, are expected to be as high as 316 C (600 F). Hence, the surface tension data had to be extrapolated. Generally, as the temperature of a liquid approaches its critical temperature (which is 498 C (927 F) for DTA), the surface tension approaches zero, because the interface between the liquid and the gas disappears at the critical point of the substance. Fig. I.21 shows surface tension data for two non-viscous fluids, as presented in Ref. 33. If a straight line were placed through the data for each fluid, then the temperature at which the surface tension becomes zero would be approximately 19 C (35 F) lower than the critical temperature of each substance. As seen in Fig. I.21, the low-temperature data for the surface tension of DTA was extrapolated by placing a line through the three low-temperature points and through the point of zero surface tension at 19C (35 F) less than its critical temperature. The sensitivity of the nozzle performance predictions to this assumption for the surface tension (and indeed to the assumption of a critical Weber Number of six for droplet breakup) will be examined during Phase II of this study.

I.4.3.3 Domains

As noted previously, the main difference between the Isothermal Model and the Model with Droplet Heat Transfer is that the latter includes the effects of heat transfer, since both models allow for velocity slip, droplet drag, and droplet breakup. Despite the fact that conceptually, the Isothermal Model is relatively simpler, both models must still be solved numerically with the computer, because the calculations are too tedious to be done by hand for the many small segments that are required for numerical stability. Therefore, in terms of obtaining numerical results, the Isothermal Model offers no advantage over the Model with Droplet Heat Transfer because computerized solutions are required in both instances.

For quick calculations which can be done manually, however, the isothermal model proposed by Rudinger (Ref. 4) and discussed in Section I.3.2 is very useful and convenient. In such a case, the simplification that results from the assumption of isothermal conditions is significant enough to allow hand calculations, whereas the computer would be necessary for solutions without this assumption. Generally, the isothermal model provides reasonable results for operating conditions of high loading ratio and small droplet size. As deduced from the Weber Number criterion, small droplets generally occur with

fluids that have low surface tension and/or at operating conditions where the velocity slip is large, thereby creating large aerodynamic forces for droplet breakup. The implication of a large loading ratio (r) is that the liquid acts as a heat source to the expanding gas, thereby reducing its temperature drop.

In contrast to isothermal models (either Rudinger's model or the computerized model developed in Section I.4.1), the Model with Droplet Heat Transfer applies to the full range of nozzle operating conditions, as long as droplet flow (in contrast to slug flow, for example) exists and the droplets are uniformly distributed across the nozzle cross-section. Fig. I.22 shows calculated results from the two computerized models, for a mixture of steam and Dowtherm A (DTA). Here, the gas and liquid velocities, the nozzle area, and the droplet size are calculated as a function of axial distance through the nozzle for the specified inlet conditions and pressure profile. For these operating conditions, the velocity slip between the gas and the liquid ($V_g - V_\ell$) increases as the flow proceeds through the nozzle. For droplet breakup, a Weber Number equal to six was used to calculate the local maximum droplet size throughout the nozzle. The Weber breakup criterion is not exact, and the diameter history of a given droplet varying slowly over time (Fig. I.22) is an idealization. In reality, the droplet probably breaks apart into smaller droplets at irregular intervals, with step changes in droplet size occurring. At this relatively high value of the loading ratio ($r = 40$), the results from the two models for velocity and throat area virtually overlap. The temperature drop of the liquid is about 5 C (9 F), and that of the gas is about 15 C (27 F). For steam alone expanded through this pressure, the isentropic temperature drop would be about 233 C (420 F), so that the liquid DTA does act as a heat source for the steam.

Table I.4 compares results calculated from the Isothermal Model and from the Model with Droplet Heat Transfer, at the same inlet conditions (temperature and pressure) and the same exit pressure, for four values of the loading ratio. At a given loading ratio, the exit velocities calculated with the Heat Transfer Model are lower than those calculated with the Isothermal Model. Understandably, both models are idealized, but the model with Droplet Heat Transfer is more realistic than the Isothermal Model because the effect of finite heat transfer is included in the model with Droplet Heat Transfer. The inclusion of this heat transfer effect means that the calculated velocities and efficiency are more realistic and lower than those calculated with the Isothermal Model, which actually requires heat additions to the nozzle to maintain isothermal conditions. Because both the gas and the liquid are calculated as being lower in temperature in the Model with Droplet Heat Transfer, the gas is denser. For a fixed pressure drop (which translates into a fixed amount of momentum), the gas velocity would logically be expected to be lower when the gas density is larger, and the liquid velocity would also be lower because it is related to the gas velocity by the droplet drag relationship.

With the Model with Droplet Heat Transfer, it can be seen in Table I.4 that when the loading ratio is increased, both the gas and liquid exit velocities decrease while the exit temperatures for both increase. As the loading ratio increases, the liquid phase increasingly carries more of the total momentum, but with the much higher density of the liquid, both velocities can be lower while the mixture still has the same total momentum. Similarly, as the loading ratio is increased, the heat capacity of the liquid phase is larger, and the gas temperature decrease during the expansion is counteracted by heat transferred from the larger heat source of the liquid phase.

The isentropic nozzle efficiencies (η) as calculated with the Model with Droplet Heat Transfer are lower than those with the Isothermal Model. The isentropic nozzle efficiency used here is the ratio of the kinetic energy per unit mass of the exit mixture to the ideal change of enthalpy (into kinetic energy) for the isentropic expansion of a homogeneous mixture. Because the efficiency is a measure of how much pressure energy is converted into kinetic energy (velocity), the lower efficiency is explained by the realistically lower velocities calculated using the model with Droplet Heat Transfer.

I.4.3.4 Comparison With Other Models and Test Data

The results from models developed during this program can be compared with results of models previously developed by other investigators and with pertinent experimental data. Table I.5 summarizes selected results, at one set of operating conditions, from the computerized Isothermal Model described in Section I.4.1, from Rudinger's analytical isothermal model (Ref. 4), and from the isentropic model discussed in Section I.3.1. The velocities calculated with the isentropic model are lower in all cases because the mixture temperature is lower, hence the gas is denser, and the velocity can be lower and still carry the all-liquid momentum. For the all-gas case ($\dot{m}_\ell/\dot{m}_g = 0$) and the nearly all-liquid case ($\dot{m}_\ell/\dot{m}_g = 1000$), the results for exit velocity from the computerized model and from Rudinger's model are in close agreement. Figure I.23 shows the all-gas results for velocity and area as a function of distance through the nozzle for the two isothermal models; the calculated results agree within one percent. Essentially, this comparison of the all-gas results from the two models represents a check on the formulation of the momentum equation in the computerized Isothermal Model. For the cases with $\dot{m}_\ell/\dot{m}_g = 40$, the difference between the exit velocity results can be attributed to the varying V_ℓ/V_g ratio in the computerized model, when compared to the condition that V_ℓ/V_g = constant in Rudinger's model. This assumption of V_ℓ/V_g = constant replaces the droplet drag equation that couples the liquid and the gas momentums in the computerized model. Further, Rudinger's model is for constant-diameter (solid) particles.

Table I.6 compares velocity and temperature results at the exit of a 50-inch-long nozzle (calculated by Elliot and Weinberg (Ref. 8) at their selected conditions) with the results from three other models for the two-phase flow of a mixture of water and nitrogen at inlet conditions of 150 psia and 16 C (60 F). The results from Rudinger's isothermal model are shown at $V_\ell/V_g = 0.7$, the value at the nozzle exit which is also the approximate value throughout the nozzle obtained from the results of Elliott and Weinberg. The exit velocity ($\bar{V}$) calculated with either of the two isothermal models is higher than the exit velocity calculated with either of the other two models, and hence, the isentropic nozzle efficiencies calculated with the two isothermal models are higher also. As discussed earlier, both the Isothermal Model and the Model with Droplet Heat Transfer are best solved by computer, but Rudinger's isothermal model is suitable for rapid manual calculations, although with the latter, the calculated nozzle efficiencies will be optimistically high.

Results from the Model with Droplet Heat Transfer are shown in Table I.6 for three different pressure profiles selected. The profile with dP/dX = constant is linear with distance between the inlet and the exit, while the 2-line and 3-line curvefits are shown in Figure I.24 along with the optimum pressure profile for maximum mean exit velocity as calculated by Weinberg and Elliott. The purpose behind using these selected pressure profiles is to compare the results calculated from the Model with Droplet Heat Transfer with the results presented by Weinberg and Elliot, which correspond to the optimum pressure profile. The nozzle cross-sectional area profiles which correspond to each of the three pressure profiles shown in Fig. I.24 and to the linear pressure profile are all slightly different. The liquid exit velocity (and the weighted mean velocity), the exit temperature of the liquid and of the gas, and the isentropic nozzle efficiency, all of which are calculated with either of the three pressure profiles in the computerized Model with Droplet Heat Transfer or with Elliott and Weinberg's model and their optimum pressure profile, agree within one percent. Furthermore, the liquid carries most of the momentum and enthalpy at the loading ratios expected for the two-phase nozzle in a possible marine propulsion application. The gas velocities, which were calculated in the same manner with the two models, differ by 18 percent. Apparently, the gas velocity results are much more sensitive to the pressure profile selected than are the liquid velocity results, as the results for the gas velocity calculated with the computerized Isothermal Model (which is just the momentum equation and no heat transfer equation) and seen in Table I.5 for the same linear pressure profile, are close to the results from the analytical isothermal model of Rudinger.

Both the Model with Droplet Heat Transfer and the model developed by Elliott and Weinberg use the basic principles of continuity, momentum, droplet drag, droplet breakup, energy, and heat transfer. However, the formulation

of the Model with Droplet Heat Transfer emphasizes its suitability to calculate parametric results, whereas the formulation of the Elliott and Weinberg model emphasizes nozzle design details but is too complicated for parametric analyses when many design cases need to be considered in a short period of time. The Elliott and Weinberg design procedure consists of several steps. First the optimum nozzle contour is determined with their computerized model at a condition of constant droplet diameter (because the pressure profile may be so steep at the nozzle inlet as to prevent droplet breakup). Computer runs are made for a series of values of the optimizing Lagrangian multiplier, λ, to cover the range of nozzle lengths of possible interest. Second, a preliminary guess of the optimum nozzle length is made to permit modifying the optimum cross-sectional profile into a practical nozzle contour. Nozzles that are too short may have large velocity slip while nozzles that are too long may have large friction losses; the result in either extreme case is a low mean exit velocity (and, hence low nozzle efficiency). This procedure, while eminently suitable for nozzle design, is too detailed for evaluating numerous possible nozzle operating conditions.

In contrast, the Model with Droplet Heat Transfer is formulated with regard to parametric analysis, but local velocity and temperature conditions are also calculated and available throughout the nozzle. This model neglects friction, but this assumption is reasonable since the nozzles for a two-phase turbine application must be short in length in order to accommodate them into the available space. Further, frictional effects did not appear to be large even in results for the 50-inch-long nozzle of Table I.6.

Experimental data, as discussed in Section I.1.1, have been taken for a number of two-phase nozzles. However, only some of these data were taken with a two-component mixture, the type of system to which the Model with Droplet Heat Transfer applies. A complication arises when comparing experimental data for the performance (both design-point and off-design) of a given nozzle with the calculated results from a design model. Essentially, a design model is used to plan families of nozzles for one set of operating conditions, whereas a performance model is used in the reverse manner, that is, to calculate the performance of one nozzle at many sets of operating conditons. Experimental performance data (Ref. 7) for a six-inch nozzle tested with a mixture of water and air are shown in Fig. I.25. Also shown are performance lines predicted for the actual nozzle contour by Elliott and Weinberg with their model (Ref. 8). The Elliott and Weinberg prediction labeled "Real" is based on a model that includes velocity slip, droplet breakup, and heat transfer, but no friction; while their prediction labeled "With Friction" includes friction in terms of wall boundary layer losses.

Both of the computerized models presented in Sections I.4.1 and I.4.2 were also used to make nozzle designs for a range of loading ratios at the inlet temperatures, velocities, and pressure of this six-inch nozzle, by assuming a linear variation of pressure drop with distance through the nozzle. (As discussed, the nozzle contour produced from these design models would be different at each value of the loading ratio.) The results from these design models are also shown in Fig. I.25. The design-point performances of a series of nozzles compare well with the experimental data and show the same trend as the off-design performance of one nozzle. The predictions from the Model with Droplet Heat Transfer are realistically lower than those from the Isothermal Model, and the difference is larger at lower values of the loading ratio where the temperature of the gas phase after expansion is lower because the gas represents a relatively larger heat sink at lower values of the loading ratio.

I.4.4 Preliminary Parametric Calculations

As part of an effort to check the computer models, some preliminary parametric calculations were made to show their versatility. Figure I.26 shows the effect of inlet temperature on temperatures, velocities, and cross-sectional area through the nozzle. In one case, the inlet temperatures of the gas and the liquid are the same at 316 C (1060 R), while in the other case the inlet gas temperature is 56 C (100 R) cooler than the inlet liquid temperature of 1060 R. The liquid inlet temperatures were selected to be the same because the liquid contains the bulk of the mixture enthalpy at a loading ratio of 40. Near the inlet for the case with the 100 R differential, the steam is rapidly heated by the higher-temperature liquid DTA, until the steam expands sufficiently for both temperatures to begin falling shortly beyond the nozzle exit. The results for the liquid velocity in both cases overlap, as also do the gas velocities. For the case with the cooler gas, slightly less nozzle area is required, because the cooler gas is denser than in the case with the higher inlet temperature.

The effect of nozzle length on performance is shown in Table I.7. As the length is increased, the residence time of the two-phase mixture in the nozzle increases, and more enthalpy and momentum can be transferred between the gas phase and the liquid phase. The weighted exit velocity is higher, and as a result, the nozzle efficiency increases with increased nozzle length. At this value of the loading ratio, the liquid temperature decreases only 0.3 C (0.6 R) as the nozzle length is increased from 3 in. to 12 in; for these operating conditions, the nozzle efficiency increases by three percentage points with the added length.

The effect of loading ratio ($\dot{m}_\ell/\dot{m}_g$) on nozzle performance is shown in Table I.4 for one set of operating conditions. As the loading ratio increases, the two-phase flow in the nozzle tends to become increasingly isothermal, because the thermal capacity of the liquid phase dominates.

The preliminary parametric calculations presented here indicate that the computerized Model with Droplet Heat Transfer is appropriately formulated for parametric analyses of two-phase nozzles.

REFERENCES

1. Tangren, R. F., C. H. Dodge and H. S. Siefert: Compressibility Effects in Two-Phase Flow. J. Appl. Phys., Vol. 20, No. 7, pp. 637-645, 1949.

2. Shapiro, A. H.: Dynamics and Thermodynamics of Compressible Fluid Flow. Ronald Press, 1953.

3. Kliegel, J. R.: One Dimensional Flow of a Gas-Particle System. Report No. TR-59-0000-00746, Space Technology Laboratories, Los Angeles, 1959.

4. Rudinger, G.: "Relaxation in Gas-Particle Flow", Chapter in Non-equilibrium Flows - Part I, P.P. Wegener, ed., pp. 119-161. Marcel Dekker, Inc., 1969.

5. Netzer, D. W.: Calculations of Flow Characteristics for Two-Phase Flow in Annular Converging-Diverging Nozzles. Report No. TM-62-3, Jet Propulsion Center, School of Mechanical Engineering, Purdue University, 1962.

6. Hultberg, J. A. and S. L. Soo: Two-Phase Flow Through a Nozzle. Astronautica Acta, Vol. 11, No. 3, pp. 207-216, 1965.

7. Elliott, D. G.: "Theoretical and Experimental Investigation of a Gas-Driven Jet Pump for Rocket Engines", in Liquid Rockets and Propellants, Progress in Astronautics and Rocketry - Vol. 2, pp. 497-541. Academic Press, 1960.

8. Elliott, D. G. and E. Weinberg: Acceleration of Liquids in Two-Phase Nozzles. JPL Report 32-987, 1968.

9. Crowe, C. T., M. P. Sharma and D. E. Stock: The Particle-Source-In Cell (PSI-Cell) Model for Gas Droplet Flows. ASME J. of Fluids Eng'g., pp. 325-332, 1977.

10. Comfort, W. J., T. W. Alger, W. H. Giedt and C. T. Crowe: Calculation of Two-Phase Dispersed Droplet-In-Vapor Flows Including Normal Shock Waves. ASME J. of Fluids Eng'g., pp. 355-362, 1978.

11. Starkman, E. S., V. E. Schrock, K. F. Neusen, and D. J. Maneely: Expansion of a Very Low Quality Two-Phase Fluid Through a Convergent-Divergent Nozzle. ASME J. of Basic Eng'g., pp. 247-254, 1964.

12. Schrock, V. E., E. S. Starkman, and R. A. Brown: Flashing Flow of Initially Subcooled Water in Convergent-Divergent Nozzles. ASME J. of Heat Transfer, pp. 263-268, 1977.

REFERENCES (Cont'd)

13. Alger, T. W.: Droplet Phase Characteristics in Liquid-Dominated Steam-Water Nozzle Flow. Report UCRL-52534, Lawrence Livermore Laboratory, 1978.

14. Cerini, D. J.: Demonstration of a Rotary Separator for Two-Phase Brine and Steam Flows. Report TID-28519, DOE, 1978.

15. Elliott, D. G., and L. G. Hays: Two-Phase Turbine Engines. Proceedings of the 11th IECEC, pp. 222-228, 1976.

16. Davison, W. R., and T. J. Sadowski: Water-Augmented Turbofan Engines. J. Hydronautics, Vol. 2, No. 1, pp. 14-20.

17. Comfort, W. J. and C. W. Beadle: Design Considerations for a Two-Phase Turbine, in "Polyphase Flow in Turbomachinery," ASME Publication, 1978.

18. Ahmad, S. and L. G. Hays: A Biphase Turbine Bottoming Cycle for a Diesel Engine. ERDA Report SAN 1207-1, 1977.

19. McAdams, W. H.: Heat Transmission. Third Edition, McGraw-Hill, 1954.

20. Rudinger, G.: Some *Effects of Finite Particle* Volume on the Dynamics of Gas-Particle Mixtures. AIAA J., Vol. 3, pp. 1217-1222, 1965.

21. Comfort, W. I. and C. T. Crowe: Dependence of Shock Characteristics on Droplet Size in Supersonic Two-Phase Mixtures, in "Polyphase Flow In Turbomachinery," ASME Publication, 1978.

22. Rudinger, G.: Wave Propagation in Suspensions of Solid Particles in Gas Flow. Applied Mechanics Reviews, Vol. 26, pp. 273-279, 1973.

23. Wallis, G. B.: One-Dimensional Two-Phase Flow. McGraw Hill, 1969.

24. Hanson, A. R., E. G. Domich, H. S. Adams: Shock Tube Investigation of the Breakup of Drops by Air Blasts. Physics of Fluids, Vol. 6, No. 8, pp. 1070-1080, 1963.

25. Hatsopoulos, G. N. and J. H. Keenan: Principles of General Thermodynamics. John Wiley, 1965.

26. Perry, R. H., C. H. Chilton, S. D. Kirkpatrick: Chemical Engineers' Handbook. Fourth Edition, McGraw-Hill, 1963.

REFERENCES (Cont'd)

27. Ingebo, R. D.: Drag Coefficients for Droplets and Solid Spheres in Clouds Accelerating in Air Streams. NACA TN 3762, 1956.

28. Rudinger, G.: Effective Drag Coefficient for Gas-Particle Flow in Shock Tubes. ASME J. of Basic Eng'g, pp. 165-172, 1970.

29. Gluckman, M. J., R. Pfeffer, S. Weinbaum: A New Technique for Treating Multiparticle Slow Viscous Flow: Axisymmetric Flow Past Spheres and Spheroids. J. Flu. Mech., Vol. 50, pp. 705-740, 1971.

30. Kreith, F.: Principles of Heat Transfer. Third Edition, Intext Educational Publishers, 1973.

31. Keenan, J. H., F. G. Keyes, P. G. Hill, and J. G. Moore: Steam Tables. John Wiley, 1978..

32. Anon.: Dowtherm A Heat Transfer Fluid. Dow Chemical Company.

33. Rohsenow, W. M. and H. Y. Choi: Heat, Mass and Momentum Transfer. Prentice-Hall, 1961.

TABLE I.1

SUMMARY OF ANALYTICAL TWO-PHASE-NOZZLE MODELS

Investigator	Year	Droplet Size	Droplet Loading	Droplet Breakup	Velocity Slip	Heat Transfer	Isothermal Between Phases	Shock Effects	
Tangren	1949	Small, as Homogeneous	Not Spec.	NO	NO	-	YES	YES	
Kliegel	1959	1 to 10 μm	$\epsilon_o < 0.05$	NO	Constant	YES	-	NO	
Rudinger	1969	<2000 μm	All / All	NO / NO	Constant / Constant	- / -	NO / YES	NO / NO	Computerized / Simplified
Netzer	1962			YES	YES		YES		
Hultberg	1965	Typ 200 μm	All	NO	YES	YES	-	YES	
Elliott	1960 1968	<2000 μm	All	YES	YES	YES	-	NO	
Crowe	1977	Typ 1000 μm	Not Spec.	NO	YES	YES	-	NO	
Comfort	1978	<10 μm	<2	YES	YES	-	YES	YES	

R80-954624-2

TABLE I.2

POTENTIAL TWO-PHASE NOZZLE APPLICATIONS

Low-RPM Two-Phase Turbines
- Marine Propulsion
- Automobile

Two-Phase Turbines for Geothermal Power

Water Injection for Jet Engine Thrust Augmentation

Two-Phase Nozzles for Liquid-Metal MHD Power

Two-Phase Turbines for Diesel Bottoming

Two-Phase Water Piston Turbines

Rocket Thrustors

Gas-Driven Jet Pumps for Rocket Engines

Two-Phase Water Jet Thrustors

TABLE I.3

PARAMETERS OF PREVIOUS TWO-PHASE-NOZZLE INVESTIGATIONS

Investigator	Gas/Liquid Combination	Inlet Temp/Press	Liquid Mass Fraction	Liquid Vol. Fraction	Droplet Diameter
Alger	Geothermal Steam/Water	435 F/360 psia	0.81 inlet	0.06 inlet	1 to 10 μm
Comfort & Beadle	Geothermal Steam/Water	434 F/360 psia	0.81 inlet 0.65 exit	0.06 inlet 0.01 exit	6.5 μm
Elliot & Hayes	Power Turbine Steam/oil	620 F/1450 psia	0.95		∿ 25 μm
Elliot & Weinberg	MHD Power Cesium/Lithium	1800 F/137 psia	0.93	0.28	1270 μm
	Nitrogen/Water	60 F/150 psia	0.976	0.33	780 μm
	Freon 1301/ Water	50 F/150 psia	0.75 to 0.93		
Elliot	Air/Water	50 F/514 psia	0.75 to 0.97		
Starkman et al	Steam/Water	580 F/1000 psia	0.8 to 1.0		250 μm
Schrock et al	Steam/Water	550 F/1305 psia	0.9 to 1.0		
Ahmad & Hayes	Bottoming Cycle Steam/Dowtherm A	660 f/2365 psia	0.8		

Table I.4

DROPLET HEAT TRANSFER MODEL VERSUS ISOTHERMAL MODEL

Six-Inch Nozzle Steam/DTA Inlet: 1060 R and 1000 psia
Exit: 100 psia

Model	$\dot{m}_\ell/\dot{m}_g$	At Exit					
		V_g	V_ℓ	$\bar{V}$	T_g	T_ℓ	η
		ft/sec			^oR		
Heat Transfer	5	1665	1383	1430	957	1009	0.89
Isothermal	5	1698	1417	1464	-	1060	0.93
Heat Transfer	10	1312	1065	1087	993	1030	0.88
Isothermal	10	1326	1080	1102	-	1060	0.90
Heat Transfer	20	1036	822	832	1017	1043	0.88
Isothermal	20	1041	829	839	-	1060	0.89
Heat Transfer	40	838	654	658	1033	1051	0.90
Isothermal	40	840	656	661	-	1060	0.91

Table I.5

COMPARISON OF ISOTHERMAL MODELS ($T_\ell = T_g = T_{inlet}$ = constant)

6-inch Nozzle
Steam/DTA

Inlet: 1060 R, 1000 psia
Exit: 100 psia

Model	$\dot{m}_\ell/\dot{m}_g$	V_ℓ/V_g	At Exit			
			V_g	V_ℓ	$\bar{V}$	
			ft/sec			
Isothermal	0	0	3674	-	3674	All-Gas
Rudinger	0	0	3674	-	3674	
Isentropic	0	0	3245	-	3245	
Isothermal (Varying V_ℓ/V_g)	40	0.78	840	656	661	
Rudinger (V_ℓ/V_g=const=0.83)	40	0.83	792	657	660	
Rudinger (V_ℓ/V_g=const=0.78)	40	0.78	824	643	657	
Isentropic	40	1.00	571	571	571	
Isothermal	1000	0.82	508	417	417	Nearly
Rudinger ($V_\ell=V_g$=const=0.82)	1000	0.82	510	418	418	All-Liquid
Isentropic	1000	1.00	116	116	116	

Table I.6

COMPARISON OF FOUR MODELS

50-inch Nozzle with Nitrogen/Water
Inlet: 520 R and 150 psia
Exit: 14.1 psia
$\dot{m}_\ell/\dot{m}_g = 40$

Model	Exit Values					
	V_g	V_ℓ	$\bar{V}$	T_g	T_ℓ	η
	ft/sec			^oR		
Rudinger Isothermal Model $V_\ell/V_g = 0.7$	437	306	309	520	-	0.758
Isothermal Model Varying V_ℓ/V_g	502	301	306	520	-	0.743
Droplet Heat Transfer Model dP/dX = const	496	300	305	503	518.6	0.736
2-line Curvefit to Elliott and Weinberg P Profile	504	298	302	502	518.6	0.726
3-line Curvefit to Elliott and Weinberg P Profile	462	300	303	505	518.6	0.730
Elliott and Weinberg Model Optimum dP/dX	425	300	303	508	518.3	0.729

FIG. I.1

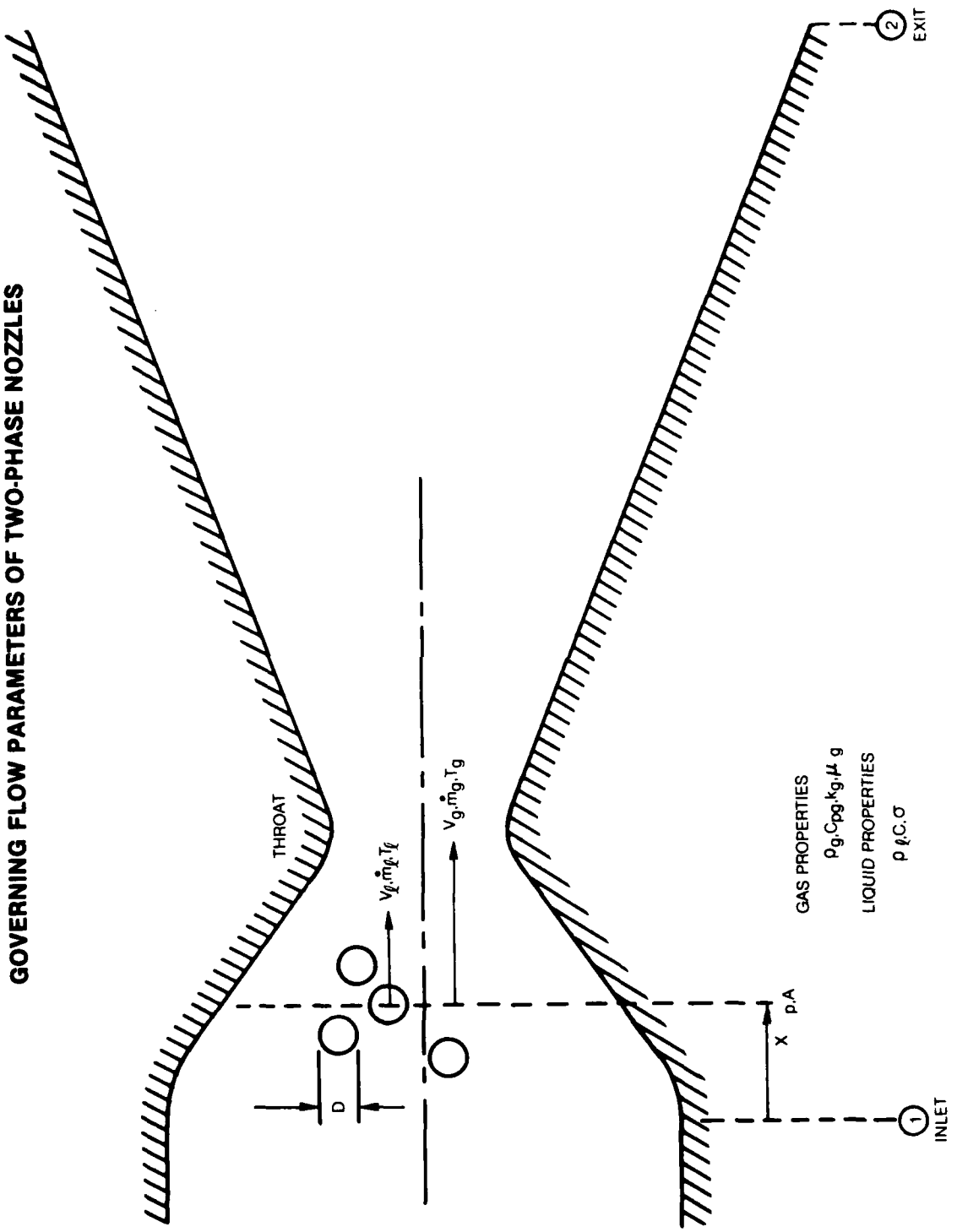
GOVERNING FLOW PARAMETERS OF TWO-PHASE NOZZLES
THROAT
EXIT
INLET
D
$V_\ell, \dot{m}_\ell, T_\ell$
$V_g, \dot{m}_g, T_g$
p,A
x
GAS PROPERTIES
$\rho_g, C_{pg}, k_g, \mu_g$
LIQUID PROPERTIES
ρ_ℓ, C, σ
79-11-106-17

EFFECT OF LOADING RATIO ON TEMPERATURE DROP OF A HOMOGENEOUS TWO-PHASE MIXTURE THROUGH A NOZZLE

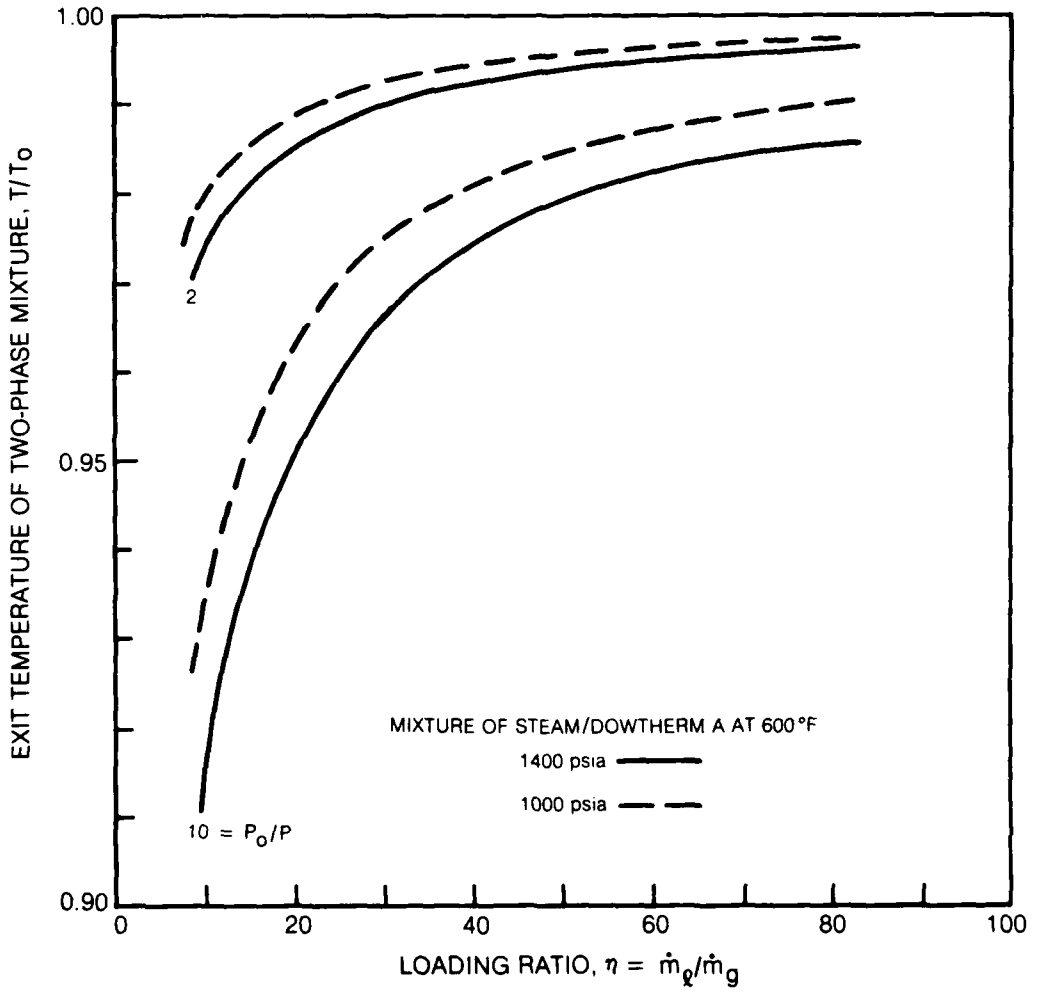

79-11-106-16

T-S CYCLE PATHS FOR TWO-PHASE AND SINGLE-PHASE TURBINES

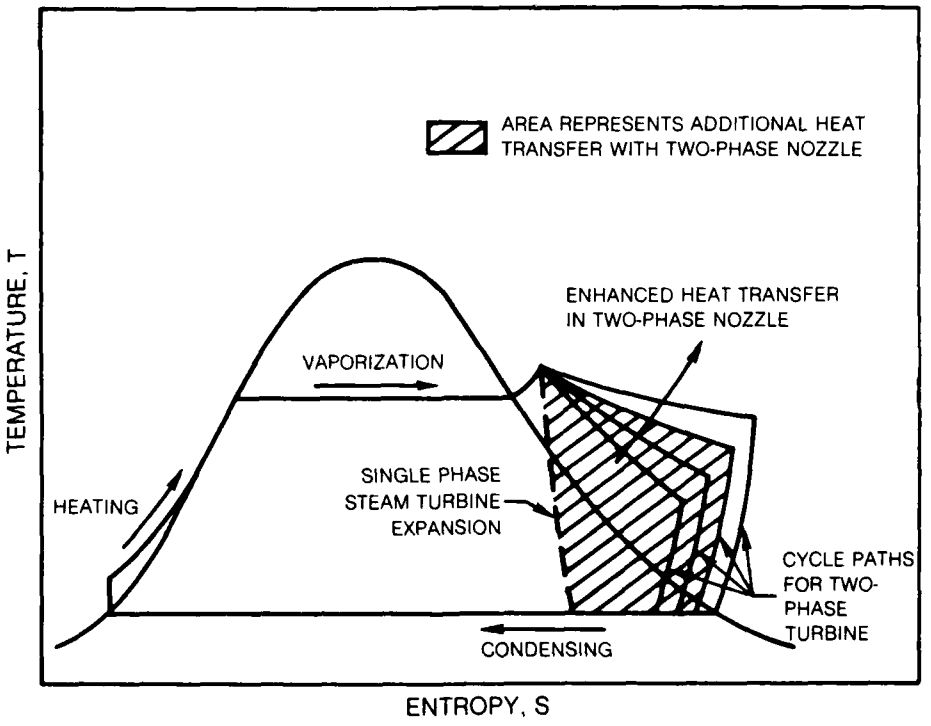

78-11-08-6

MAXIMUM DROPLET SIZE BASED ON WEBER DROPLET BREAKUP CRITERION

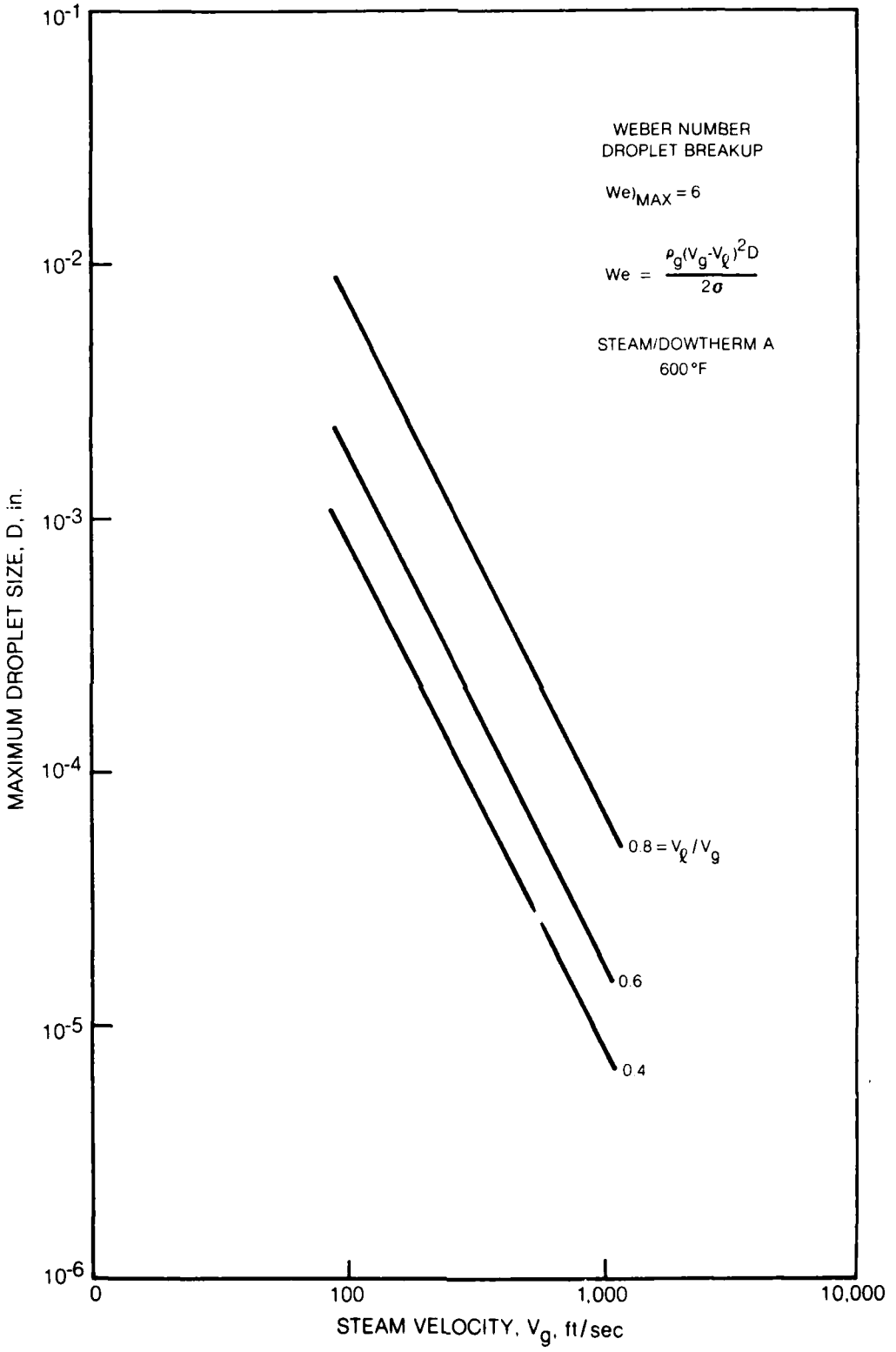

80-5-123-1

FIG. I.5

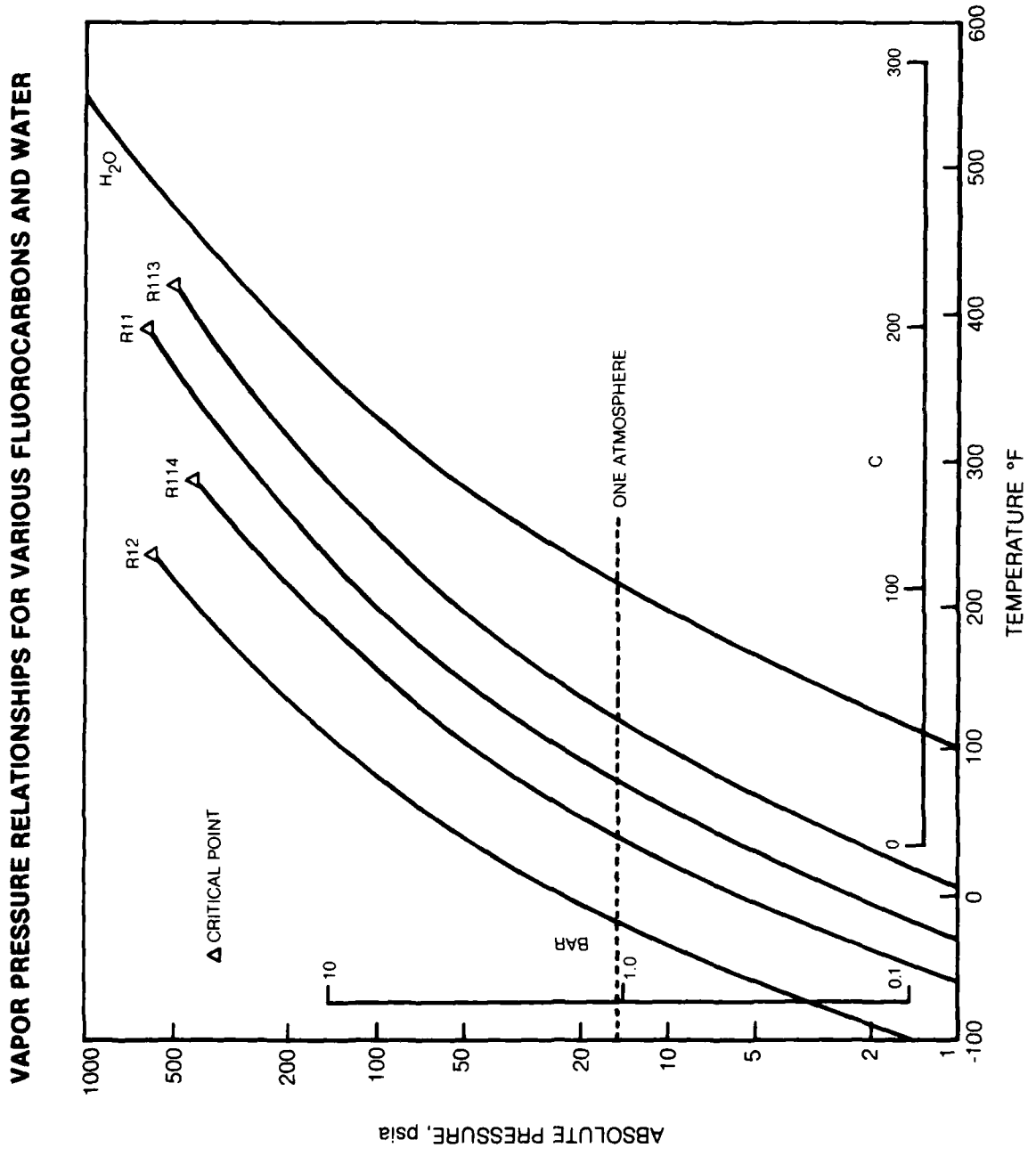
VAPOR PRESSURE RELATIONSHIPS FOR VARIOUS FLUOROCARBONS AND WATER
ABSOLUTE PRESSURE, psia
1000
500
200
100
50
20
10
5
2
1
BAR
10
1.0
0.1
H_2O
R11
R113
R12
R114
CRITICAL POINT
ONE ATMOSPHERE
C
0
100
200
300
TEMPERATURE °F
-100
0
100
200
300
400
500
600
79-11-106-14

FIG. I.6

MOMENTUM FLUX AND VELOCITY OF HOMOGENEOUS GAS — DROPLET MIXTURES

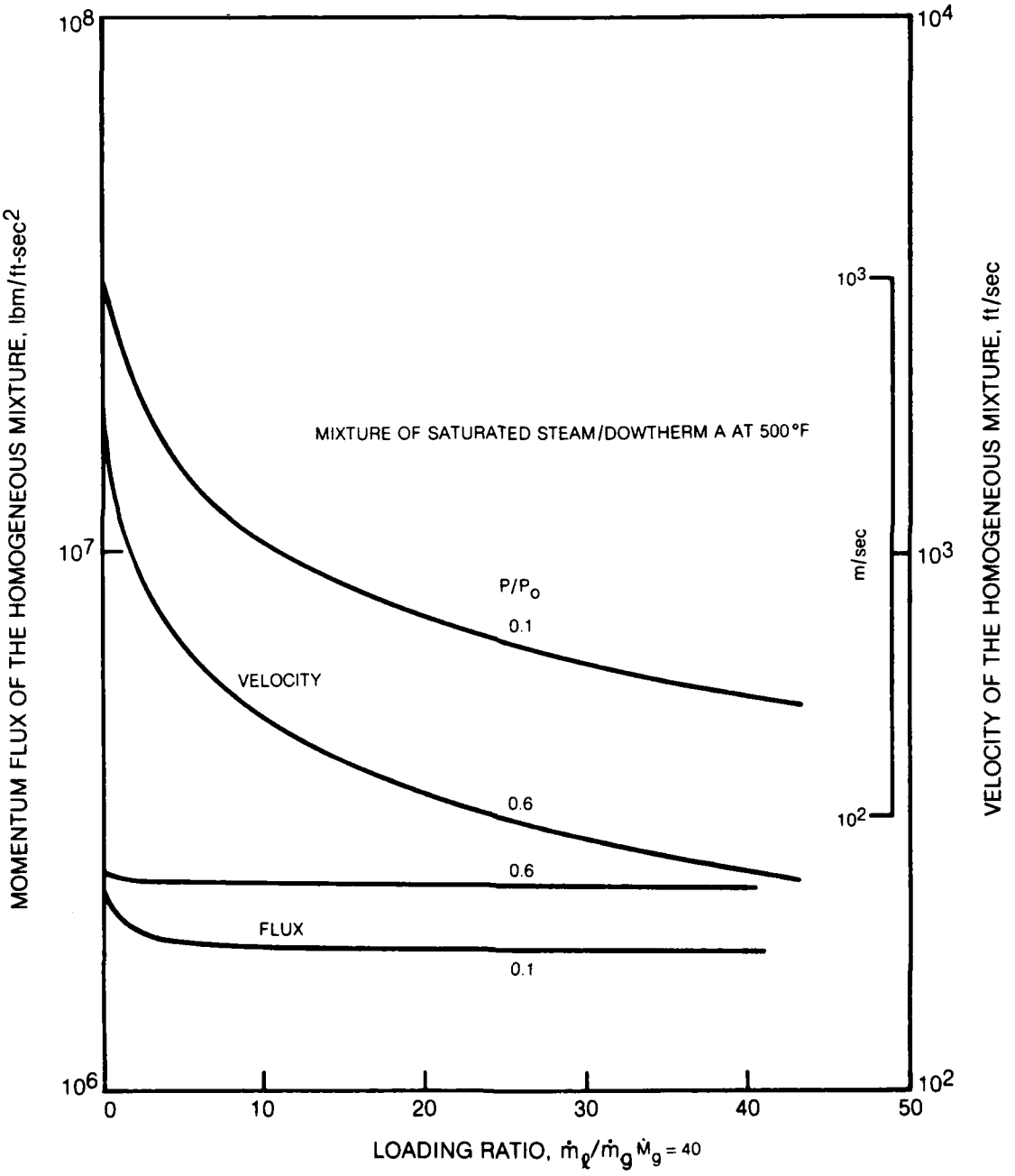

79-11-106-13

RELATIONSHIP BETWEEN LOADING RATIO, DENSITY RATIO, AND PARTICLE VOLUME FRACTION

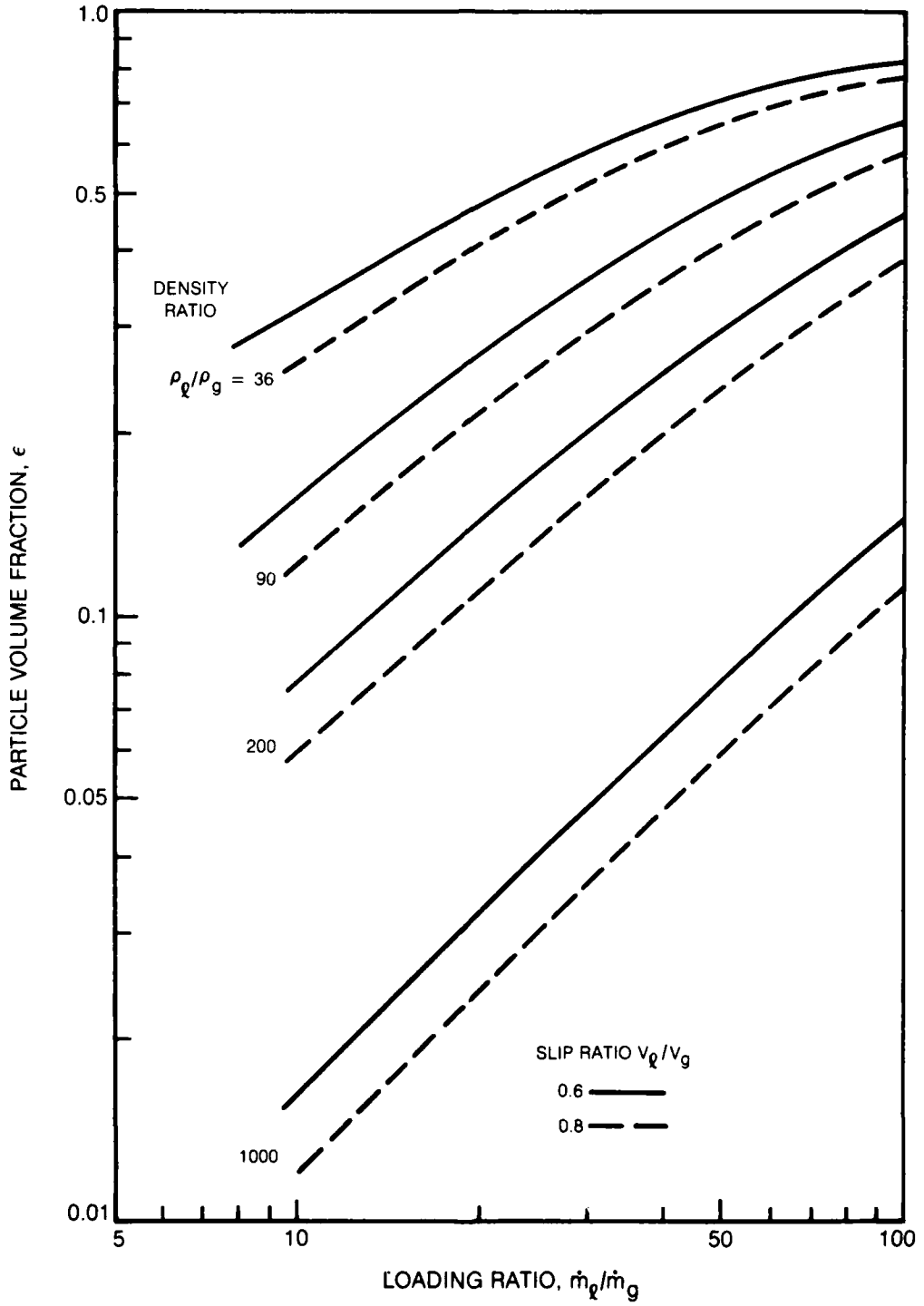

79-11-106-12

NOZZLE PARAMETERS CALCULATED WITH THE ISOTHERMAL RUDINGER MODEL

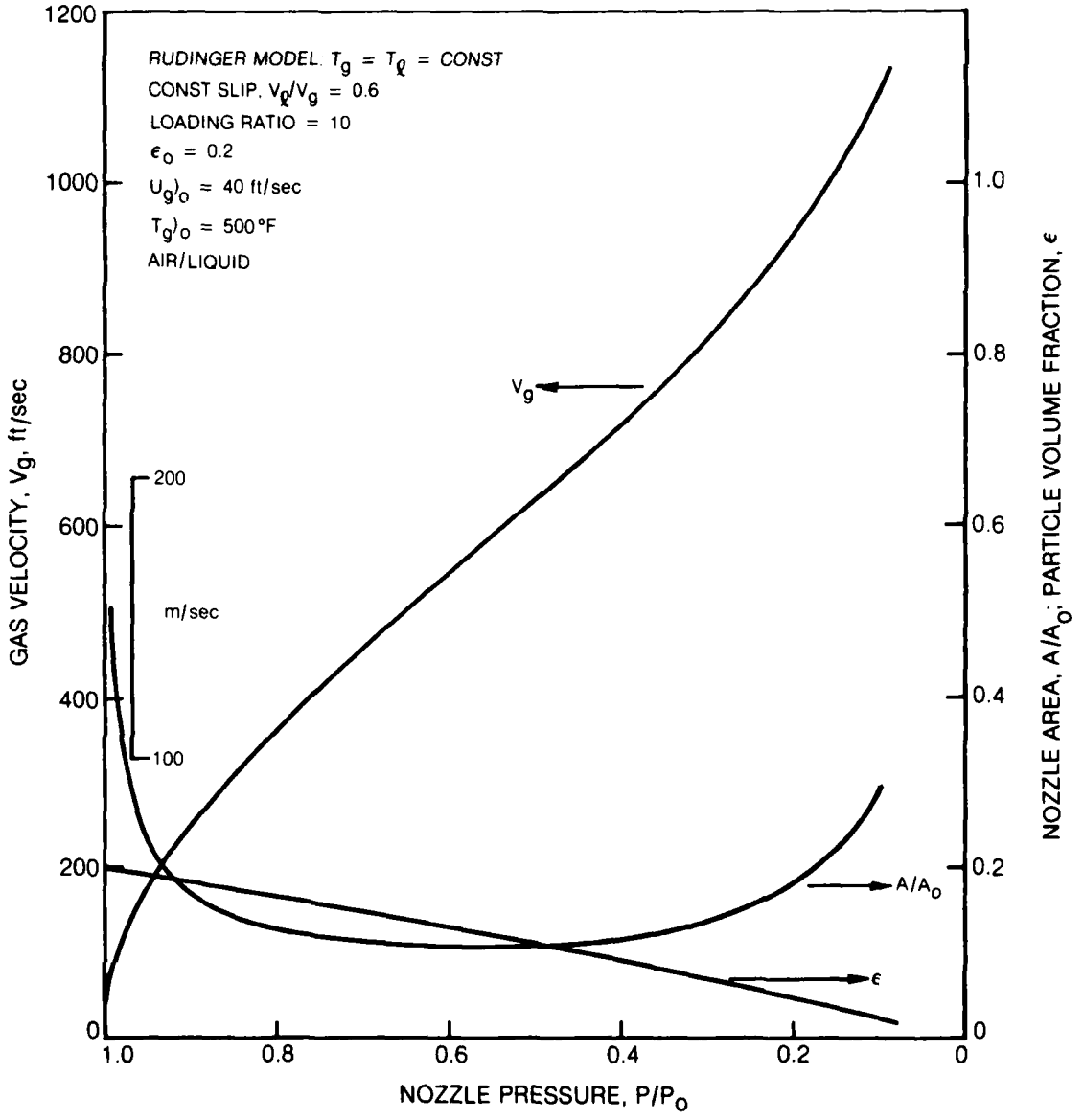

79-11-106-11

EFFECT OF INLET PARTICLE VOLUME ON GAS EXIT VELOCITY

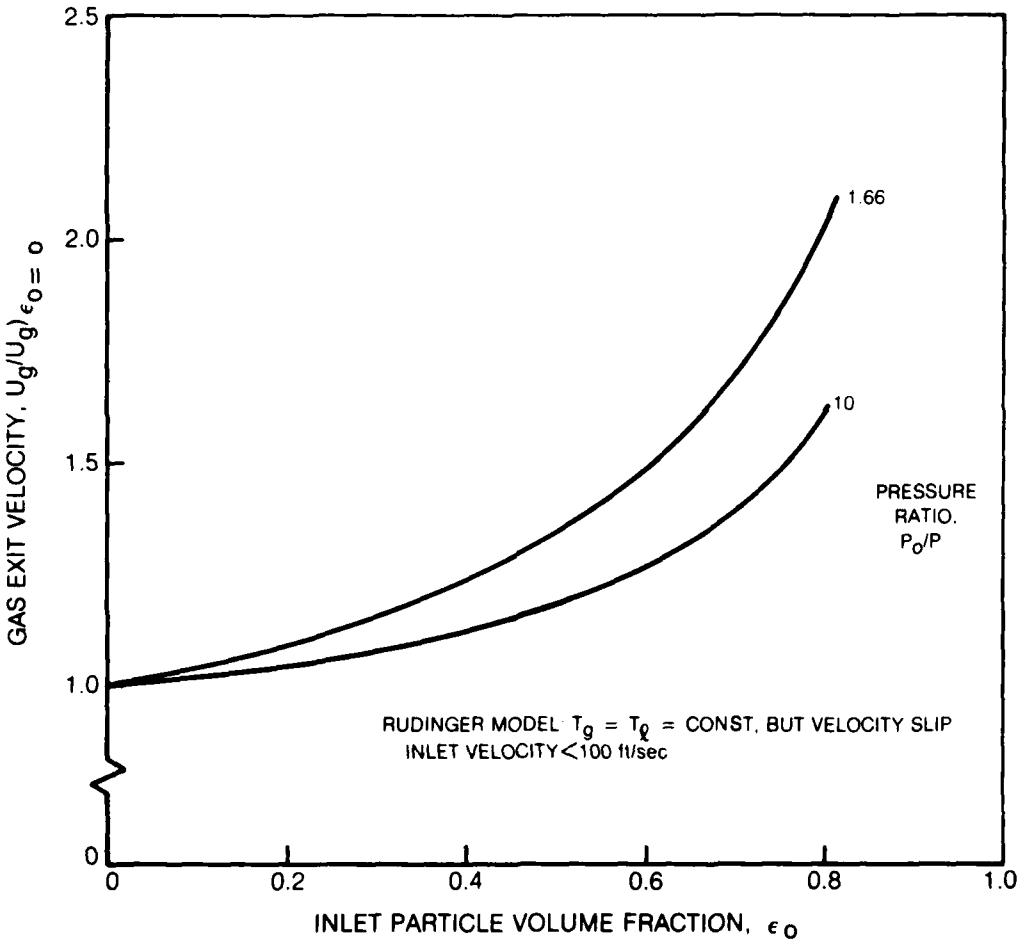

79-11-106-10

EFFECT OF INLET PARTICLE VOLUME ON THROAT PRESSURE RATIO

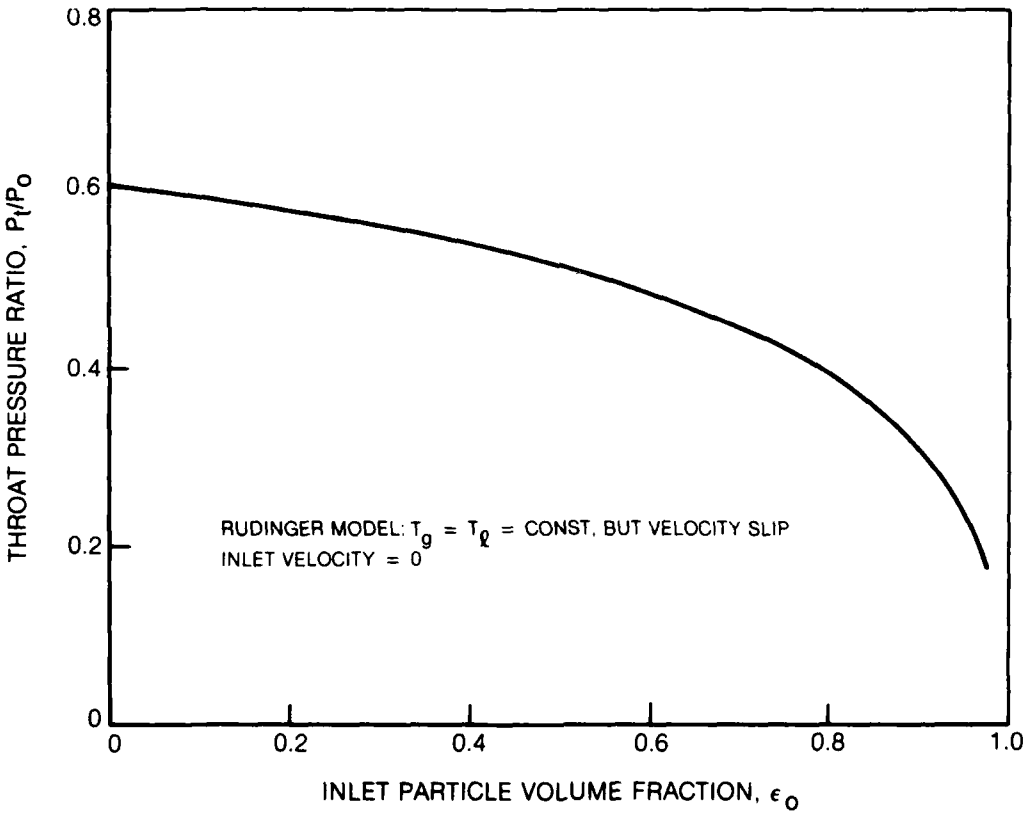

79-11-106-9

COMPARISON OF HOMOGENEOUS WITH SEPARATED MODELS

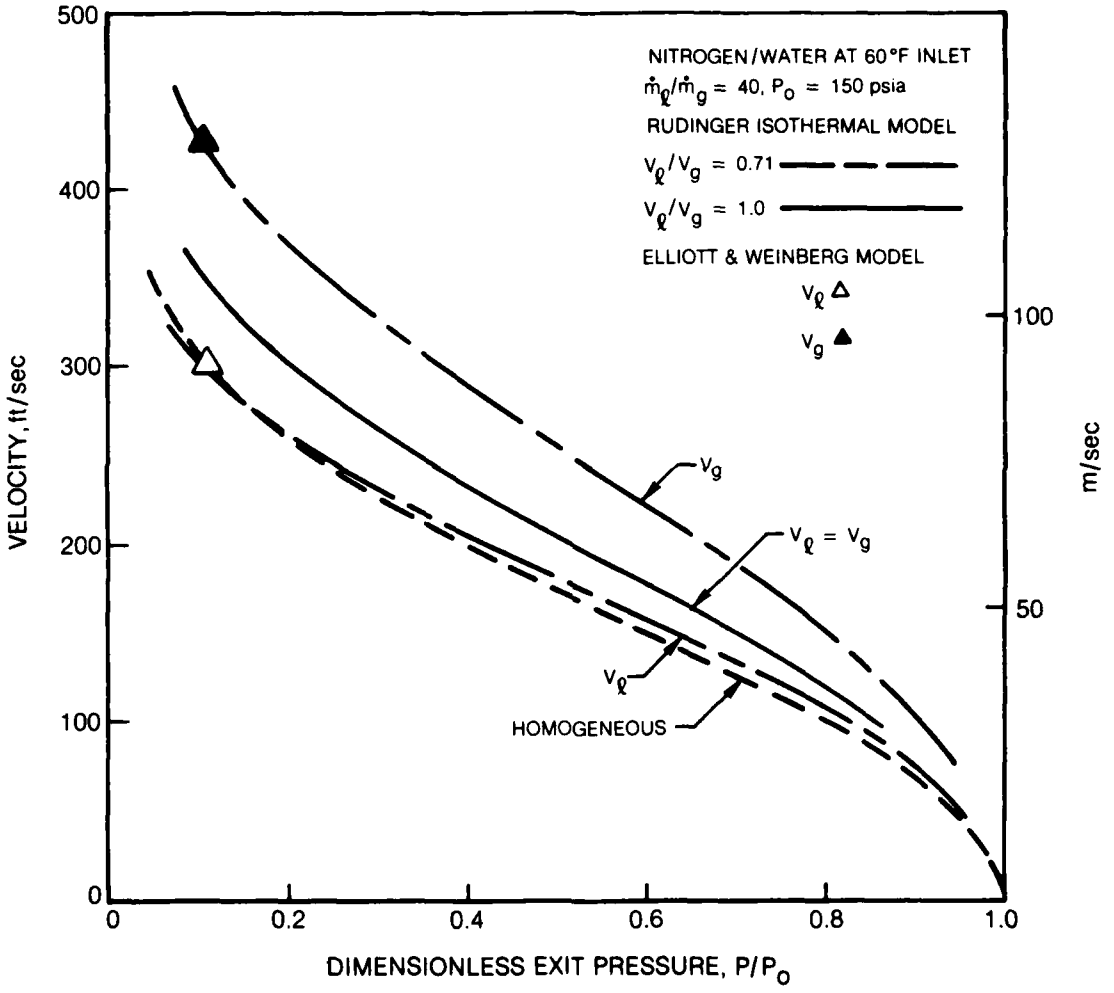

79-11-106-8

COMPARISON OF HOMOGENEOUS WITH PARTIALLY SEPARATED MODEL

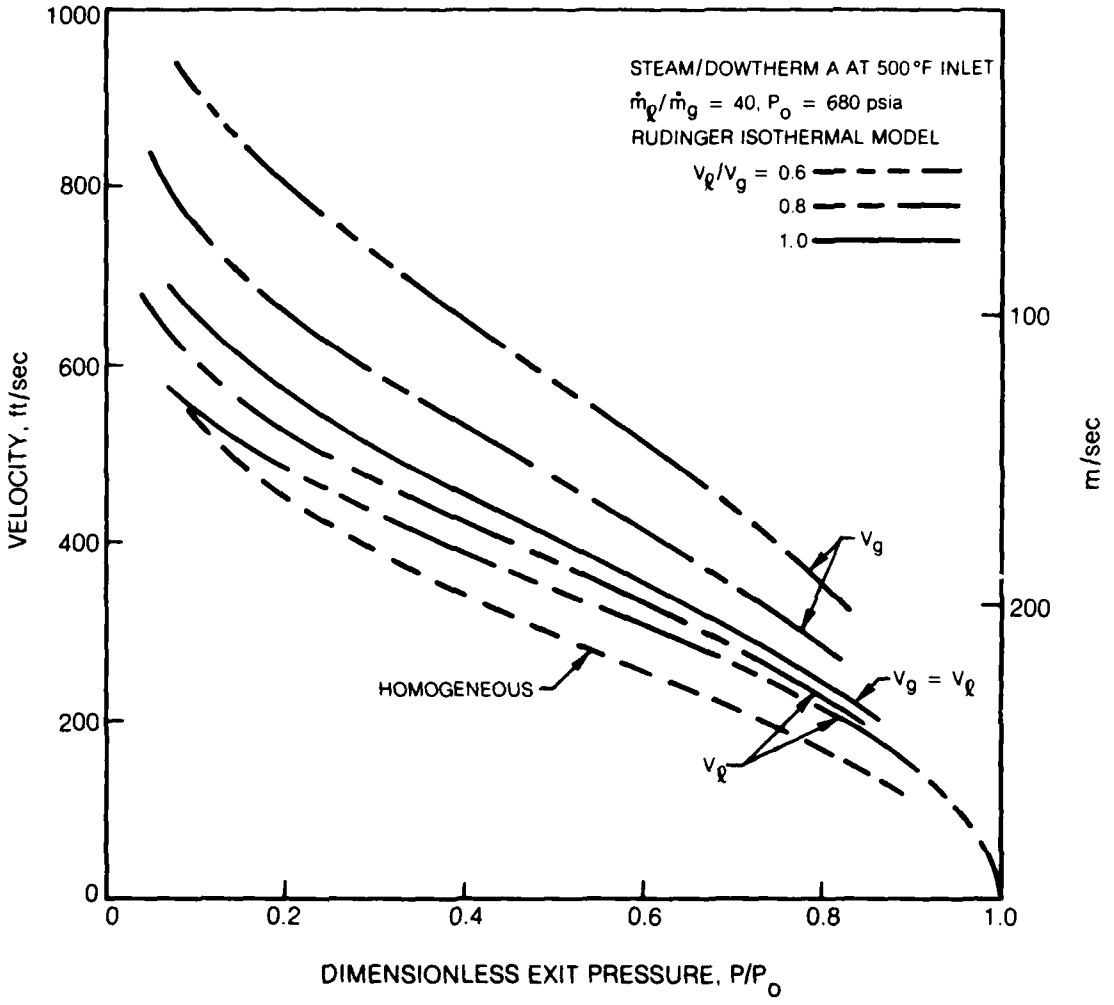

79-11-106-7

COMPARISON OF MOMENTUM FLUX AS CALCULATED WITH THE HOMOGENEOUS AND ISOTHERMAL MODELS

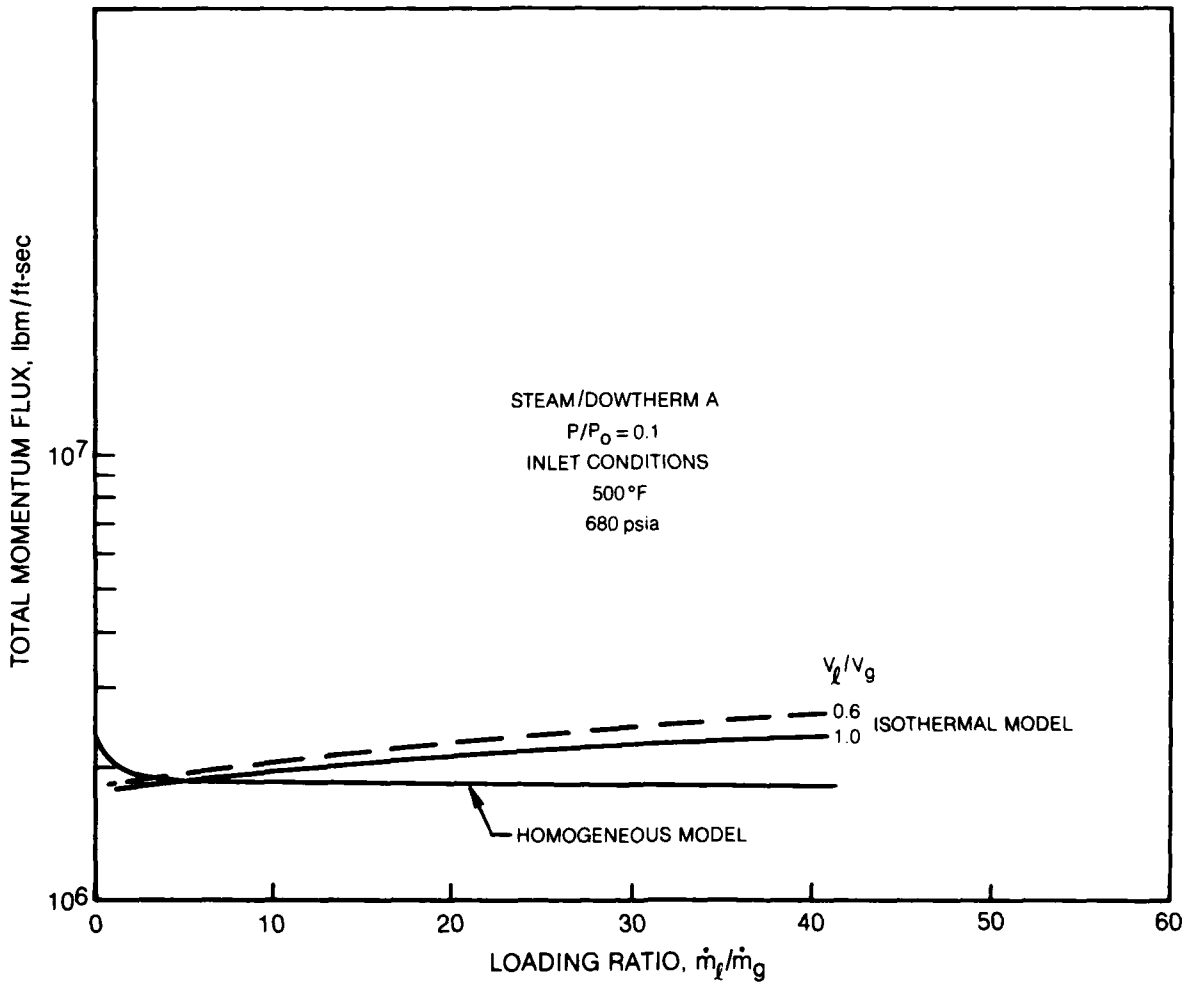

79-11-106-6

FIG. I.14

SIMPLIFIED MODEL TO ESTIMATE HEAT TRANSFER RATE EFFECTS

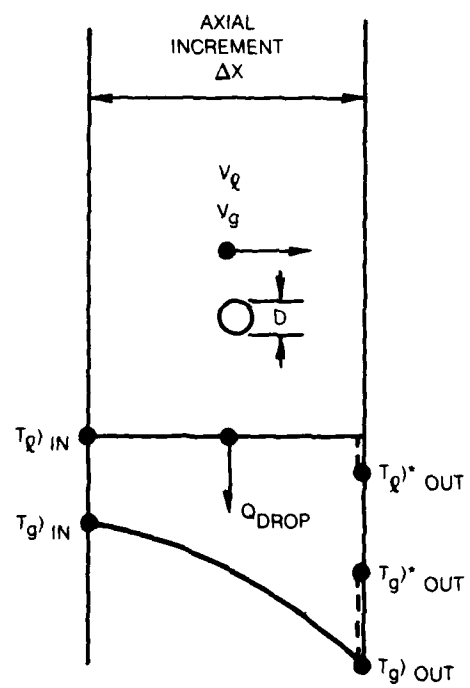

79-11-106-5

EFFECT OF DROPLET SIZE AND VELOCITY ON DROPLET HEAT TRANSFER

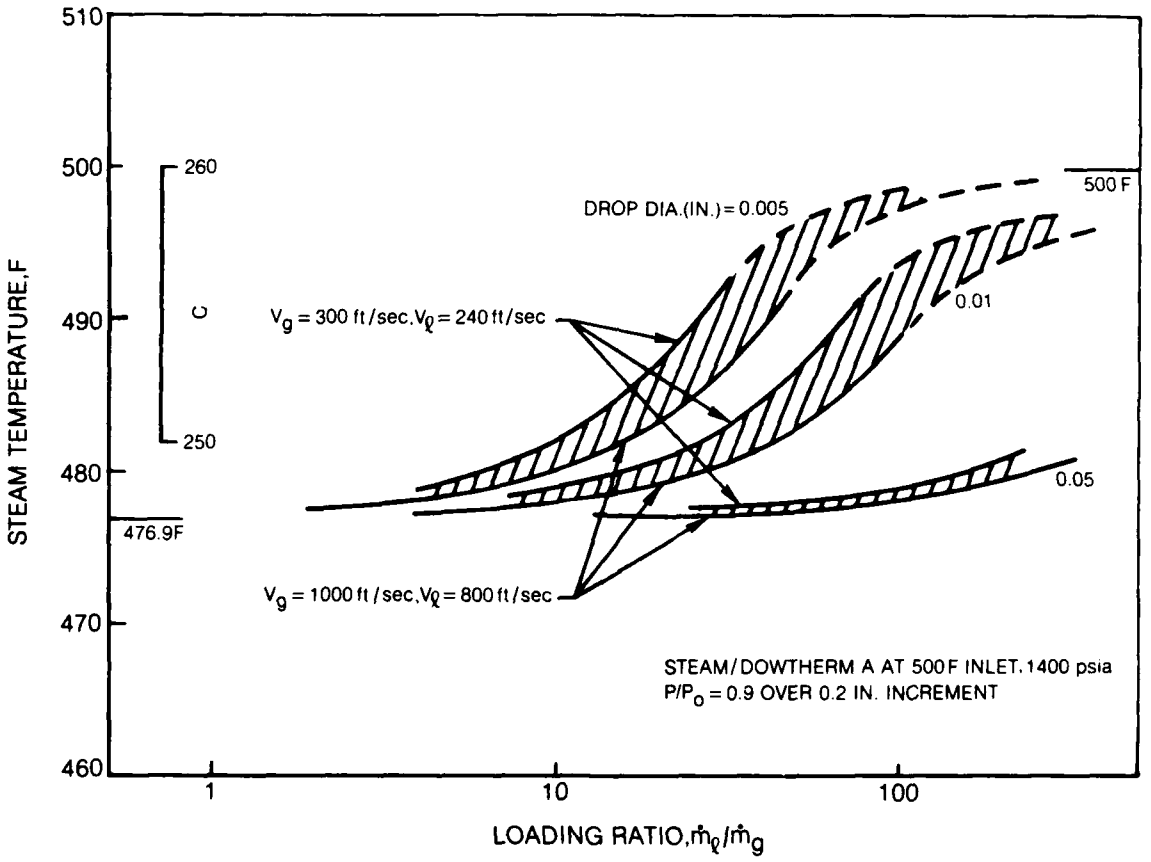

79-11-106-4

FIG. I.16

EFFECT OF LIQUID-GAS TEMPERATURE DIFFERENTIAL ON DROPLET HEAT TRANSFER

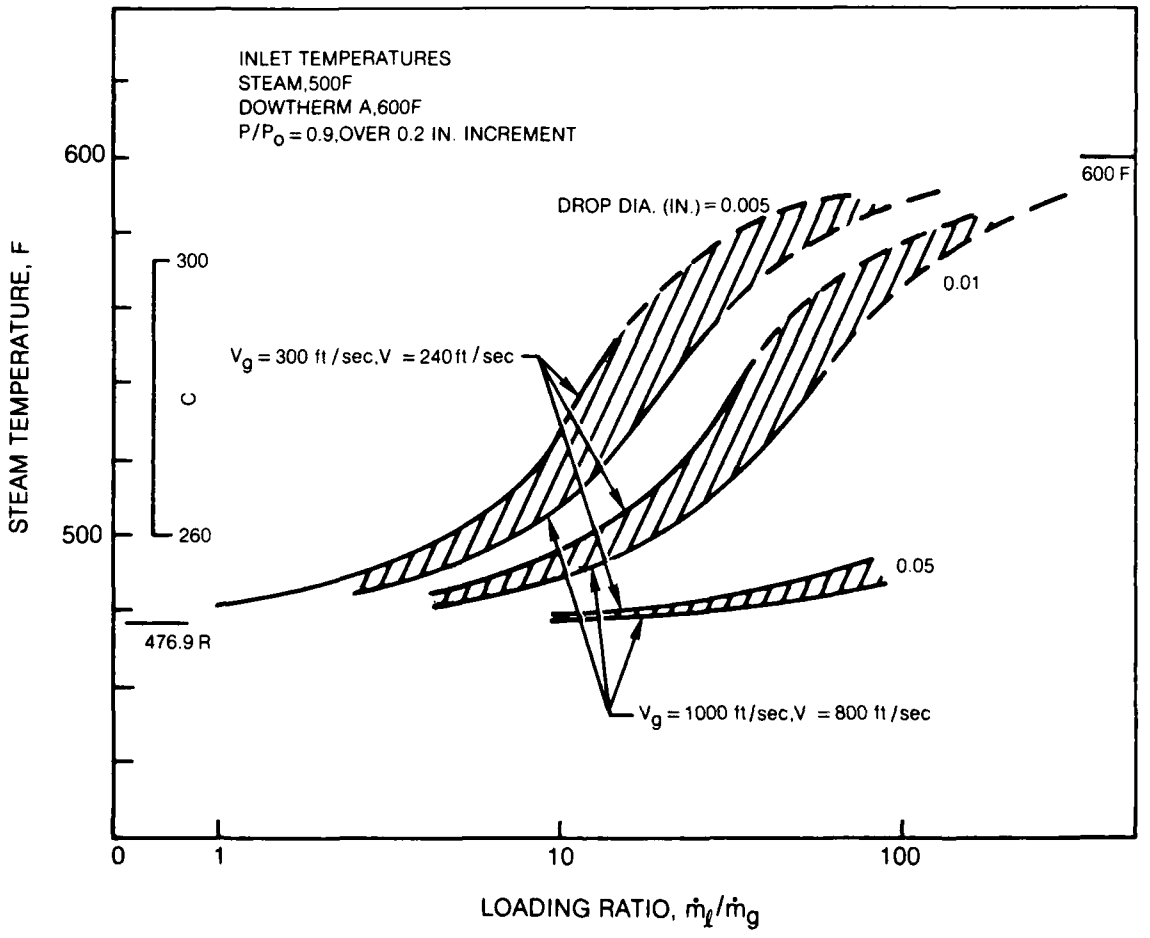

79-11-106-3

EQUILIBRIUM SPEED OF SOUND IN A HOMOGENEOUS TWO-PHASE MIXTURE

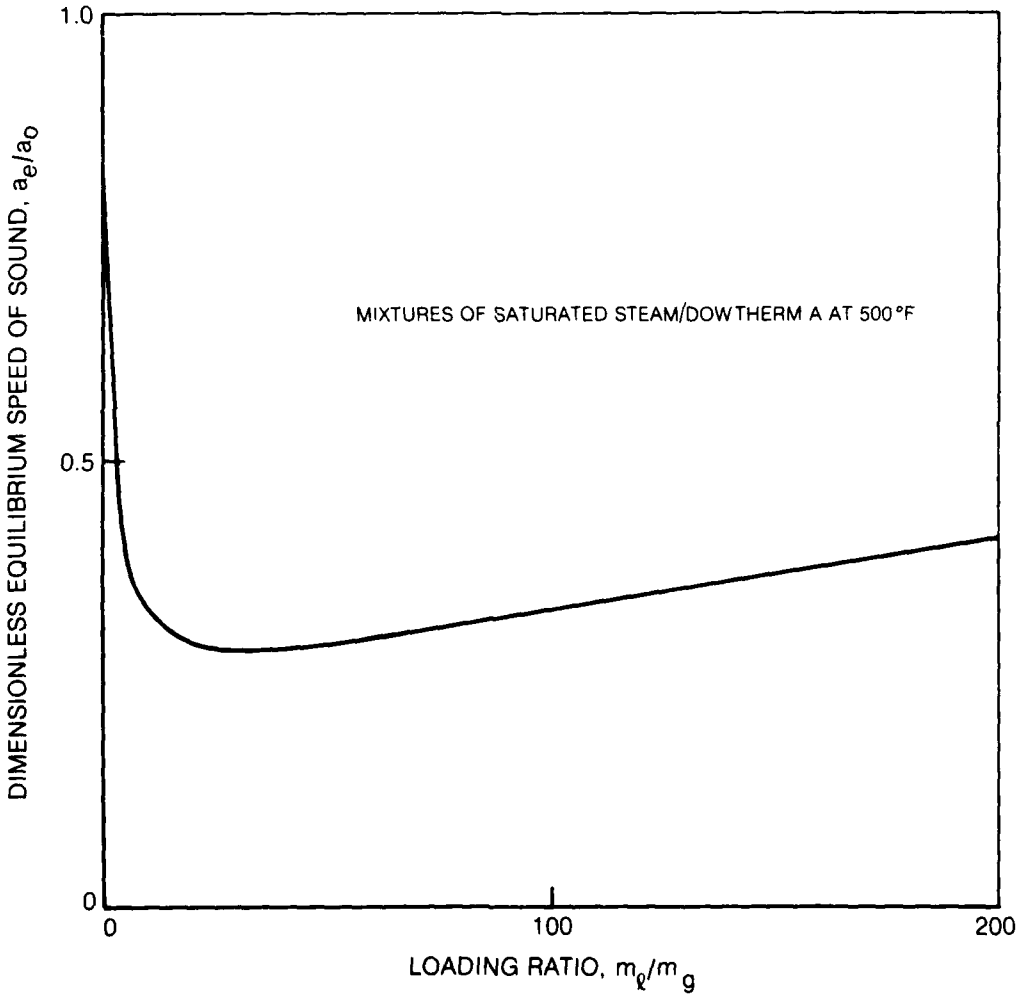

79-11-106-2

FIG. I.18

DIMENSIONLESS RESIDENCE TIME FOR VELOCITY EQUILIBRIUM

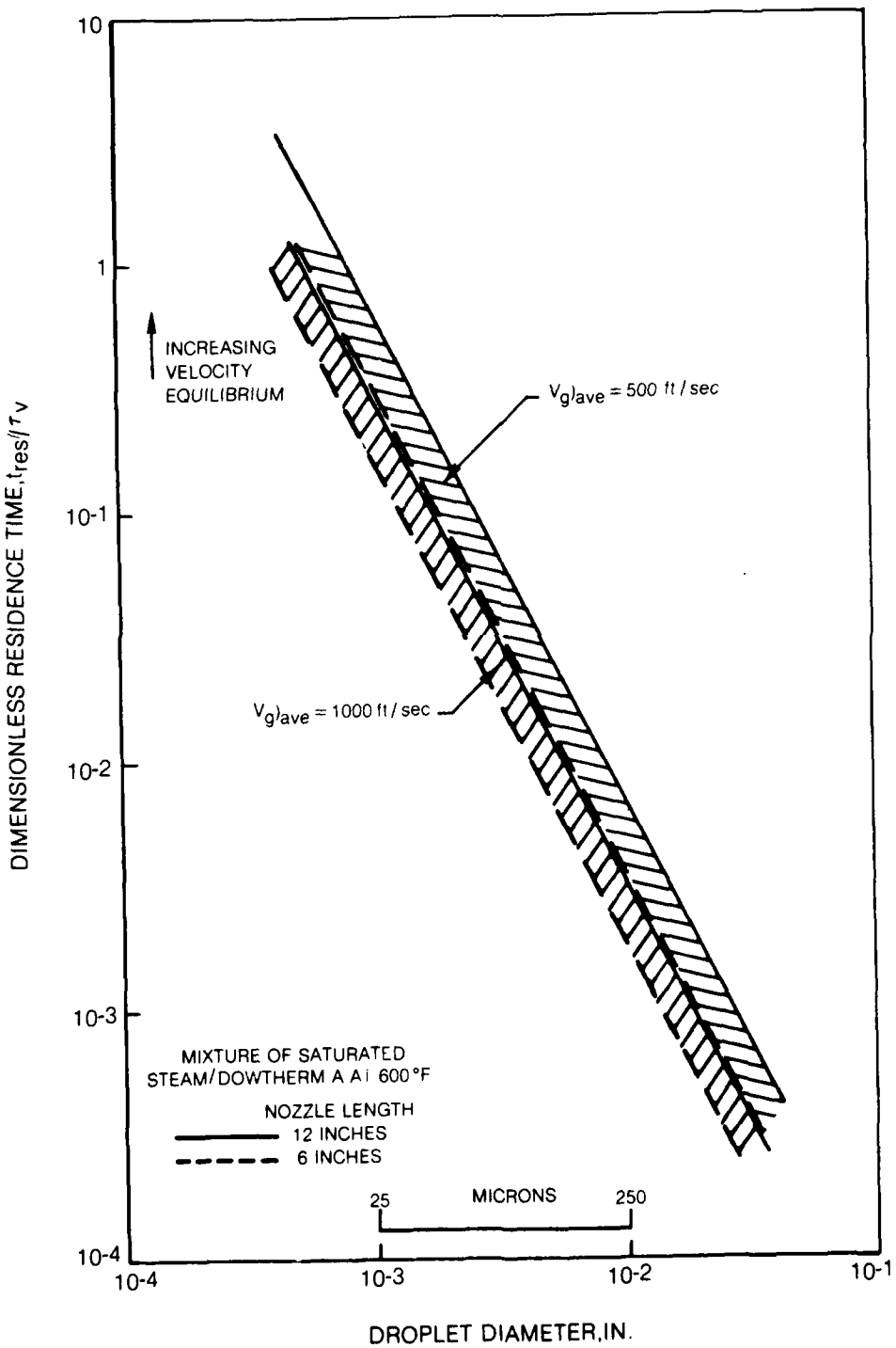

79-11-106-1

FIG. I.19

FORCE BALANCE WITH DRAG ON LIQUID DROPLET

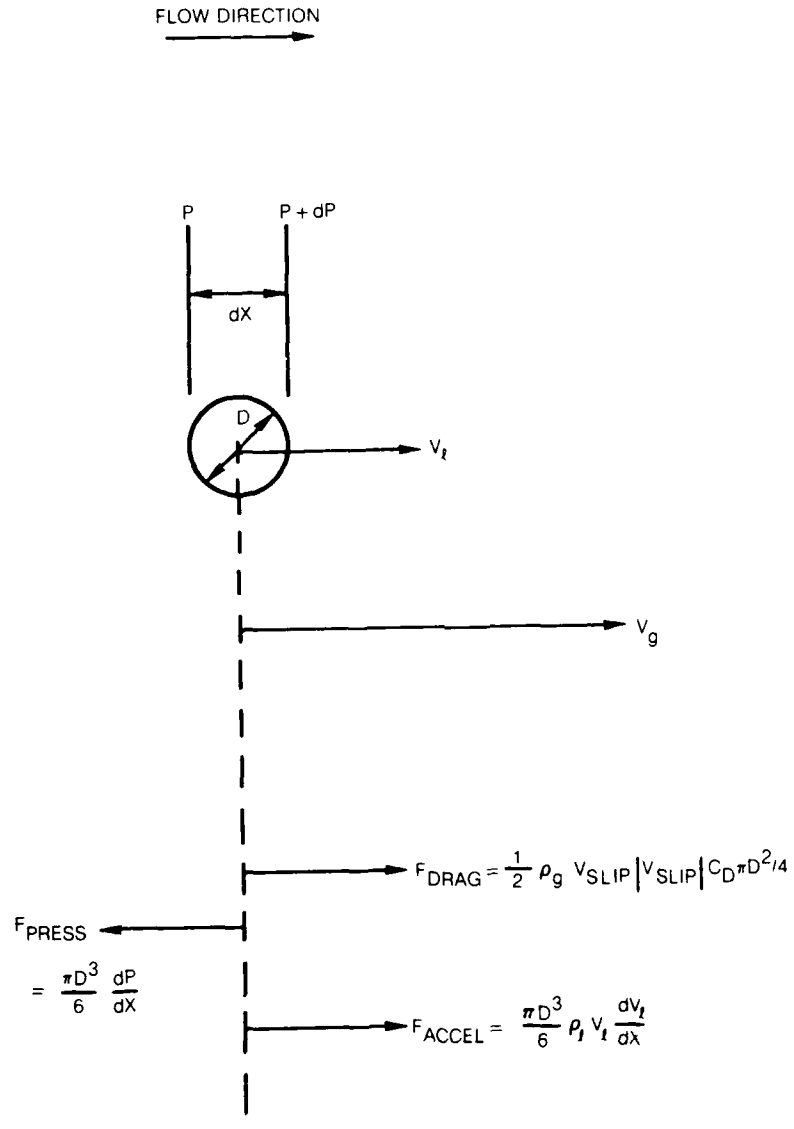

$$F_{DRAG} - F_{PRESS} = F_{ACCEL}$$

80-5-123-9

FIG. I.20

COMPARISON OF DRAG COEFFICIENTS

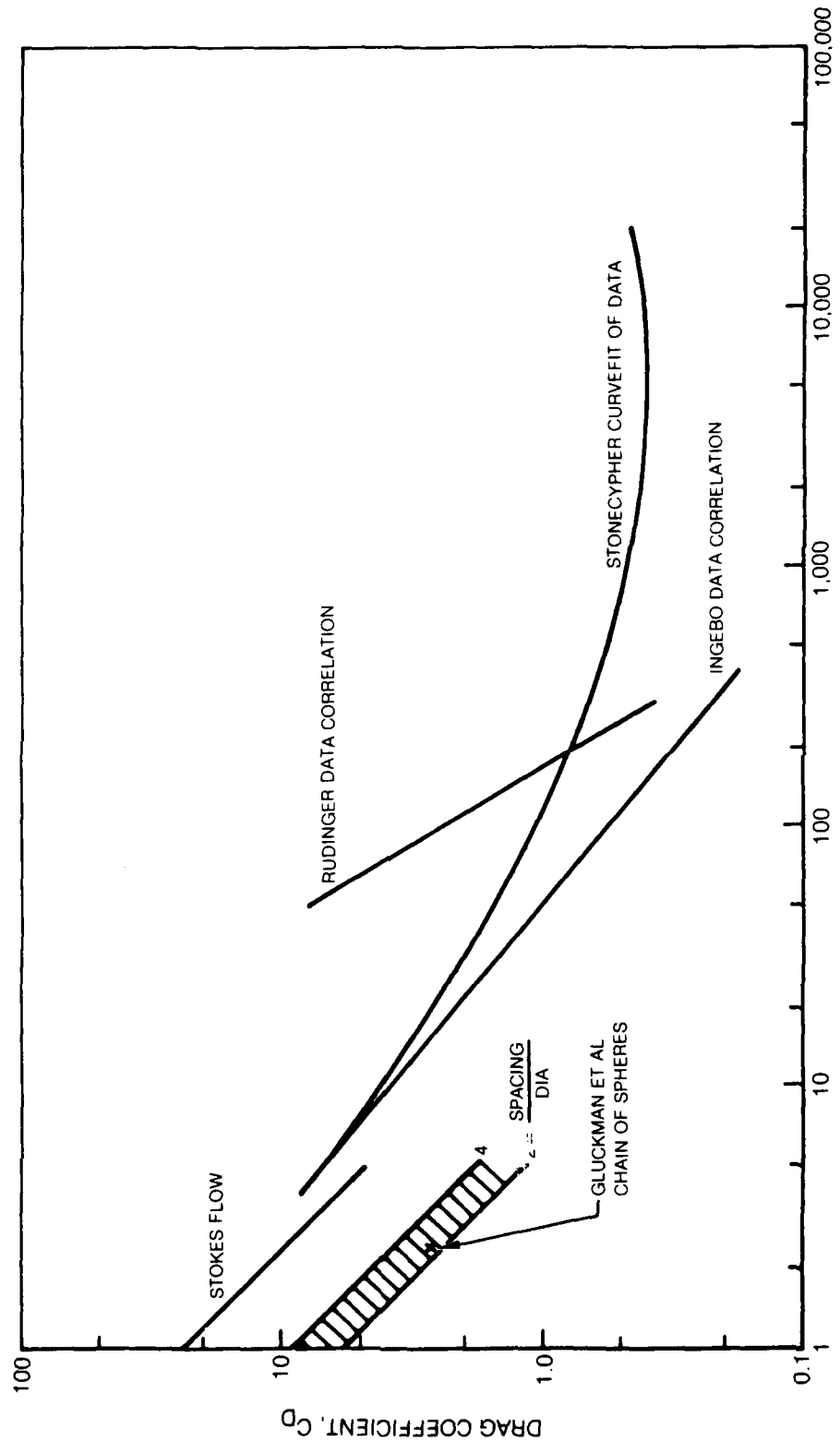

80-6-123-8

SURFACE TENSION OF SELECTED FLUIDS

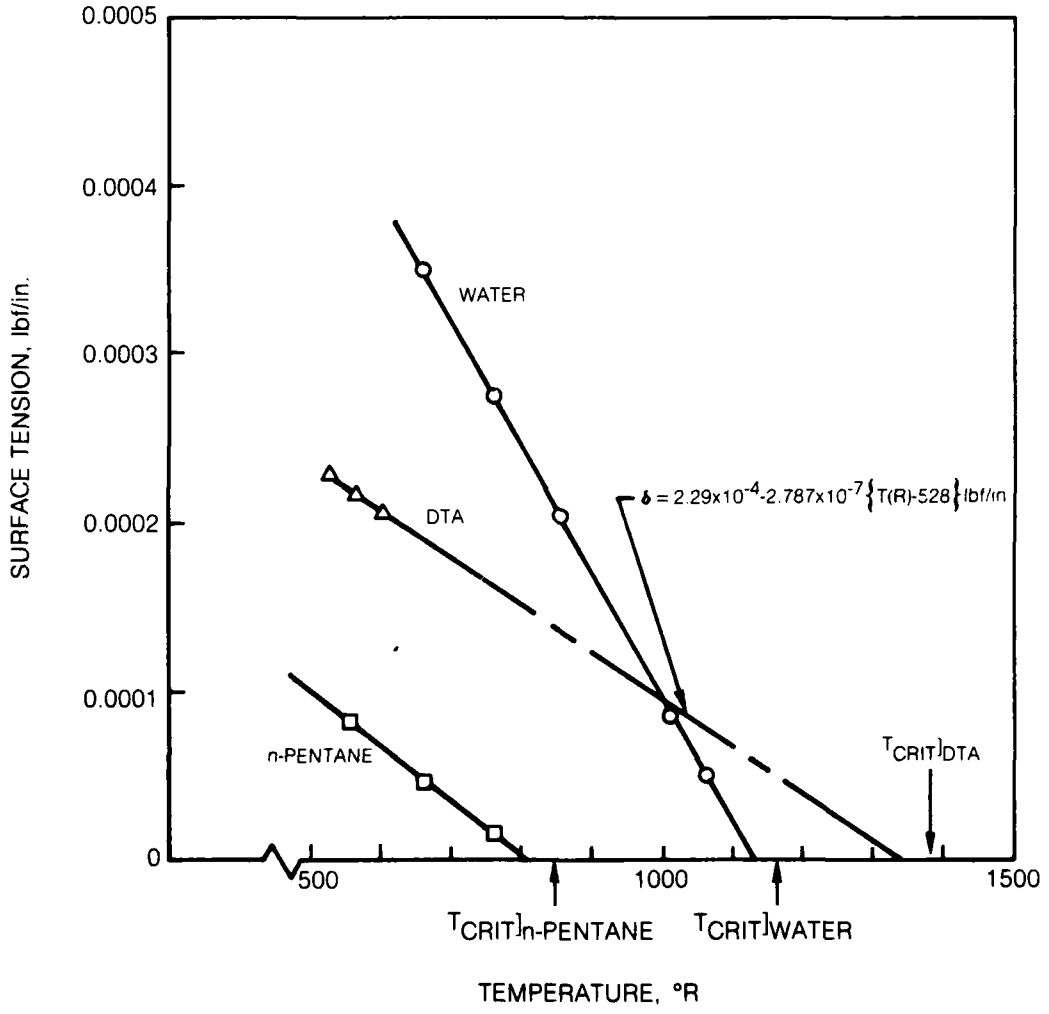

80-5-123-7

FIG. I.22

RESULTS FROM COMPUTERIZED TWO-PHASE NOZZLE MODELS

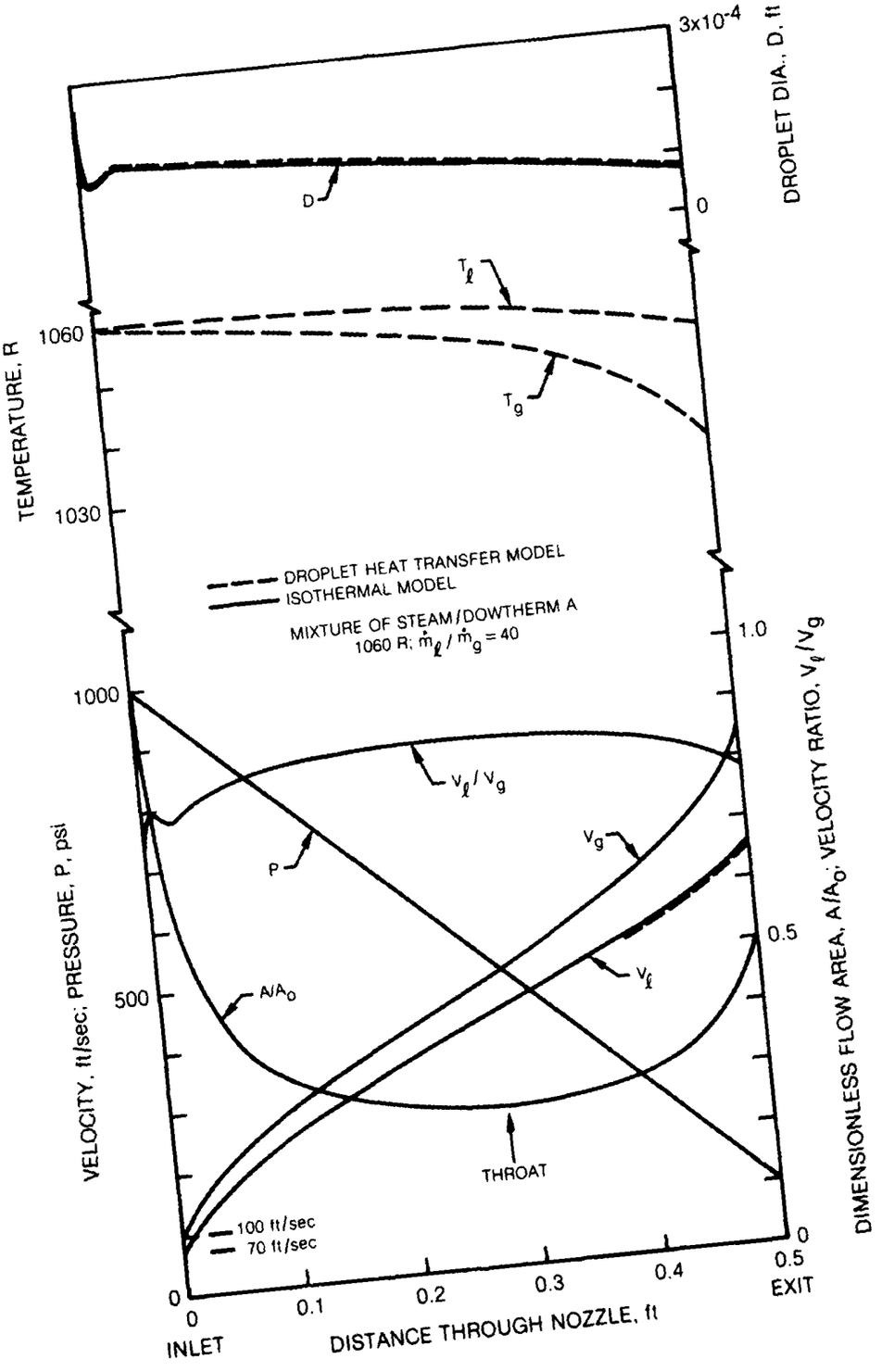

80-6-123-6

FIG. I.23

ALL-GAS RESULTS FROM ISOTHERMAL MODELS

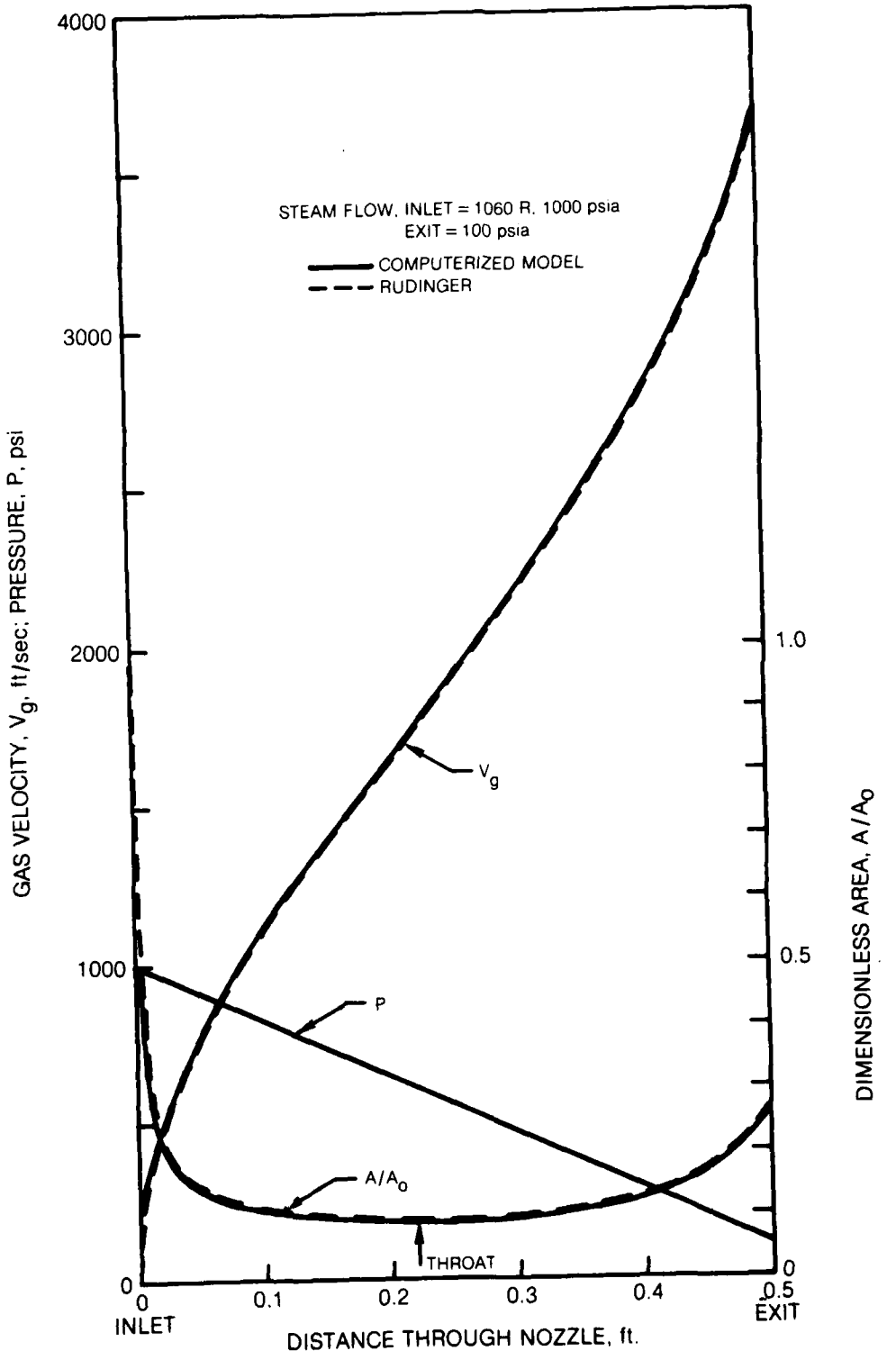

80-5-123-5

PRESSURE PROFILES FOR 50-INCH WATER/NITROGEN NOZZLE

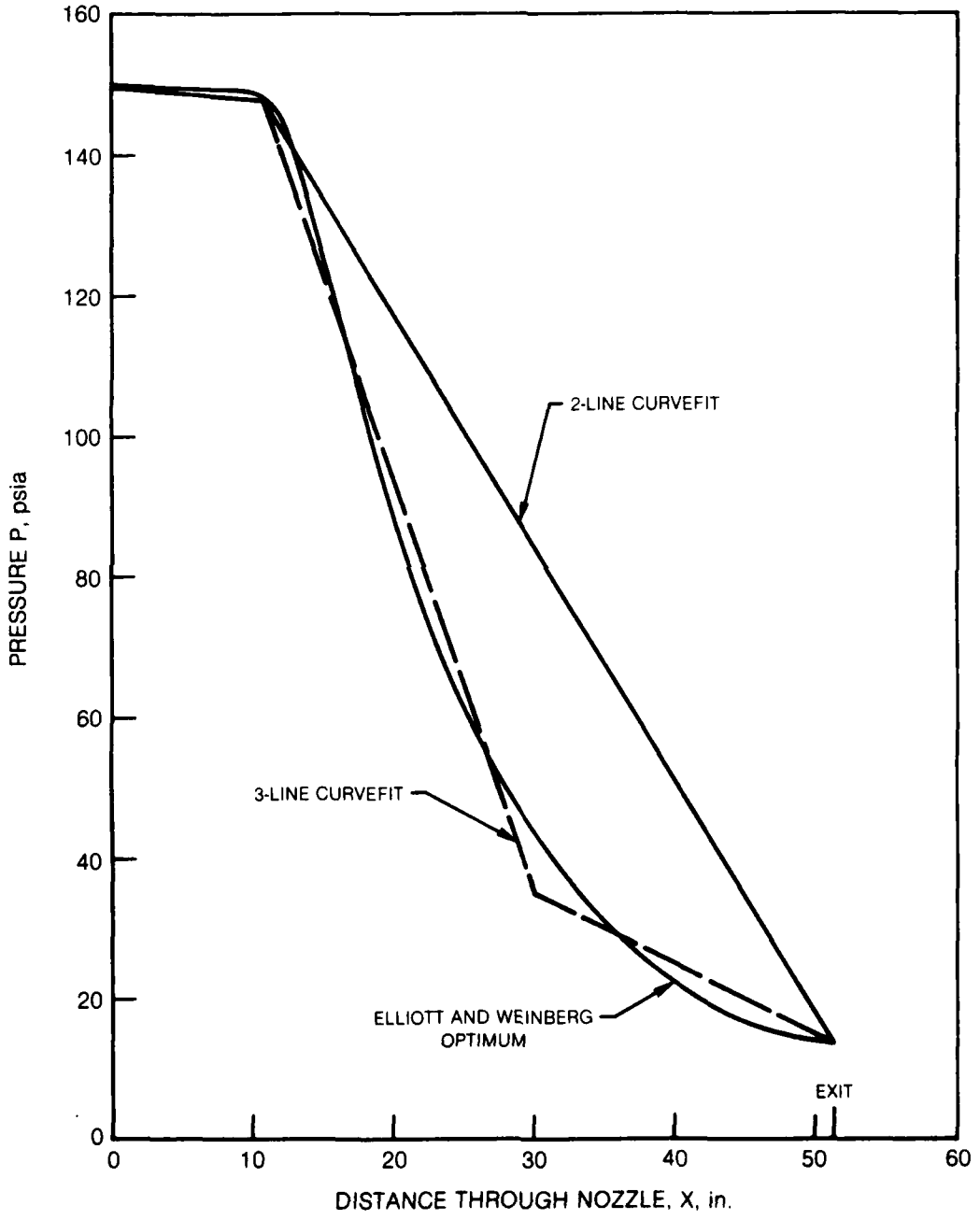

80-6-123-4

FIG. I.25

COMPARISON OF COMPUTERIZED MODELS WITH EXPERIMENTAL EXIT VELOCITIES FOR SIX-INCH NOZZLE AND WITH ELLIOTT AND WEINBERG MODELS

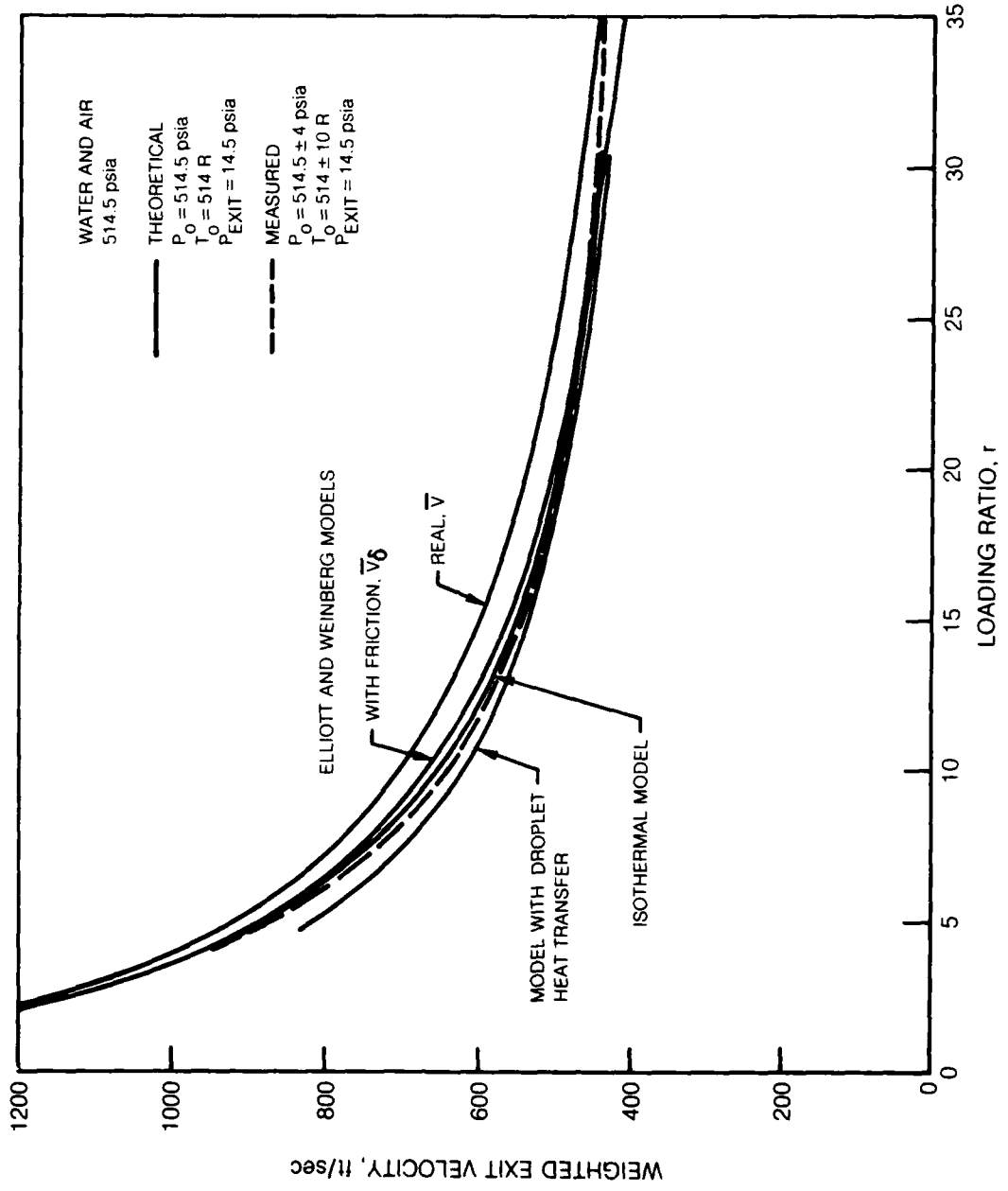

80-5-123-3

FIG. I.26

EFFECT OF INLET TEMPERATURE DIFFERENTIAL ON NOZZLE RESULTS

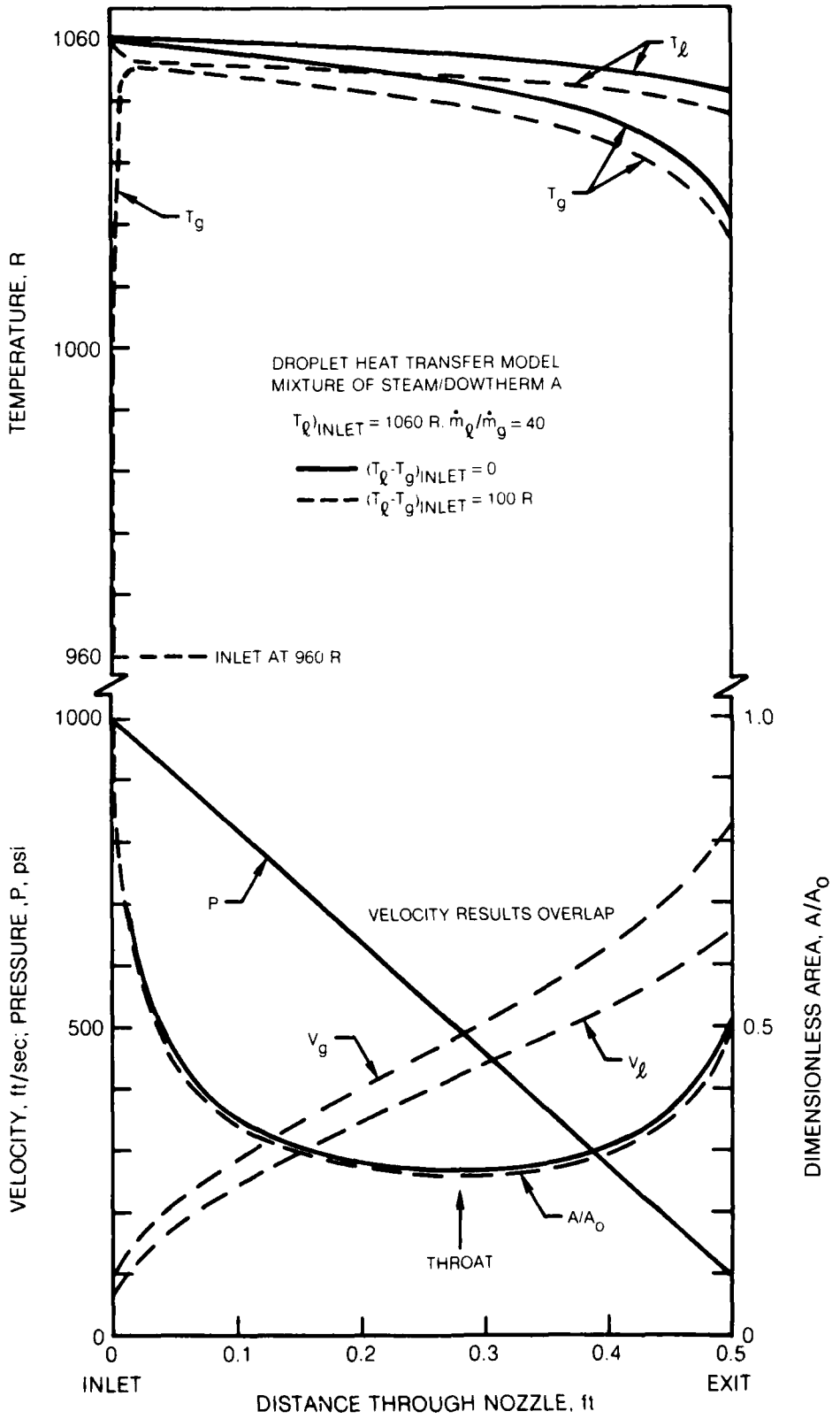

80-5-123-2

DISTRIBUTION LIST

TWO PHASE FLOW

	One copy except as noted
Mr. M. Keith Ellingsworth Power Program, Code 473 Office of Naval Research 800 N. Quincy Street Arlington, VA 22217	5
Defense Documentation Center Building 5, Cameron Station Alexandria, VA 22314	12
Technical Information Division Naval Research Laboratory 4555 Overlook Avenue SW Washington, DC 20375	6
Professor Paul Marto Department of Mechanical Engineering US Naval Post Graduate School Monterey, CA 93940	
Professor Bruce Rankin Naval Systems Engineering US Naval Academy Annapolis, MD 21402	
Dr. Al Wood Office of Naval Research Eastern/ Central Regional Office Bldg. 114, Section D 666 Summer Street Boston, Massachusetts 02210	
Mr. Mike Chaszeyka Office of Naval Research Branch Office 536 South Clark Street Chicago, Ill. 60605	
Mr. Charles Miller, Code 05R13 Crystal Plaza #6 Naval Sea Systems Command Washington, DC 20362	2

Steam Turbines Branch, Code 5221
National Center #4
Naval Sea Systems Command
Washington, DC 20362

Mr. Ed Ruggiero, NAVSEA 08
National Center #2
Washington, DC 20362

Dr. Earl Quandt Jr., Code 272
David Taylor Ship R&D Center
Annapolis, MD 21402

Mr. Wayne Adamson, Code 2722
David Taylor Ship R&D Center
Annapolis, MD 21402

Dr. George Lea, Director
Fluid Mechanics Program
National Science Foundation
Washington, DC 20550

Mr. Michael Perlsweig
Department of Energy
Mail Station E-178
Washington, DC 20545

Professor J. A. C. Humphrey
Department of Mechanical Engineering
University of California, Berkeley
Berkeley, CA 94720

Professor Brian Launder
Thermodynamics and Fluid Mechanics Division
University of Manchester
Institute of Science & Technology
P088 Sackville Street
Manchester M601QD England

Professor Shi-Chune Yao
Department of Mechanical Engineering
Carnegie-Mellon University
Pittsburgh, PA 15213

Dr. Branko Leskovar
Electronics R&D Group
Lawrence Berkeley Laboratory
University of California
Berkeley, CA 94720

Dr. Ryszard Gajewski, Director
Division of Advanced Energy Projects
Office of Basic Energy Sciences
Department of Energy
Washington, DC 20545

Dr. David Elliot
NASA Jet Propulsion Laboratory
4800 Oak Grove Drive
Stop 67-201
Pasadena, CA 91103

Mr. Lance Hays, President
BiPhase Energy Systems
2800 Airport Blvd.
Santa Monica, CA 90405

Professor Paul A. Libby
Department of Applied Mechanics and Engineering Sciences
University of California San Diego
P.O. Box 109
La Jolla, CA 92037

Professor C. Forbes Dewey Jr.
Fluid Mechanics Laboratory
Massachusetts Institute of Technology
Cambridge, Massachusetts 02139

Professor Warren Rohsenow
Mechanical Engineering Department
Massachusetts Institute of Technology
77 Massachusetts Avenue
Cambridge, Massachusetts 02139

Professor A. Louis London
Mechanical Engineering Department
Bldg. 500, Room 501B
Stanford University
Stanford, CA 94305

Professor T. N. Veziroglu
Clean Energy Research Institute
University of Miami
Coral Gables, Florida 33124

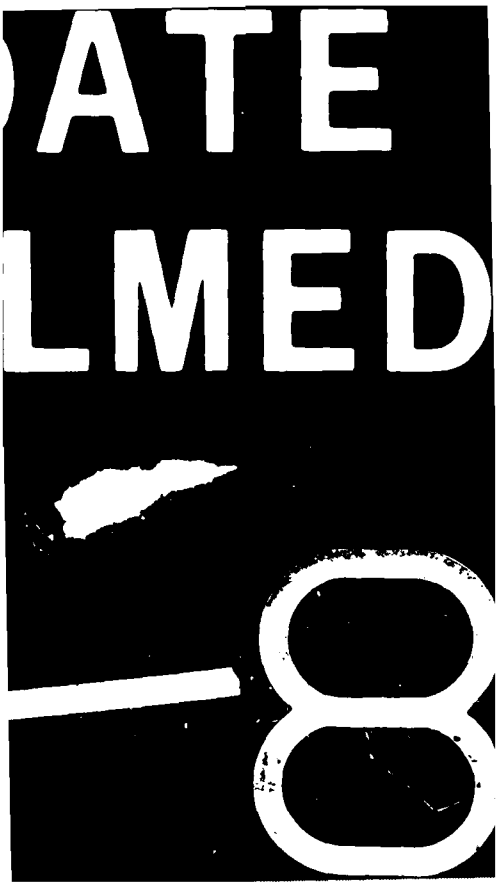
ATE
LMED
8